

THE KINETICS OF ZINC EXTRACTION IN THE DI(2-ETHYLHEXYL) PHOSPHORIC  
ACID, n-HEPTANE - ZINC PERCHLORATE, PERCHLORIC ACID, WATER SYSTEM

by

DONALD WILLIAM JOHN MacLEAN

B.A.Sc., The University of British Columbia, 1988

A THESIS SUBMITTED IN PARTIAL FULFILLMENT OF  
THE REQUIREMENTS FOR THE DEGREE OF  
MASTER OF APPLIED SCIENCE

in

THE FACULTY OF GRADUATE STUDIES  
Department of Metals and Materials Engineering

We accept this thesis as conforming  
to the required standard

THE UNIVERSITY OF BRITISH COLUMBIA

April 1991

© Donald William John MacLean, 1991

In presenting this thesis in partial fulfilment of the requirements for an advanced degree at the University of British Columbia, I agree that the Library shall make it freely available for reference and study. I further agree that permission for extensive copying of this thesis for scholarly purposes may be granted by the head of my department or by his or her representatives. It is understood that copying or publication of this thesis for financial gain shall not be allowed without my written permission.

Department of Metals and Materials Engineering

The University of British Columbia  
Vancouver, Canada

Date April 9, 1991

---

## *ABSTRACT*

---

The kinetics of zinc extraction from perchlorate solutions with di(2-ethylhexyl) phosphoric acid in n-heptane have been measured using the rotating diffusion cell technique.

The extraction of zinc is controlled by the mass transfer of reactants ( $Zn^{2+}$  and D2EHPA) to the interface. At low zinc concentrations, the system is controlled by the aqueous transport of  $Zn^{2+}$  to the interface; at higher zinc concentrations transport of D2EHPA becomes rate controlling. For the range of D2EHPA concentrations examined, the transport of D2EHPA is rate controlling. Bulk pH has a negligible effect, except perhaps at the lowest pH values examined, where there may be a slight decrease in extraction rate. This decrease was attributed to less favourable thermodynamics at low interfacial pH values. It appears that the chemical reaction rate is fast enough that it has a negligible effect on the overall extraction rate. A basic mathematical model was developed which is adequate for predicting the extraction rate under variable conditions of zinc concentration, D2EHPA concentration, and pH.

The effect of using a partially loaded organic extractant was also investigated, and the system was found to be mass transfer controlled. An extended mathematical model was developed which predicts that the speciation of organic complexed zinc changes with increasing preload, and at high loadings the direction of  $ZnL_2 \cdot HL$  and  $ZnL_2 \cdot (HL)_2$  flux reverses, with these species providing extractant to the interface. At very high loadings,  $ZnL_2 \cdot HL$  provides almost all the extractant to the interface.

Experimental studies of the effect of temperature on the rate of zinc extraction resulted in a calculation of the activation energy which was consistent with a diffusion controlled mechanism. Finally, the effect of different filter pore sizes on extraction was examined. The extraction rate decreases significantly with a very small filter pore size, while there appeared to be little or no effect for larger filter pore sizes. For the filter pore size used in this study, it was therefore concluded that the filter pores do not pose an additional resistance to mass transfer.

# Table of Contents

Abstract .....	ii
List of Tables .....	vi
List of Figures .....	vii
List of Symbols .....	xiii
Acknowledgements .....	xv
CHAPTER 1 - Introduction .....	1
CHAPTER 2 - Literature Review .....	3
2.1 Industrial Solvent Extraction Practice .....	3
2.1.1 Solvent Extraction Reagents .....	3
2.1.2 Industrial Solvent Extraction Circuits .....	4
2.1.2.1 Uranium .....	4
2.1.2.2 Copper .....	5
2.2 Di(2-ethylhexyl) Phosphoric Acid .....	6
2.2.1 Applications .....	7
2.2.2 Chemistry .....	8
2.2.3 Parameter Estimation .....	10
2.3 Solvent Extraction Kinetics .....	11
2.3.1 Interfacial Mechanisms .....	13
2.3.2 Mass Transfer Control .....	16
2.3.3 Mixed Regime (Mass Transfer with Chemical Reaction) .....	18
2.3.4 Other considerations .....	21
2.3.5 Summary .....	22
2.4 Kinetic Contactors .....	22

2.4.1 Lewis Cell (constant interface area cells) .....	22
2.4.2 AKUFVE .....	24
2.4.3 Single Drop Cell (Moving Drop Cell) .....	24
2.4.4 Growing Drop Cell .....	25
2.4.5 Laminar Liquid Jet (Liquid Jet Recycle Reactor) .....	26
2.5 Rotating Diffusion Cell .....	27
2.5.1 Apparatus .....	27
2.5.2 Theory .....	28
2.5.3 Previous Work using the RDC .....	29
2.5.4 Summary .....	32
2.6 Zn-D2EHPA equilibrium and kinetics .....	32
2.6.1 Zn-D2EHPA equilibrium .....	32
2.6.2 Zn-D2EHPA Kinetics .....	34
2.7 Supported Liquid Membranes .....	37
2.8 Summary .....	39
<b>CHAPTER 3 - Experimental Methods .....</b>	<b>41</b>
3.1 Reagents .....	41
3.1.1 D2EHPA Purification .....	41
3.1.2 Preparation of Preloaded Zinc-D2EHPA .....	42
3.2 Solution Analysis .....	43
3.3 Rotating Diffusion Cell Apparatus .....	44
3.4 Filter Preparation .....	45
3.5 Experimental Procedure .....	46

<b>CHAPTER 4 - Results and Discussion</b> .....	49
4.1 Initial Data from Test Runs .....	49
4.2 Basic Mathematical Model .....	54
4.3 Basic Model Predictions .....	61
4.3.1 Basic Model Verification .....	61
4.3.2 Basic Model Predictions .....	70
4.4 Extended Mathematical Model .....	79
4.5 Preload Results .....	84
4.5.1 Extended Model Verification .....	84
4.5.2 Extended Model Predictions .....	88
4.6 Variable Temperature .....	96
4.7 Filter Characterization .....	98
4.8 SLM Applications .....	100
<b>CHAPTER 5 - Conclusions</b> .....	101
<b>CHAPTER 6 - Recommendations for Further Work</b> .....	102
<b>REFERENCES</b> .....	103
<b>APPENDIX A - Optical Tachometer</b> .....	109
<b>APPENDIX B - Data Acquisition Hardware and Software</b> .....	112
<b>APPENDIX C - Raw Experimental Data</b> .....	121
<b>APPENDIX D - Basic Mathematical Model</b> .....	123
<b>APPENDIX E - Extended Mathematical Model</b> .....	130

## List of Tables

Table 2.1	Physical and Chemical Properties of D2EHPA .....	9
Table 2.2	Diffusion Coefficients predicted by the Wilke-Chang Relationship .....	11
Table 2.3	Results of Patel's study of Ni, Co, Cu and Zn extraction .....	31
Table 2.4	Survey of Equilibrium Studies using Zinc and D2EHPA .....	33
Table 2.5	Survey of Kinetic Studies using Zinc and D2EHPA .....	34
Table 4.1	Experimental Conditions .....	50
Table 4.2	Membrane Filter Characteristics .....	98
Table B.1	Pascal Listing of Data Acquisition Computer Program .....	113
Table D.1	Pascal Listing of Basic Mathematical Model .....	123
Table E.1	Pascal Listing of Extended Mathematical Model .....	130

## List of Figures

Figure 2.1	Flow Sheet of the DAPEX Process .....	4
Figure 2.2	Bluebird Mine Solvent Extraction and Electrowinning Flowsheet .....	6
Figure 2.3	Structural diagram of a D2EHPA dimer .....	8
Figure 2.4	Viscosity of solutions of the Zn(II)-HDEHP complex at 0.01M total Zn(II) in dodecane at 20°C as a function of the excess HDEHP concentration .....	10
Figure 2.5	Schematic diagram of the reaction zone and aqueous/organic boundary layers .....	12
Figure 2.6	Concentration profile for an interfacial reaction mechanism .....	14
Figure 2.7	Interfacial Profile : Mass transfer limited reaction .....	16
Figure 2.8	Schematic diagram of the reaction zone and aqueous/organic boundary layers - Mass transfer with chemical reaction model .....	18
Figure 2.9	The original Lewis Cell .....	23
Figure 2.10	The moving drop cell .....	25
Figure 2.11	The growing drop cell .....	26
Figure 2.12	The inner portion of the Liquid-Jet Recycle Reactor .....	27
Figure 2.13	The Rotating Diffusion Cell .....	28
Figure 2.14	Fluid flow patterns near the Rotating Diffusion Cell .....	29
Figure 2.15	The extraction of Co, Ni, Cu, and Zn by D2EHPA .....	31
Figure 2.16	Extraction processes in a SLM .....	38
Figure 2.17	Axial and cross-sectional view of a hollow-fibre SLM module .....	38
Figure 3.1	Sample Gran Plots .....	44
Figure 3.2	The Rotating Diffusion Cell .....	45
Figure 3.3	A Sample RDC Plot showing lines from three different experiments : Formal [D2EHPA] = 0.05 M, pH = 4.5, T = 25°C, filter = 0.45µm .....	47

Figure 4.1	Effect of changing bulk zinc concentration on zinc flux : Formal [D2EHPA] = 0.05 M, pH = 4.5, T = 25°C, filter = 0.45µm, ω = 100 rpm .....	52
Figure 4.2	Effect of changing D2EHPA concentration on zinc flux : [Zn] = 0.05 M, pH = 4.5, T = 25°C, filter = 0.45µm, ω = 100 rpm .....	52
Figure 4.3	Effect of changing bulk pH on zinc flux : [Zn] = 0.05M, Formal [D2EHPA] = 0.05 M, T = 25°C, filter = 0.45µm, ω = 100 rpm .....	53
Figure 4.4	Effect of changing temperature on zinc flux : [Zn] = 0.05 M, Formal [D2EHPA] = 0.05 M, pH = 4.5, filter = 0.45µm, ω = 100 rpm .....	53
Figure 4.5	Diagram of species and flux direction definitions for the VMR model .....	55
Figure 4.6	VMR predictions and experimental data for changes in bulk zinc concentration : Formal [D2EHPA] = 0.05 M, pH = 4.5, T = 25°C, filter = 0.45µm, ω = 100 rpm .....	57
Figure 4.7	VMR predictions and experimental data for changes in bulk D2EHPA concentration : [Zn] = 0.05 M, pH = 4.5, T = 25°C, filter = 0.45µm, ω = 100 rpm .....	57
Figure 4.8	Basic program structure of the simple mathematical model .....	61
Figure 4.9	Effect of changing bulk zinc concentration on zinc flux : Formal [D2EHPA] = 0.05 M, pH = 4.5, T = 25°C, filter = 0.45µm, ω = 100 rpm .....	64
Figure 4.10	Effect of changing bulk zinc concentration on zinc flux : Formal [D2EHPA] = 0.05 M, pH = 4.5, T = 25°C, filter = 0.45µm, ω = 300 rpm .....	64
Figure 4.11	Effect of changing D2EHPA concentration on zinc flux : [Zn] = 0.05M, pH = 4.5, T = 25°C, filter = 0.45µm, ω = 100 rpm .....	65
Figure 4.12	Effect of changing D2EHPA concentration on zinc flux : [Zn] = 0.05M, pH = 4.5, T = 25°C, filter = 0.45µm, ω = 300 rpm .....	65
Figure 4.13	Effect of changing bulk pH on zinc flux : [Zn] = 0.05M, Formal [D2EHPA] = 0.05 M, T = 25°C, filter = 0.45µm, ω = 100 rpm .....	66
Figure 4.14	Effect of changing bulk pH on zinc flux : [Zn] = 0.05M, Formal [D2EHPA] = 0.05 M, T = 25°C, filter = 0.45µm, ω = 300 rpm .....	66
Figure 4.15	Zinc flux vs. zinc concentration for changes in the organic species diffusion coefficients : Formal [D2EHPA] = 0.05 M, pH = 4.5, T = 25°C, filter = 0.45µm, ω = 100 rpm .....	67

Figure 4.16	Zinc flux vs. D2EHPA concentration for changes in the organic species diffusion coefficients : [Zn] = 0.05M, pH = 4.5, T = 25°C, filter = 0.45µm, ω = 100 rpm .....	67
Figure 4.17	Zinc flux vs. zinc concentration for changes in the equilibrium constant $K_{ex}$ : Formal [D2EHPA] = 0.05 M, pH = 4.5, T = 25°C, filter = 0.45µm, ω = 100 rpm .....	68
Figure 4.18	Zinc flux vs. D2EHPA concentration for changes in the equilibrium constant $K_{ex}$ : [Zn] = 0.05M, pH = 4.5, T = 25°C, filter = 0.45µm, ω = 100 rpm .....	68
Figure 4.19	Zinc flux vs. zinc concentration for changes in the filter equivalent thickness $L/\alpha$ : Formal [D2EHPA] = 0.05 M, pH = 4.5, T = 25°C, filter = 0.45µm, ω = 100 rpm .....	69
Figure 4.20	Zinc flux vs. D2EHPA concentration for changes in the filter equivalent thickness $L/\alpha$ : [Zn] = 0.05M, pH = 4.5, T = 25°C, filter = 0.45µm, ω = 100 rpm .....	69
Figure 4.21	Predicted change in association factor ( $n_{avg}$ ) with bulk zinc concentration : Formal [D2EHPA] = 0.05 M, pH = 4.5, T = 25°C, filter = 0.45µm, ω = 100 rpm .....	73
Figure 4.22	Predicted change in interfacial pH with bulk zinc concentration : Formal [D2EHPA] = 0.05 M, pH = 4.5, T = 25°C, filter = 0.45µm, ω = 100 rpm .....	73
Figure 4.23	Predicted change in interfacial zinc concentration with bulk zinc concentration : Formal [D2EHPA] = 0.05 M, pH = 4.5, T = 25°C, filter = 0.45µm, ω = 100 rpm .....	74
Figure 4.24	Predicted change in interfacial D2EHPA concentration with bulk zinc concentration : Formal [D2EHPA] = 0.05 M, pH = 4.5, T = 25°C, filter = 0.45µm, ω = 100 rpm .....	74
Figure 4.25	Predicted change in association factor ( $n_{avg}$ ) with bulk D2EHPA concentration : [Zn] = 0.05M, pH = 4.5, T = 25°C, filter = 0.45µm, ω = 100 rpm .....	75
Figure 4.26	Predicted change in interfacial pH with bulk D2EHPA concentration : [Zn] = 0.05M, pH = 4.5, T = 25°C, filter = 0.45µm, ω = 100 rpm .....	75
Figure 4.27	Predicted change in interfacial zinc concentration with bulk D2EHPA concentration : [Zn] = 0.05M, pH = 4.5, T = 25°C, filter = 0.45µm, ω = 100 rpm .....	76

Figure 4.28	Predicted change in interfacial D2EHPA concentration : [Zn] = 0.05M, pH = 4.5, T = 25°C, filter = 0.45µm, ω = 100 rpm .....	76
Figure 4.29	Predicted change in association factor ( $n_{avg}$ ) with bulk pH : [Zn] = 0.05M, Formal [D2EHPA] = 0.05 M, T = 25°C, filter = 0.45µm, ω = 100 rpm .....	77
Figure 4.30	Predicted change in interfacial pH with bulk pH : [Zn] = 0.05M, Formal [D2EHPA] = 0.05 M, T = 25°C, filter = 0.45µm, ω = 100 rpm .....	77
Figure 4.31	Predicted change in interfacial zinc concentration with bulk pH : [Zn] = 0.05M, Formal [D2EHPA] = 0.05 M, T = 25°C, filter = 0.45µm, ω = 100 rpm .....	78
Figure 4.32	Predicted change in interfacial D2EHPA concentration with bulk pH : [Zn] = 0.05M, Formal [D2EHPA] = 0.05 M, T = 25°C, filter = 0.45µm, ω = 100 rpm .....	78
Figure 4.33	Basic program structure of the extended mathematical model .....	83
Figure 4.34	Comparison of experimental data and extended model predictions for flux vs. preload for selected values of $\beta_{12}/\beta_{13}$ : [Zn] = 0.05M, Formal [D2EHPA] <sub>total</sub> = 0.05 M, pH = 4.5, T = 25°C, filter = 0.45µm, ω = 100 rpm .....	85
Figure 4.35	Effect of preload on zinc flux : [Zn] = 0.05M, Formal [D2EHPA] <sub>total</sub> = 0.05 M, pH = 4.5, T = 25°C, filter = 0.45µm, ω = 100 rpm, $\beta_{12}/\beta_{13} = 6 \times 10^{-5}$ .....	86
Figure 4.36	Effect of preload on zinc flux : [Zn] = 0.05M, Formal [D2EHPA] <sub>total</sub> = 0.05 M, pH = 4.5, T = 25°C, filter = 0.45µm, ω = 300 rpm, $\beta_{12}/\beta_{13} = 6 \times 10^{-5}$ .....	86
Figure 4.37	Zinc flux vs. preload for changes in the organic species diffusion coefficients : [Zn] = 0.05M, Formal [D2EHPA] <sub>total</sub> = 0.05 M, pH = 4.5, T = 25°C, filter = 0.45µm, ω = 100 rpm, $\beta_{12}/\beta_{13} = 6 \times 10^{-5}$ .....	87
Figure 4.38	Zinc flux vs. preload for changes in the equilibrium constant $K_{ex}$ : [Zn] = 0.05M, Formal [D2EHPA] <sub>total</sub> = 0.05 M, pH = 4.5, T = 25°C, filter = 0.45µm, ω = 100 rpm, $\beta_{12}/\beta_{13} = 6 \times 10^{-5}$ .....	87
Figure 4.39	Zinc flux vs. preload for changes in the filter equivalent thickness $L/\alpha$ : [Zn] = 0.05M, Formal [D2EHPA] <sub>total</sub> = 0.05 M, pH = 4.5, T = 25°C, filter = 0.45µm, ω = 100 rpm, $\beta_{12}/\beta_{13} = 6 \times 10^{-5}$ .....	88

Figure 4.40	Predicted change in interfacial zinc concentration (aqueous) with preload : [Zn] = 0.05M, Formal [D2EHPA] <sub>total</sub> = 0.05 M, pH = 4.5, T = 25°C, filter = 0.45µm, ω = 100 rpm, β <sub>12</sub> /β <sub>13</sub> = 6 × 10 <sup>-5</sup> .....	91
Figure 4.41	Predicted change in interfacial pH with preload : [Zn] = 0.05M, Formal [D2EHPA] <sub>total</sub> = 0.05 M, pH = 4.5, T = 25°C, filter = 0.45µm, ω = 100 rpm, β <sub>12</sub> /β <sub>13</sub> = 6 × 10 <sup>-5</sup> .....	91
Figure 4.42	Predicted change in bulk D2EHPA concentration with preload : [Zn] = 0.05M, Formal [D2EHPA] <sub>total</sub> = 0.05 M, pH = 4.5, T = 25°C, filter = 0.45µm, ω = 100 rpm, β <sub>12</sub> /β <sub>13</sub> = 6 × 10 <sup>-5</sup> .....	92
Figure 4.43	Predicted change in interfacial D2EHPA concentration with preload : [Zn] = 0.05M, Formal [D2EHPA] <sub>total</sub> = 0.05 M, pH = 4.5, T = 25°C, filter = 0.45µm, ω = 100 rpm, β <sub>12</sub> /β <sub>13</sub> = 6 × 10 <sup>-5</sup> .....	92
Figure 4.44	Predicted association factors vs. preload : [Zn] = 0.05M, Formal [D2EHPA] <sub>total</sub> = 0.05 M, pH = 4.5, T = 25°C, filter = 0.45µm, ω = 100 rpm, β <sub>12</sub> /β <sub>13</sub> = 6 × 10 <sup>-5</sup> .....	93
Figure 4.45	Predicted fractions of zinc species vs. preload : [Zn] = 0.05M, Formal [D2EHPA] <sub>total</sub> = 0.05 M, pH = 4.5, T = 25°C, filter = 0.45µm, ω = 100 rpm, β <sub>12</sub> /β <sub>13</sub> = 6 × 10 <sup>-5</sup> .....	93
Figure 4.46	Predicted change in bulk zinc concentrations (organic) with preload : [Zn] = 0.05M, Formal [D2EHPA] <sub>total</sub> = 0.05 M, pH = 4.5, T = 25°C, filter = 0.45µm, ω = 100 rpm, β <sub>12</sub> /β <sub>13</sub> = 6 × 10 <sup>-5</sup> .....	94
Figure 4.47	Predicted change in interfacial zinc concentrations (organic) with preload : [Zn] = 0.05M, Formal [D2EHPA] <sub>total</sub> = 0.05 M, pH = 4.5, T = 25°C, filter = 0.45µm, ω = 100 rpm, β <sub>12</sub> /β <sub>13</sub> = 6 × 10 <sup>-5</sup> .....	94
Figure 4.48	Predicted change in organic zinc concentrations with preload : [Zn] = 0.05M, Formal [D2EHPA] <sub>total</sub> = 0.05 M, pH = 4.5, T = 25°C, filter = 0.45µm, ω = 100 rpm, β <sub>12</sub> /β <sub>13</sub> = 6 × 10 <sup>-5</sup> .....	95
Figure 4.49	Predicted flux of organic species with preload : [Zn] = 0.05M, Formal [D2EHPA] <sub>total</sub> = 0.05 M, pH = 4.5, T = 25°C, filter = 0.45µm, ω = 100 rpm, β <sub>12</sub> /β <sub>13</sub> = 6 × 10 <sup>-5</sup> .....	95
Figure 4.50	VMR predictions and experimental data for changes in temperature : [Zn] = 0.05M, Formal [D2EHPA] = 0.05 M, pH = 4.5, filter = 0.45µm, ω = 100 rpm .....	97

Figure 4.51	Arrhenius Plot for experimental temperature data with linear regression fit : [Zn] = 0.05M, Formal [D2EHPA] = 0.05 M, pH = 4.5, filter = 0.45 $\mu$ m, $\omega$ = 100 rpm .....	97
Figure 4.52	Effect of changing filter pore size on zinc flux : [Zn] = 0.05M, Formal [D2EHPA] = 0.05 M, pH = 4.5, T = 25 $^{\circ}$ C, $\omega$ = 100 rpm .....	99
Figure 4.53	Effect of changing filter pore size on zinc flux : [Zn] = 0.05M, Formal [D2EHPA] = 0.05 M, pH = 4.5, T = 25 $^{\circ}$ C, $\omega$ = 300 rpm .....	99
Figure A.1	The RDC and the Optical RPM Sensor .....	109
Figure A.2	The Tachometer Circle .....	110
Figure A.3	Schematic Diagram of Optical Counter Signal Conditioner .....	111
Figure B.1	Chart Feed pin-out specifications .....	112
Figure B.2	Major elements of the data acquisition program .....	113

# List of Symbols

$c$	organic species concentration ( kmol/m <sup>3</sup> )
$C$	aqueous species concentration ( kmol/m <sup>3</sup> )
$D$	diffusion coefficient ( m <sup>2</sup> /s )
$F$	formal D2EHPA concentration ( kmol/m <sup>3</sup> )
$J$	species flux ( kmol/m <sup>2</sup> /s )
$k$	mass transfer coefficient of specified species ( m/s )
$K_{ex}$	concentration-based equilibrium constant ( (kmol/m <sup>3</sup> ) <sup>(2-n)</sup> )
$K_D$	dimerization constant ( (kmol/m <sup>3</sup> ) <sup>-1</sup> )
$L$	effective filter thickness ( m )
$M$	solvent molecular weight ( kg/kmol )
$m$	valence of metal cation
$n$	association factor (number of dimerized extractant molecules complexing the divalent metal)
$P$	Partition coefficient
$T$	temperature ( °C )
$V_B$	molar volume of the solute at the normal boiling point ( m <sup>3</sup> /kmol )
$x$	solvent association factor
$z_{D,aq}$	aqueous equivalent boundary layer thickness ( m )
$z_{D,org}$	organic equivalent boundary layer thickness ( m )

## *Subscripts for c, C*

$Zn^{2+}$	aqueous zinc
HL	organic D2EHPA monomer
(HL) <sub>2</sub>	organic D2EHPA dimer
(HL) <sub>2,total</sub>	total organic D2EHPA concentration, expressed as dimer

$ZnL_2$	organic $n=1$ zinc-D2EHPA complex
$ZnL_2 \cdot HL$	organic $n=1.5$ zinc-D2EHPA complex
$ZnL_2 \cdot (HL)_2$	organic $n=2$ zinc-D2EHPA complex
$ZnL_2 \cdot (HL)_{x,total}$	total organic zinc-extractant complex, all forms
$Zn_{total}$	total organic zinc, all forms

### *Superscripts for c, C*

<i>bulk</i>	bulk species
<i>i</i>	interfacial species

### *Superscripts*

— (overbar) property or species in the organic phase

### *Greek Symbols*

$\alpha$	filter porosity
$\beta_{12}$	$ZnL_2$ metal-extractant complex formation constant
$\beta_{13}$	$ZnL_2 \cdot HL$ metal-extractant complex formation constant ( $(\text{kmol}/\text{m}^3)^{-1}$ )
$\beta_{14}$	$ZnL_2 \cdot (HL)_2$ metal-extractant complex formation constant ( $(\text{kmol}/\text{m}^3)^{-2}$ )
$\delta_{aq}$	aqueous diffusion boundary layer thickness
$\delta_{org}$	organic diffusion boundary layer thickness
$\delta_r$	reaction zone thickness
$\mu$	absolute viscosity ( $\text{N}\cdot\text{s}/\text{m}^2$ )
$\nu$	kinematic viscosity ( $\text{m}^2/\text{s}$ )
$\omega$	RDC angular velocity ( radians/s )

# Acknowledgements

I would like to take this opportunity to thank some of the many special people who have helped me in this endeavour.

Thanks to my research supervisor, Dr. David Dreisinger, who has not only been an academic guide but an encourager; constantly exhorting me to press on towards excellence, and leading by example.

With much appreciation I acknowledge the many "rays of sunshine" that Joan, Merlin, Moyra, and Celeste have brought my way. You have brightened up more than a few "rainy" days.

Thanks to Ken Scholey, Mike Lo, and Ish Grewal for your friendship and companionship; I know that I am richer for having known you, and I hope that you feel the same way.

Thanks to Fred Rink, who has demonstrated to me in his life the true meaning of the word perseverance, and who has been a burden bearer and pray-er.

And last, but very definitely not least, I would like to thank my parents, my sister Heather, and my aunts Win and Dot for their unconditional love and support through this difficult time.

Thanks are also extended to the Cy and Emerald Keyes Foundation and the Natural Sciences and Engineering Research Council of Canada for their financial support.

---

## CHAPTER 1 - Introduction

---

Solvent extraction is a metals purification process that has grown from its roots in analytical chemistry to become a major unit operation in industrial practice. The first large-scale use of solvent extraction processes was in the early 1940's, when it was used to produce super high-purity uranium by extracting uranyl nitrate with diethyl ether; this Manhattan Project production of uranium was used to produce both the  $^{235}\text{U}$  and  $^{239}\text{Pu}$  that was used in the first atomic bombs. Since that time, the number of applications involving solvent extraction techniques has grown dramatically. Currently, metals that are produced (or purified) by solvent extraction techniques include, but are not limited to, copper, nickel, cobalt, uranium, tungsten, vanadium, chromium, niobium, tantalum, platinum group metals, and rare-earths. Copper is one of the highest volume metals processed by solvent extraction techniques; world production by solvent extraction has been estimated at 282,000 tpy (1984 figures).<sup>[1]</sup>

The rapid growth of solvent extraction has now slowed somewhat, with the industry entering a more mature phase of development. As a result, research is now being directed at more fundamental topics, with new discoveries more likely in the realm of incremental improvements rather than radical breakthroughs.

Modern plant practice is still fraught with many problems. Poor mixing results in larger-than-necessary contactors to provide long residence times. A poorly mixed system can also result in excessive solvent entrainment in a third phase which does not easily disengage, resulting in high solvent losses and low settler capacity. Extractants can coat particulates carried over from earlier processing stages, resulting in a "crud" formation which interferes with phase separation.<sup>[2]</sup> Finally, since solvent extraction circuits run at low temperatures (unlike pyrometallurgical systems), acceleration of slow kinetics is important in ensuring the economical operation of a solvent extraction plant.

Research is therefore being focused on the above as well as other areas. Chemists are constantly searching for new reagents which will extract metals faster, with greater selectivity, and at a lower overall cost. The use of a higher priced extractant can often be justified if it has a lower solubility in the aqueous phase (and therefore lower losses) or a higher rate of extraction (reducing equipment capital costs). New applications for solvent extraction technology are

constantly being explored. For example, research is under way on techniques for extracting impurities from copper refinery electrolytes. Strong extractants which remove heavy metals from acidic waste waters are currently being marketed. Efforts are also being expended to develop new types of contactors which operate more efficiently or with lower capital costs than present designs. One example is a supported liquid membrane (SLM), where an extractant-impregnated membrane is contacted with a feed solution on one side and a strip solution on the other side. Metal ions in the feed react with the organic in the membrane, the metal-organic complex diffuses through the membrane, and the metal is then transferred to the strip solution on the opposite side. Such systems look very promising for the treatment of very dilute metal-containing waste streams.

The objective of this thesis is to study the kinetics of zinc extraction from perchlorate solutions by di(2-ethylhexyl) phosphoric acid (D2EHPA) in heptane. This particular topic was selected to increase our understanding of the rate controlling processes at or near the aqueous/organic interface. The results of this work should contribute to 1) the design of extractants with superior metal extraction kinetics, 2) the optimization of current solvent extraction processes using D2EHPA, and 3) the development of supported liquid membrane contactors.

This work is divided into six major sections. Chapter 2 consists of a summary of a literature search of solvent extraction kinetics with a critical discussion of present theory and practice. Chapter 3 describes the experimental procedures used in the current study, and Chapter 4 is a discussion of the experimental results. The results are summarized in Chapter 5, and recommendations for further work are presented in Chapter 6.

---

## **CHAPTER 2 - Literature Review**

---

### **2.1 Industrial Solvent Extraction Practice**

This introduction to industrial solvent extraction practice will consist of two sections. First, the types of solvent extraction reagents and their general properties will be discussed. Two examples of industrial solvent extraction circuits will then be given.

#### **2.1.1 Solvent Extraction Reagents**

There are three general types of solvent extractants: acid, basic, and solvating.<sup>[2]</sup> Acid extractants can be further divided into two subcategories: acidic extractants and acid chelating extractants.

Acidic extractants exchange a hydrogen ion for a metal cation; their reactions are thus pH dependent. The alkylphosphoric acids (including di(2-ethylhexyl) phosphoric acid, or D2EHPA) are the most commonly used members of this group, and are widely used for extracting many metals including uranium, cobalt/nickel, and rare-earths.

Acid chelating extractants typically form bidentate (2-membered) complexes with the target metal cation; examples are the 8-hydroxyquinoline and hydroxyoxime derivatives. The LIX series of reagents, including LIX63 and LIX65N, are hydroxyoximes. They are primarily used for copper extraction, and have enjoyed great commercial success.

Basic extractants are amines or quaternary ammonium salts which extract anionic metal species. In the case of primary, secondary, and tertiary amines, the organic extractant molecule is first protonated forming an amine salt which is then able to anion exchange with the target anionic metal species. The resulting metal-amine is then transferred to the organic phase. An example of a basic extractant currently used in industrial practice is Alamine 336, a tertiary amine which is used for uranium, cobalt, tungsten, and vanadium extraction.

Solvating extractants extract neutral complexes from the aqueous phase. The most common donor groups are oxygen bonded to carbon, or oxygen or sulphur bonded to phosphorous. A solvating extractant widely used in industrial practice is tributylphosphate

(TBP), which is an oxygen-phosphorous bond extractant. This particular extractant is commonly used in nuclear metallurgy where it is used to refine uranium and reprocess spent nuclear reactor fuel.<sup>[1,2]</sup>

## 2.1.2 Industrial Solvent Extraction Circuits

### 2.1.2.1 Uranium

The DAPEX (Di-AlkylPhosphoric acid EXtraction) process is used to concentrate and purify uranium extracted from ore leach solutions. In this process, extraction is achieved by using both D2EHPA and TBP (there is a synergistic effect). The uranium feed is clarified and injected into the extraction system - 5 stages are typically used. The loaded organic solution is stripped using a 15%  $\text{Na}_2\text{CO}_3$  solution, forming a uranium tricarbonate complex and D2EHPA sodium salt. In the extraction stages, acid is added to replenish the acid lost due to the presence of the D2EHPA sodium salt. The purified aqueous solution is filtered to remove any iron or titanium precipitated during stripping. Uranium is recovered after solution neutralization by adding peroxide and precipitating uranyl peroxide, which is then dried to produce yellow cake ( $\text{Na}_2\text{UO}_4 \cdot 2\text{H}_2\text{O}$ ).<sup>[1]</sup> A typical process flowsheet is shown in Figure 2.1.

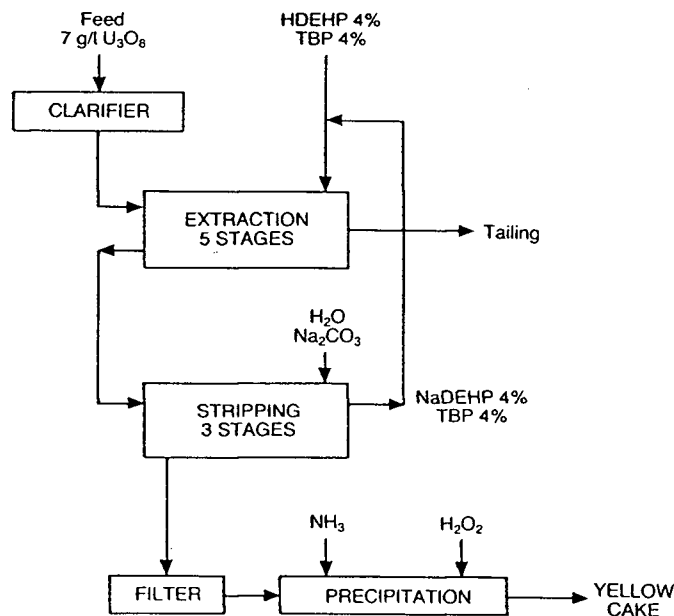


Figure 2.1 Flow sheet of the DAPEX process (after Alegret<sup>[1]</sup>)

### 2.1.2.2 Copper

The most common copper solvent extraction system is found in a leach-extraction-electrowinning system. In this process, low-grade oxidized copper ores are first leached with sulphuric acid. The dilute leach solution is then processed through a solvent extraction circuit, where the solution is purified and the copper concentration increases to a level which is practical for electrowinning.

The first copper plant to use this process was the Ranchers Exploration and Development Corporation Bluebird plant at Miami, Arizona, which started operation in 1968; a process flowsheet is shown in Figure 2.2. The copper ore is sequentially leached in 9 ponds, with a total leaching time of ~135 days. The solution is then filtered, heated, and sent to the solvent extraction plant where the copper is extracted by a 9.5% LIX64N solution in a Napoleum 470 diluent. Three mixer settlers are used in a countercurrent configuration with an organic/aqueous ratio of 2.5:1, resulting in a throughput of ~22000 l/min. The copper feed concentration is 1.8 to 2.4 gpl Cu; the raffinate contains ~250 ppm Cu and is returned to the leaching ponds.

The loaded organic is stripped in two mixer settlers; the strip solution contains ~140 gpl H<sub>2</sub>SO<sub>4</sub> and ~30 gpl Cu, and the final copper solution sent for electrowinning contains ~34 gpl Cu. The electrowinning plant produces ~18.2 tpd Cu.<sup>[1,3]</sup>

Since the Ranchers plant was built, many other copper solvent extraction plants have been constructed. As of 1984, the largest plant constructed is the Nchanga plant in Zambia, which operates an acid leach of mine tailings. This plant produces 182 tpd Cu using four solvent extraction streams, one using SME529 and the other three using LIX64N.<sup>[1]</sup>

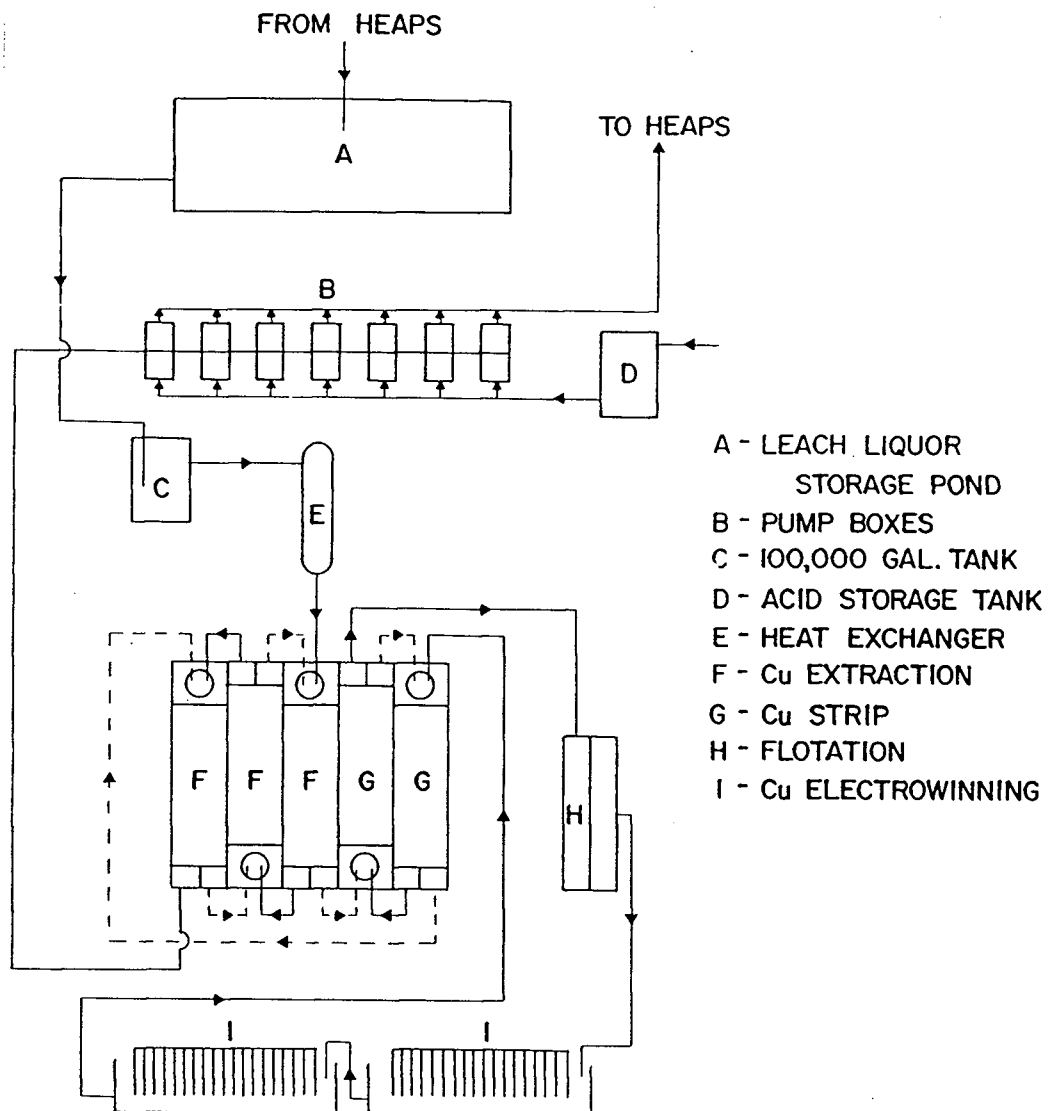


Figure 2.2 Bluebird Mine Solvent Extraction and Electrowinning Flowsheet (after Ritcey and Ashbrook<sup>(3)</sup>)

## 2.2 Di(2-ethylhexyl) Phosphoric Acid

Di(2-ethylhexyl) phosphoric acid (hereafter referred to as D2EHPA in the text and as HL in formulae) is an alkylphosphoric acid that has become widely used in solvent extraction practice. First used in 1949, this general-purpose extractant is used for extracting a wide variety of metals, including uranium, cobalt/nickel, and rare-earths. It has adequate kinetics, moderate separation capability, low aqueous solubility, and is chemically stable.<sup>(1)</sup> Its wide availability and low cost keep it popular when compared to other reagents.

### 2.2.1 Applications

As mentioned above, D2EHPA is used extensively in nuclear applications, particularly the DAPEX process. Although it is used to extract many other metals, this discussion will focus exclusively on the extraction of zinc with D2EHPA.

The traditional pyrometallurgical/hydrometallurgical methods for the primary production of zinc from zinc ores (and more advanced hydrometallurgical methods such as the zinc pressure leach) are already quite efficient and well established. Therefore, there is little need for the use of solvent extraction technology in primary metal production. However, solvent extraction is a particularly effective unit process for the recovery and concentration of zinc from dilute aqueous process streams, and several processes have been developed. A significant impetus for the further development and implementation of these processes is developing as a result of legislation requiring either proper waste disposal or metal recovery.<sup>[4]</sup>

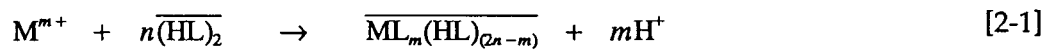
The Zincex process<sup>[2,5-7]</sup> uses two solvent extraction circuits to recover zinc from pyrite cinder leach solutions. An amine extractant is used in the first circuit to produce a purified zinc chloride solution; D2EHPA is then used in the second circuit to extract zinc. The zinc is then stripped with spent sulphuric acid electrolyte and recovered in a conventional electrowinning plant. Even after passing through the first circuit, some iron remains in the purified solution; it is removed by bleeding of some of the D2EHPA and treating it with strong HCl. A Zincex plant producing 22 tpd of 99.99% pure zinc is currently in operation at Bilbao, Spain; the value of recovered zinc pays the plant operating costs.

The METSEP process<sup>[8,9]</sup> was developed to recover zinc and iron from galvanizing pickling solutions. Zinc is removed using an ion exchange column; the column is then eluted with HCl and the zinc is extracted with D2EHPA. Zinc is stripped using sulphuric acid, and then electrowon. The iron is removed from the pickling effluent by pyrohydrolysis, which recovers Fe as iron oxide. HCl is then recovered in an absorber along with the HCl from the SX circuit, and recycled. A plant was in operation in South Africa, but was closed due to poor process economics.<sup>[9]</sup>

Finally, the Valberg process<sup>[7,9,10]</sup> is used to extract zinc from rayon manufacturing waste waters. A plant in Sweden uses D2EHPA in kerosene in a two-step countercurrent process to reduce the zinc concentration from ~0.2 gpl to less than 2 ppm. Sulphuric acid is used to strip the zinc from the organic solution; the resulting 80 gpl zinc solution is recycled back to the rayon spinning bath. Although process installation was required by environmental legislation, the value of recovered zinc pays all operating costs.

### 2.2.2 Chemistry

The basic physiochemical properties of D2EHPA are outlined in Table 2.1. It is a weak acid, and is relatively insoluble in water. The reaction between a metal cation and the D2EHPA dimer can be expressed by the generalized formula:



where M represents the metal being extracted, L is the extractant (D2EHPA),  $m$  is the valence of the metal cation,  $n$  represents the number of dimerized extractant molecules participating in the reaction, and a bar indicates a compound in the organic phase.

The D2EHPA molecule usually exists as a dimer in nonpolar media (i.e. most aromatic and aliphatic solvents<sup>[11]</sup>), and is monomeric in highly polar media (i.e. alcohols, carboxylic acids, and water).<sup>[12]</sup> The D2EHPA dimer consists of two D2EHPA monomers, joined by hydrogen bonds between adjacent P=O and P-OH groups, as shown in Figure 2.3.

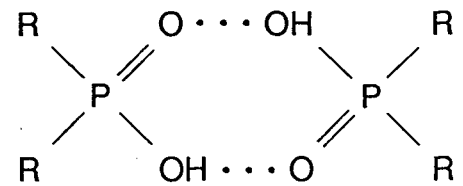


Figure 2.3 Structural diagram of a D2EHPA dimer

The non-ideal behaviour of D2EHPA at high extractant concentrations was investigated by Danesi and Vandegrift<sup>[13]</sup>, who examined results from equilibrium studies of  $Eu^{3+}$ ,  $Tm^{3+}$ , and  $Ca^{2+}$  extraction by D2EHPA in n-dodecane. They concluded that the D2EHPA dimer activity coefficient  $\gamma_D$  is fitted fairly well by the expression:

$$\log \gamma_D = 0.83 \sqrt{\frac{F}{2}} \quad [2-2]$$

where  $F$  is the formal D2EHPA concentration.

**Table 2.1** Physical and Chemical Properties of D2EHPA

chemical name:	Bis(2-ethylhexyl) phosphoric acid	
CAS registry number:	[298-07-7]	
formula:	$(C_8H_{17}O)_2POOH^*$	
structure: (monomer)		
molecular weight	322 g/mole (monomer)*	
specific gravity (20/20 °C)	0.977 ± 0.003*	
viscosity (cps/25 °C)	35*	
liquid molar volume, $V_B$	422.9 m <sup>3</sup> /kmol (monomer) <sup>†</sup> 845.8 m <sup>3</sup> /kmol (dimer) <sup>†</sup>	
$D_{(HL)_2, \text{heptane}}$	1.003 × 10 <sup>-9</sup> m <sup>2</sup> /sec (dimer) <sup>‡</sup>	
pK <sub>a</sub> 0.1M(H,Na)NO <sub>3</sub> /heptane	1.49	Komasawa <i>et al.</i> [14]
0.1M(H,Na)ClO <sub>4</sub> /hexane	1.30	Komasawa <i>et al.</i> [14]
0.0001-1M(H,Na)ClO <sub>4</sub> /octane	1.36 to 1.44	Ul'yanov <i>et al.</i> [15]
distribution constant (H,Na)ClO <sub>4</sub> /octane	log K <sub>d</sub> = 3.44	Ul'yanov <i>et al.</i> [15]
0.1M(H,Na)NO <sub>3</sub> /heptane	log K <sub>d</sub> = 3.20	Komasawa <i>et al.</i> [14]
dimerization constant (H,Na)ClO <sub>4</sub> /octane	log K <sub>D</sub> = 4.47	Ul'yanov <i>et al.</i> [15]
0.1M(H,Na)NO <sub>3</sub> /heptane	log K <sub>D</sub> = 4.50	Komasawa <i>et al.</i> [14]
(H,Na)ClO <sub>4</sub> /Isopar-H	log K <sub>D</sub> = 4.70	Sastre <i>et al.</i> [1]

\*source: manufacturer's information sheet

<sup>†</sup>calculated by the method of Le Bas as reported in Perry<sup>[16]</sup>

<sup>‡</sup>calculated by the Wilke-Chang relationship<sup>[17]</sup>

The extracted metal-D2EHPA complex can have a variable number of additional D2EHPA molecules associated with it. At high metal loadings, the metal:D2EHPA ratio approaches the theoretical limit of 1:2; as this limit is approached the mixture polymerizes, resulting in an increase in viscosity. For zinc/D2EHPA in dodecane, there is a threefold increase in viscosity as the loading increases from 75% to 100%, while for cobalt/D2EHPA in dodecane, there is a fourfold increase in viscosity as the loading increases from ~85% to 100%; Figure 2.4 shows this change in viscosity for Zn-D2EHPA complexes. Evidence suggests that the polymers formed at high metal loadings can be very large, perhaps even approaching molecules with thousands of monomeric elements.<sup>[18]</sup>

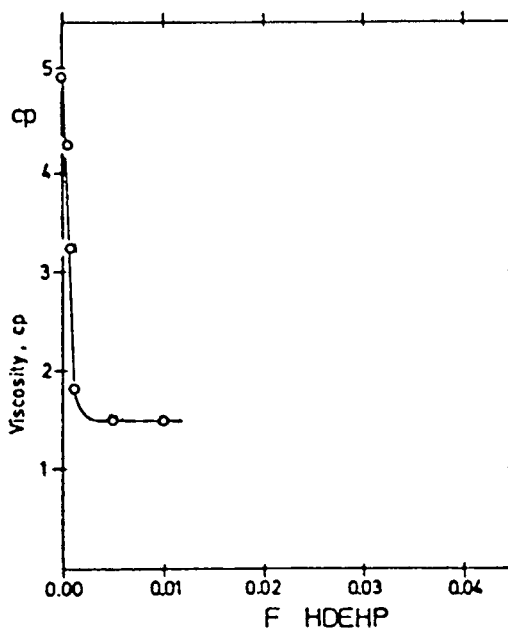


**Figure 2.4** Viscosity of solutions of the Zn(II)-HDEHP complex at 0.01M total Zn(II) in dodecane at 20°C as a function of the excess HDEHP concentration (after Kolarík & Grimm<sup>[18]</sup>)

---

### 2.2.3 Parameter Estimation

The Wilke-Chang<sup>[17]</sup> relationship, shown in equation [2-3], was used to estimate the diffusion coefficients of the various organic species.

$$\frac{D \mu}{T} = \frac{7.4 \times 10^{-12} (x M)^{0.5}}{V_B^{0.6}} \quad [2-3]$$

Dreisinger<sup>[19]</sup> has previously shown that this correlation is acceptable for predicting diffusion coefficients - a predicted value for the diffusion coefficient of HEHEHP (mono 2-ethylhexyl phosphonic acid mono 2-ethylhexyl ester) in heptane was within 2% of the measured value.

The diffusion coefficients calculated using equation [2-3] are shown in Table 2.2. Data<sup>[16,20]</sup> used in the calculations are: absolute viscosity,  $\mu(\text{heptane}) = 0.386 \text{ cP}$ ; solvent association factor,  $x(\text{heptane}) = 1.0$ ; solvent molecular weight,  $M(\text{heptane}) = 100.21$ ; and temperature,  $T = 298 \text{ K}$ . The molar volume of the solute at the normal boiling point,  $V_B$ , was estimated by using the method of Le Bas<sup>[16]</sup>; these values for different organic species are also shown in Table 2.2.

---

**Table 2.2** Diffusion Coefficients predicted by the Wilke-Chang Relationship.

Species	$V_B$ ( $\text{m}^3 \text{ kmol}^{-1}$ )	$D$ (heptane) ( $\text{m}^2 \text{ s}^{-1}$ )
HL	422.9	$1.520 \times 10^{-9}$
(HL) <sub>2</sub>	845.8	$1.003 \times 10^{-9}$
ZnL <sub>2</sub>	858.4	$0.993 \times 10^{-9}$
ZnL <sub>2</sub> ·HL	1281.7	$0.781 \times 10^{-9}$
ZnL <sub>2</sub> ·(HL) <sub>2</sub>	1704.2	$0.659 \times 10^{-9}$

---

### 2.3 Solvent Extraction Kinetics

In pyrometallurgical systems, thermodynamics and mass transfer are the primary considerations when determining the feasibility of a process; systems are generally near equilibrium since chemical reaction kinetics are fast at elevated temperature. However, in hydrometallurgical systems reactions occur at much lower temperatures and chemical reaction kinetics can become very important. It follows that the study and evaluation of the different

reaction mechanisms are important to consider if hydrometallurgical systems are to be applied effectively and economically in industrial practice. Danesi and Chiarizia<sup>[21]</sup> have written an excellent review of solvent extraction kinetics, and it is not the purpose of this section to repeat their conclusions. Instead, there will be a brief introduction to the subject of solvent extraction kinetics, followed by a discussion of a few reaction models which have been proposed by researchers.

The rate controlling step in solvent extraction systems can be mass transfer, chemical reaction, or both. In most solvent extraction contactors, the aqueous and organic phases are well mixed, and therefore any resistance to mass transfer generally occurs in the diffusion layers between the bulk (stirred) phases and the reaction zone. If the extraction of a metal ion by D2EHPA occurs according to the reaction stoichiometry given in Equation 2-1, then a simplified diagram of the region near the reaction zone can be drawn as shown in Figure 2.5. Extractant diffuses through the organic boundary layer to the reaction zone, where it reacts with the metal species which has diffused through the aqueous boundary layer. The product species then diffuse back through the organic and aqueous boundary layers and into the bulk phases.

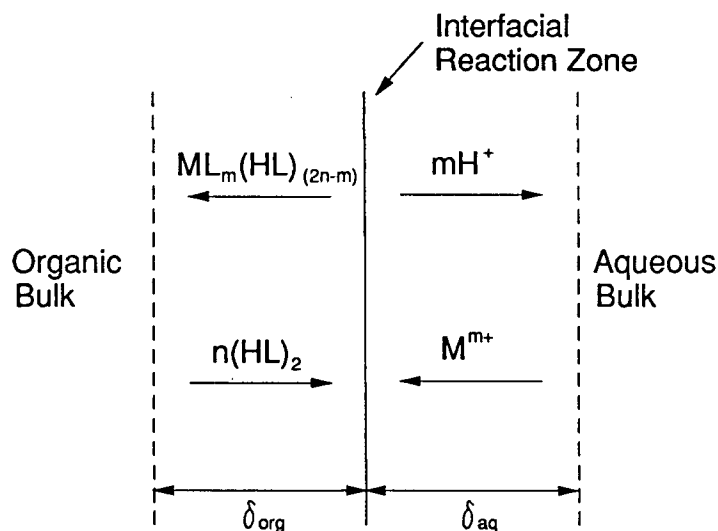


**Figure 2.5** Schematic diagram of the reaction zone and aqueous/organic boundary layers

In some systems, the rate of diffusion of reactants to, and products from, the reaction zone determines the rate of reaction; such a system is said to be operating in the "diffusional regime", or "mass transfer controlled with instantaneous chemical reaction." Such systems tend to be either those that are not well agitated (i.e. the diffusion layer thickness is large) or those in which one or more reactants have small concentrations.

In contrast, systems in which some chemical step is very slow are said to be in the "kinetic regime", where the contribution to slow reaction rates by mass transfer resistances can be ignored. In such systems, either the thickness of the diffusion layer approaches zero, or the diffusion coefficient is large enough relative to the rate constant that there are no significant diffusional gradients between the bulk phases and the reaction zone.<sup>[21]</sup>

Most solvent extraction systems operate neither in the purely diffusional regime nor in the purely kinetic regime; instead, they operate in a mixed regime where both mass transfer and chemical reaction kinetics are significant. Many experimenters have worked on the problem of accurately characterizing the mechanisms and methods by which these reactions occur. In spite of all their work, the field of solvent extraction kinetics is still largely empirical, with a large body of isolated (and sometimes conflicting) data having been gathered on many systems using many types of apparatus. The determination of the rate controlling step for most solvent extraction systems is further complicated since the observed rate controlling step is often influenced by the measurement technique. Finally, some researchers have shown some bias in explaining the mechanisms of extraction; chemists tend to assume that rates are governed by purely kinetic mechanisms, while engineers tend to assume that mass transfer is dominant.

The following discussion on kinetic models will focus on several relevant mechanisms with examples from the literature.

### 2.3.1 Interfacial Mechanisms

If we consider the case where the system is operating in the kinetic regime; that is, there is effectively no mass transfer resistance, then one possibility is an interfacial mechanism. Although there is still a stagnant boundary layer on either side of the interface, there is no concentration gradient of either reactants or products through the boundary layer since the mass transfer rate is much greater than the chemical reaction rate, i.e.  $[ ]_{\text{int}} \approx [ ]_{\text{bulk}}$ . A reactant/product concentration profile can then be drawn as shown in Figure 2.6.

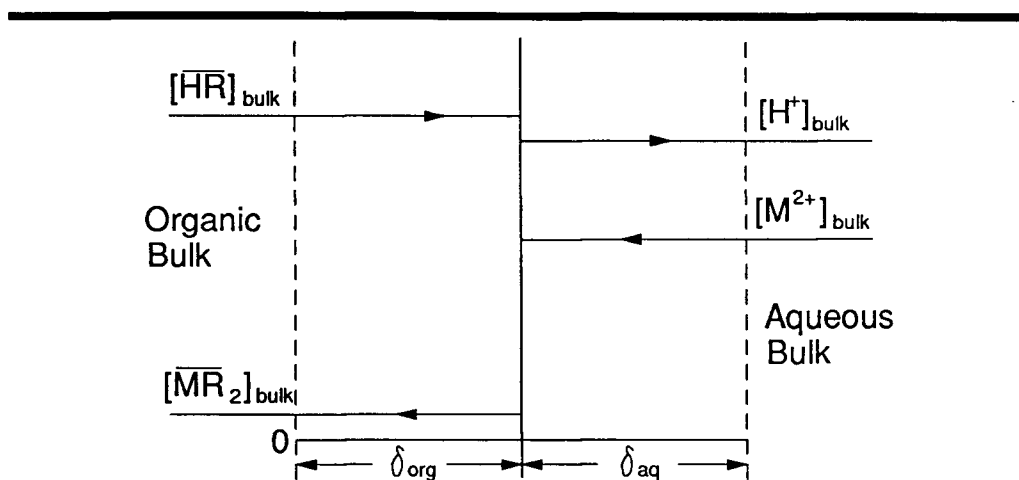
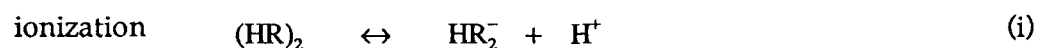


Figure 2.6 Concentration profile for an interfacial reaction mechanism

Ajawin *et al.*<sup>[7,22]</sup> investigated the extraction of zinc by D2EHPA from sulphuric acid solutions. Using a constant interfacial area contactor, the mixing speed was increased until a plateau region was reached where the reaction rate did not change with increasing speed (only to a point - very high mixing rates perturb the interface and change the interfacial area). In this plateau region, they concluded that the reaction rate was controlled by a slow chemical reaction.

It was found that the rate of reaction was proportional to the interfacial contact area and independent of solution volume, thus indicating that extraction occurs at the interface. By varying the aqueous zinc concentration, pH, and extractant concentration, it was shown that the extraction of zinc is first order with respect to zinc and D2EHPA, and inverse first order with respect to pH (hydrogen ion concentration). It was proposed that the reaction occurs in several steps. In the first step, dimeric D2EHPA ionizes and dissociates as follows:



The species  $\text{HR}_2^-$  and  $\text{HR}$  then rapidly adsorb at the interface, and react with zinc ions to form an extractable zinc-D2EHPA compound through the following two reactions:



In the reaction scheme given above, only reaction (iii) agrees with experimental findings, that is, first order with respect to  $Zn^{2+}$  and D2EHPA, and inverse first order with respect to  $H^+$ . They therefore concluded that reaction (iii) is the rate controlling step.

While the analysis that Ajawin *et al.* have made with respect to the rate controlling mechanism may be correct, Hughes and Rod<sup>[23]</sup> have shown that it is possible that the system may be operating in a "pseudokinetic" regime. They demonstrated that the flattening of the rate-rpm curve in the plateau region may be due to the attainment of a minimum value of the diffusion layer thickness rather than the chemical reaction becoming rate controlling. Further, Danesi *et al.*<sup>[24]</sup> have demonstrated that diffusion coupled with a fast chemical reaction at the interface can mimic a multi-step interfacial process. It is therefore possible that the results found in Ajawin's study can be explained by mass transfer processes rather than a multi-step interfacial reaction.

Other authors have postulated interfacial mechanisms to explain the results of various kinetic studies. Roddy *et al.*<sup>[25]</sup> studied the extraction of  $Fe^{3+}$  from acid perchlorate solutions using D2EHPA in n-octane. They concluded that the extractable species  $FeR_3 \cdot 3HR$  is formed by a multi-step reaction which occurs at the interface. They also demonstrated that reaction rates could be increased by introducing species which replace water as a solvating ligand and allow faster ligand exchange.

Komasawa and Otake<sup>[26]</sup> concluded that the extraction of Co, Cu, and Ni from nitrate media with D2EHPA proceeded by a two-step interfacial mechanism. The effects of aliphatic (heptane) and aromatic (benzene, toluene) diluents on the overall extraction rate were studied, and it was found that the extraction rate was much higher when an aliphatic diluent was employed. However, diluent type had little effect on the stripping rate, indicating that the enhancement of extraction was due to a change in the forward reaction rate constant.

Albery *et al.*<sup>[27]</sup> found that the extraction of copper from sulphate media by Acorga P50 (an oxime extractant) in n-heptane was governed by an interfacial reaction. At low reagent concentrations, extraction was first order for both copper and extractant; at higher concentrations the reaction approached a limiting rate which suggests a saturated interface.

Danesi and Vandegrift<sup>[28]</sup> examined the extraction of  $\text{Eu}^{3+}$  and  $\text{Am}^{3+}$  from a chloride media using D2EHPA in n-dodecane. They attempted to fit their data to two models: a pure interfacial model assuming no diffusional resistances and a mass transfer model coupled to a fast chemical reaction. Both models gave a qualitative fit, but the kinetic model yielded the best quantitative fit.

The combined body of research suggests that interfacial mechanisms are generally dominant in the extraction of metal ions using alkylphosphoric acids. However, in those cases when reaction kinetics have been evaluated using constant interface stirred cells operating at low mixing rates, some doubt remains as to whether the results have been correctly interpreted.

### 2.3.2 Mass Transfer Control

In the case where bulk phase mixing is complete but the mass transfer resistance is much greater than the kinetic resistance, then the system is mass transfer controlled. Since the chemical reaction is fast, it occurs instantaneously at or immediately adjacent to the interface. Diffusion is therefore the only important process, and the rate of reaction is determined solely by the rate of transport of reactants and products. Under these circumstances, the interfacial concentrations must be computed from the flux equations and chemical equilibria at the interface. A typical profile showing concentration gradients near the interface for a mass transfer limited reaction is shown in Figure 2.7.

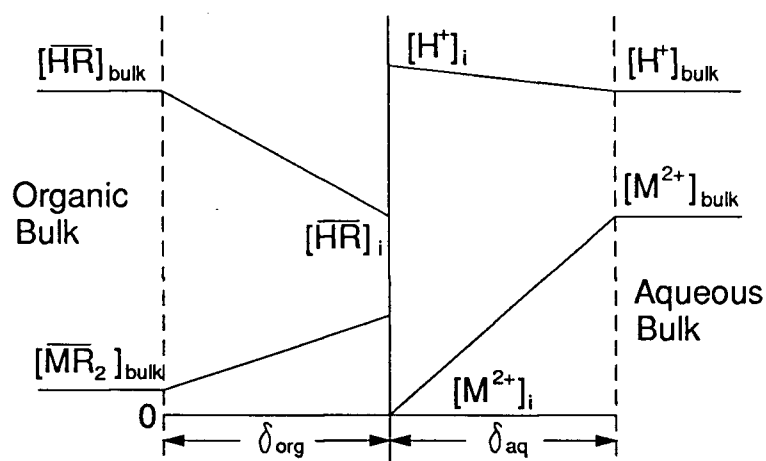
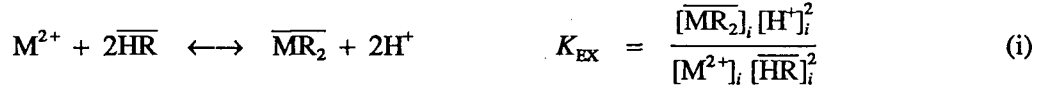


**Figure 2.7** Interfacial Profile : Mass transfer limited reaction

The extraction equilibrium for a divalent metal reacting with an organic acid can be written as:



If we assume steady-state conditions and no chemical reactions in the boundary layer, then the fluxes to and from the interface must obey equation (i), and therefore,

$$J_{M^{2+}} = -\frac{1}{2}J_{\overline{HR}} = J_{\overline{MR_2}} = -\frac{1}{2}J_{H^+} \quad (ii)$$

Expressions can be written for the fluxes to and from the interface for each species by Fick's first law, i.e.

$$J_{M^{2+}} = \frac{D_{M^{2+},aq}}{\delta_{M^{2+},aq}} \{ [M^{2+}]_{bulk} - [M^{2+}]_i \} \quad (iii)$$

$$J_{\overline{HR}} = \frac{D_{\overline{HR},org}}{\delta_{\overline{HR},org}} \{ [\overline{HR}]_i - [\overline{HR}]_{bulk} \} \quad (iv)$$

$$J_{\overline{MR_2}} = \frac{D_{\overline{MR_2},org}}{\delta_{\overline{MR_2},org}} \{ [\overline{MR_2}]_i - [\overline{MR_2}]_{bulk} \} \quad (v)$$

$$J_{H^+} = \frac{D_{H^+,aq}}{\delta_{H^+,aq}} \{ [H^+]_{bulk} - [H^+]_i \} \quad (vi)$$

If the diffusion coefficients, bulk concentrations, and boundary layer thicknesses are known, and if a value for  $K_{EX}$  is available, then the mass transfer limited flux of species  $M^{2+}$  can be found by substituting equations (ii) - (vi) into equation (i) and solving for  $J_{M^{2+}}$ :

$$K_{EX} = \frac{\left( [\overline{MR_2}]_{bulk} + J_{M^{2+}} \delta_{\overline{MR_2},org} / D_{\overline{MR_2},org} \right) \left( [H^+]_{bulk} + 2J_{M^{2+}} \delta_{H^+,aq} / D_{H^+,aq} \right)^2}{\left( [M^{2+}]_{bulk} - J_{M^{2+}} \delta_{M^{2+},aq} / D_{M^{2+},aq} \right) \left( [\overline{HR}]_{bulk} - 2J_{M^{2+}} \delta_{\overline{HR},org} / D_{\overline{HR},org} \right)^2} \quad (vii)$$

Fleming *et al.*<sup>[29]</sup> found that the extraction of copper with LIX63 and LIX64N in chloroform from aqueous nitrate media was controlled by mass transfer in the organic phase. They determined that the extraction reaction occurred at the interface, and that while stirring in the aqueous phase had no effect, changes in the stirring rate of the organic phase caused a proportional shift in the rate of extraction.

Miyake *et al.*<sup>[30]</sup> studied the extraction of copper(II) and cobalt(II) by 2-ethylhexyl phosphonic acid mono-2-ethylhexyl ester. They found that the rate of extraction is limited by the transport of the metal-extractant complex from the interface to the organic bulk.

### 2.3.3 Mixed Regime (Mass Transfer with Chemical Reaction)

The above two rate models can be combined to create the mass transfer with chemical reaction (MTWCR) model. In this model, it is assumed that the system operates in a mixed regime, with neither kinetic nor diffusional mechanisms dominant. The reactants diffuse from the well mixed bulk through the stagnant boundary layer to the reaction zone, where a slow chemical reaction occurs. Since the chemical reaction is slow, the assumption that the reaction occurs solely at the interface is no longer valid, and the reaction may occur in a zone which extends from the interface into the aqueous phase (and perhaps even into the aqueous bulk).

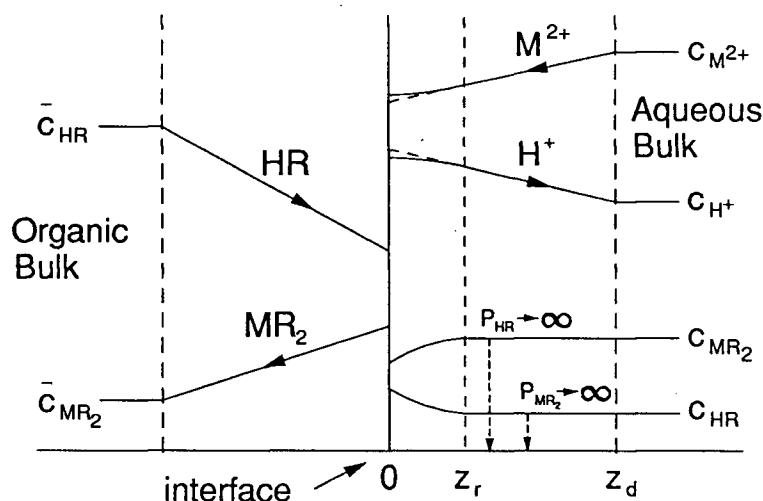


Figure 2.8 Schematic diagram of the reaction zone and aqueous/organic boundary layers - Mass transfer with chemical reaction model (after Hughes and Rod<sup>[31]</sup>)

Hughes and Rod<sup>[31]</sup> have developed a general model incorporating interfacial film diffusion and a chemical reaction in the aqueous phase which describes the extraction of metals in a mixed regime. Distribution of the extractant and the extracted metal complex between the organic and the aqueous phase is incorporated into the model through the partition coefficient ( $P_{HR}$  and  $P_{MR_2}$  respectively). For finite values of the partition coefficient and for mixed reaction conditions, extraction occurs in a reaction zone of thickness  $z_r$ .

For the purposes of their model, Hughes and Rod suggested that the reaction occurs in five steps:



with the overall reaction expressed by the equation:



Either step 3 or step 4 may be rate controlling.

If step 3 is assumed to be rate controlling, then the flux of extractant can be given by the equation:

$$J = \sqrt{\frac{\Theta_1 c_{\text{M},j}}{c_{\text{H},j}} \left[ 1 - \frac{c_{\text{H},j}^2 \overline{c}_{\text{MR}_2,j}}{K_{\text{EX}} \overline{c}_{\text{HR},j}^2 c_{\text{M},j}} \right] (\overline{c}_{\text{HR},j}^2 - P_{\text{HR}}^2 c_{\text{HR}}^2)} \quad (\text{i})$$

where

$$\Theta_1 = \frac{k_R D_{\text{HR}}}{P_{\text{HR}}^2 K_{\text{HR}}} \quad (\text{ii})$$

and

$$\overline{c}_{\text{HR},j} = \overline{c}_{\text{HR}} - \frac{J}{k_{\text{HR},\sigma g}} \quad (\text{iii})$$

$$\overline{c}_{\text{MR}_2,i} = \overline{c}_{\text{MR}_2} + \frac{J}{2k_{\text{MR}_2,\sigma g}} \quad (\text{iv})$$

$$c_{\text{HR}} = \frac{1}{P_{\text{HR}}} \left[ \frac{-P_{\text{MR}_2} D_{\text{HR}} c_{\text{H}}^2}{4P_{\text{HR}} D_{\text{MR}_2} K_{\text{EX}} c_{\text{M}}} + \quad (\text{v}) \right.$$

$$\left. \sqrt{\left[ \frac{P_{\text{MR}_2} D_{\text{HR}} c_{\text{H}}^2}{4P_{\text{HR}} D_{\text{MR}_2} K_{\text{EX}} c_{\text{M}}} \right]^2 + \frac{c_{\text{H}}}{K_{\text{EX}} c_{\text{M}}} \left( \overline{c}_{\text{MR}_2} + \frac{D_{\text{HR}} P_{\text{MR}_2} \overline{c}_{\text{HR},i}}{2D_{\text{MR}_2} P_{\text{HR}}} \right)} \right]$$

$$c_{MR_2} = K_{EX} \left( \frac{c_{HR} c_M}{c_H^2} \right) \left( \frac{P_{HR}^2}{P_{MR_2}} \right) \quad (\text{vi})$$

$$c_{M,i} = c_M - \frac{J}{2k_{M,aq}} + \frac{D_{HR}}{2D_H P_{HR}} (\bar{c}_{HR,i} - c_{HR} P_{HR}) \quad (\text{vii})$$

$$c_{H,i} = c_H + \frac{J}{k_{H,aq}} - \left( \frac{D_{HR}}{D_H P_{HR}} \right) (\bar{c}_{HR,i} - c_{HR} P_{HR}) \quad (\text{viii})$$

Special cases of the model occur under the following circumstances:

particular case	$k_R$	$P_{HR}$	$\Theta_1 = \frac{k_R D_{HR}}{P_{HR}^2 K_{HR}}$
reaction in the film	finite	finite	finite
equilibrium reaction in the film	$\infty$	finite	$\infty$
reaction at the interface	$\infty$	$\infty$	finite
instantaneous reaction at the interface	$\infty$	$\infty$	$\infty$

Hughes and Rod extended the model and used it to analyze results reported in the literature for the LIX64N/CuSO<sub>4</sub>/H<sub>2</sub>SO<sub>4</sub> system using a rising drop and a constant interface (gauze cell) contactor. The extraction of Cu from slightly acidic media with a rotating diffusion cell was also analyzed. In each case the model was able to adequately fit the results, and the addition of the first ligand (step 3) was found to be rate controlling.

Dreisinger and Cooper<sup>[32,33]</sup> used a modified version of the MTWCR model to model the extraction of Co and Ni from sulphate solutions by HEHEHP (mono 2-ethylhexyl phosphonic acid mono 2-ethylhexyl ester) and Co from perchlorate solutions by D2EHPA. The modified MTWCR model was able to fit the experimental results. However, Ni extraction from perchlorate solutions by D2EHPA was so slow that a significant portion of the extractant partitioned into the aqueous phase as either ionized extractant anion (L<sup>-</sup>) or as a NiH<sub>x</sub>L<sup>(2+x-y)+</sup> complex, and the model was unable to accommodate these conditions. The extraction of zinc from perchlorate solutions by D2EHPA was so fast that the reaction was completely mass transfer controlled; thus, the model could not be applied.

### 2.3.4 Other considerations

A mixed or kinetic regime may exist if the rate of chemical reaction is slow. Different metals have different ligand exchange rates and thus reaction rates in systems with identical extractant, diluent, and aqueous media but with different metals can vary substantially. For example, if a comparison is made between the water exchange rate constants<sup>(1)</sup> for zinc, cobalt, and nickel,

$$k_i(\text{Zn}^{2+}) = 2.5 \times 10^7 \text{ s}^{-1}$$

$$k_i(\text{Co}^{2+}) = 2.6 \times 10^5 \text{ s}^{-1}$$

$$k_i(\text{Ni}^{2+}) = 1.3 \times 10^4 \text{ s}^{-1}$$

it can be seen that there is a difference of over three orders of magnitude.<sup>[34]</sup> Since there is a general relationship between the rate of complex formation from aqueous ions and the water exchange rate, a qualitative comparison of metal chemical reaction rates may be made.<sup>[34]</sup> Thus, a system extracting zinc might be mass transfer controlled, while under the same conditions nickel might be extracted by a MTWCR mechanism.

The solubility of extractant in aqueous solutions affects not only solvent losses to the raffinate, but can also determine the location of the chemical reaction. Since water is a polar solvent, molecules which have a polar component will tend to be more soluble. Increasing the extractant carbon chain length and chain branching tends to decrease solubility. Increasing salt content in the aqueous phase has the effect of decreasing reagent solubility, while increasing temperature and pH increases solubility. High solubility can result in a significant extractant concentration in the aqueous phase, and thus metal extraction may occur in the aqueous bulk.<sup>[3]</sup>

The effect of pH on the aqueous solubility of acidic extractants must be considered when attempting to determine the reaction location. Since acidic extractants dissociate in water according to the equilibrium:



---

1 Water exchange rates are a measure of the speed at which bulk water molecules replace water molecules in the metal ion coordination shell.

decreasing the pH can substantially decrease the aqueous phase solubility of the extractant and therefore move the location of the chemical reaction from the aqueous bulk (or aqueous film) to the interface.

### **2.3.5 Summary**

In an alkylphosphoric acid extraction system, all three regimes can be found under different conditions.

If the aqueous phase metal concentration is high and the region near the interface is well mixed (i.e. the boundary layers are thin), then it is likely that the system is operating in the kinetic regime and an interfacial mechanism will be dominant.

If the same system is operated with low metal concentrations or poor mixing near the interface (but with adequate bulk phase mixing), then the system may operate in the diffusional regime with a mass transfer mechanism dominant. Under these conditions, although the chemical reaction rate may be finite, the rate of metal diffusion is much slower and therefore dominant.

Extraction may occur in the mixed regime if the mass transfer and chemical reaction resistances are of the same order of magnitude. This particular situation is most likely to occur when mixing is poor (thick boundary layer) and chemical reactions are slow.

## **2.4 Kinetic Contactors**

The earliest research on solvent extraction kinetics grew out of analytical chemistry methods for equilibrium studies, and were little more than shakeout tests, informing the experimenter of the time it took for a particular system to reach equilibrium. Since these early experiments, many researchers have developed different types of apparatus for the study of solvent extraction reaction kinetics.

### **2.4.1 Lewis Cell (constant interface area cells)**

The Lewis cell is a constant area kinetic contactor which has proved to be very popular for investigating the kinetic mechanisms of solvent extraction reactions.<sup>[2,35]</sup> The contact area between the two immiscible phases is defined by the geometry of the reaction vessel, and each phase is separately stirred by an impeller. Various researchers have improved upon the basic design of the Lewis cell, generally either by introducing some sort of phase

separating media in the interface area, by adding baffles which modify phase mixing, or by attempting to improve the stirring in either (or both) phase.<sup>[2,21]</sup> For the purposes of this discussion, the different Lewis cell variants including the Nitsch cell and the ARMOLLEX contactor will be grouped under a common heading. Problems with Lewis-type cells include the accumulation of surfactants at the organic/aqueous interface, the formation of an agitated, unstable interface, and scatter in collected data of  $\pm 30\%$ .<sup>[36]</sup>

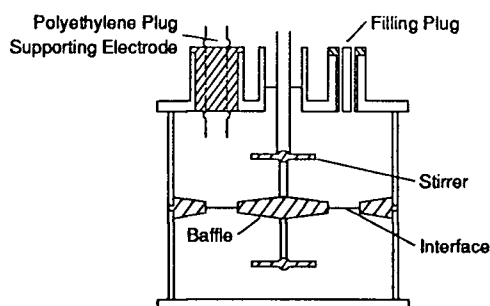


**Figure 2.9** The original Lewis Cell (after Hanna and Noble<sup>[37]</sup>)

The major difficulty in the use of the Lewis cell is the elimination (or accurate characterization) of diffusion barriers. At low mixing speeds, the diffusion layer thickness is large, and mixing of the bulk solution is incomplete. At high mixing speeds, the aqueous/organic interface is disturbed and eddies form; this type of interface is extremely difficult to characterize, and thus results obtained under these conditions are invalid. A compromise must thus be obtained between poor mixing at low speeds and interface disruption at high speeds. Experimenters have attempted to find mixing speeds somewhere between these two extremes where satisfactory mixing is obtained and yet the interface is not disrupted.<sup>[38]</sup> Researchers working in this range claim to have removed all mass transfer limitations from the system, i.e. the rate of reaction is solely determined by chemical reaction kinetics. However, as Hughes and Rod<sup>[23]</sup> have demonstrated, it is more likely that they are operating in a pseudokinetic regime, where the diffusion layer thickness is small, but is still limited to a finite value which may have an effect on the reaction rate. This effect depends on the relative magnitudes of the diffusional resistances and kinetic resistances.

## 2.4.2 AKUFVE

The AKUFVE apparatus is a highly stirred tank system which operates near equilibrium conditions.<sup>[39]</sup> The aqueous/organic media are continuous, with one phase completely dispersed in the other; this dispersion makes it impossible to define the surface area. A high stirring rate is used so that mixing is turbulent and complete, removing most mass transfer resistances. The aqueous and organic phases are continuously sampled to determine concentration changes over time.

The complete mixing found in the AKUFVE contactor makes it unsuitable for studying kinetic systems where the chemical rate constants are large and therefore reactions are primarily mass transfer limited. However, in systems which have slow reaction kinetics, the AKUFVE apparatus can be used to study the rate of chemical reaction. Since the interfacial contact area in the AKUFVE apparatus is unknown<sup>[36]</sup>, the interfacial flux cannot be measured. Thus, reaction rates can only be qualitatively compared between metal systems; a quantitative evaluation of absolute reaction rates is not possible. However, using this technique it is possible to gain valuable information about the reaction orders of different extractant systems.<sup>[21]</sup>

## 2.4.3 Single Drop Cell (Moving Drop Cell)

In the single drop cell, drops of one phase are formed on the tip of a small capillary and are then allowed to fall (or rise, depending on relative densities) through the other continuous phase.<sup>[38]</sup> While the drop is travelling to the collector, metal extraction takes place through the drop surface. If the drops are assumed to be spherical, the contact area can be computed. After many drops have been reacted, the drop phase is collected and analyzed for metal content. Thus, the metal extraction rate and interfacial flux can be calculated.

There are several difficulties with the single drop method. First, the drop may not be spherical. Also, internal drop circulation may be poor; that is, the bulk solution in the drop interior may not be well mixed.<sup>[21,38]</sup> The drop may oscillate as it moves, and there may be a stagnant region in the drop's wake.<sup>[40]</sup> Finally, in fast systems some extraction may occur during drop formation and when the drop is in the coalesced stagnant pool at the end of the cell.<sup>[40]</sup>

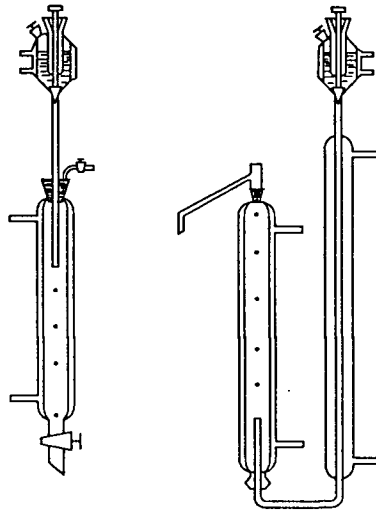


**Figure 2.10** The moving drop cell (after Danesi and Chiarizia<sup>[21]</sup>)  
Left side: falling drop; Right side: rising drop

---

#### 2.4.4 Growing Drop Cell

In a typical mixer-settler type contactor, extraction generally occurs between drops of one phase dispersed in a continuous second phase. Single-phase drops are sheared away from large drop aggregates (drop formation), they travel through the second phase, and then coalesce back into drop aggregates. Since researchers believe that extraction occurring in the drop formation phase is a significant part of the total extraction occurring over the lifetime of the drop, the growing drop method was designed to study extraction occurring during drop formation.<sup>[41]</sup>

As in the single drop cell, drops grow at the end of a small needle. After they detach, they rise a short distance and then are sucked into a collection system. When a sufficient number of drops have been created, the collected drops are analyzed for metal content. Drop formation times are typically on the order of 1 to 20 seconds, and about 100 to 200 drops are required for each data point. While the hydrodynamics around and inside the growing drop are complex<sup>[36]</sup>, researchers claim to have been able to at least partially model the behaviour of the growing drop.<sup>[41]</sup>

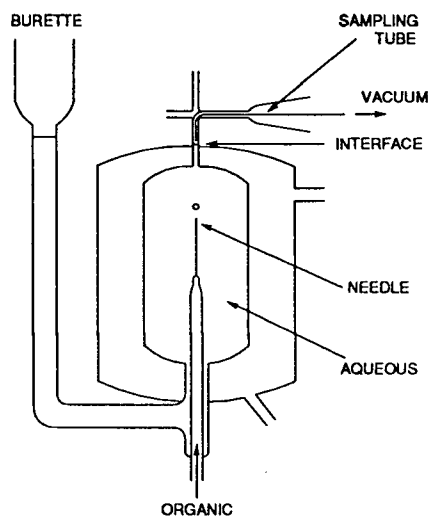


**Figure 2.11** The growing drop cell (after Hughes and Zhu<sup>[41]</sup>)

#### 2.4.5 Laminar Liquid Jet (Liquid Jet Recycle Reactor)

In the liquid jet recycle reactor, developed by Freeman and Tavlarides<sup>[42]</sup>, one phase flows as a jet through a continuous second phase. New surface is continuously created by the jet action, and the surface area is fairly well-defined. The circulating phases can be continuously monitored to determine concentration profiles, and the hydrodynamics of the jet are understood.<sup>[2,36]</sup> However, the hydrodynamic conditions cannot be widely varied if jet stability is to be maintained.

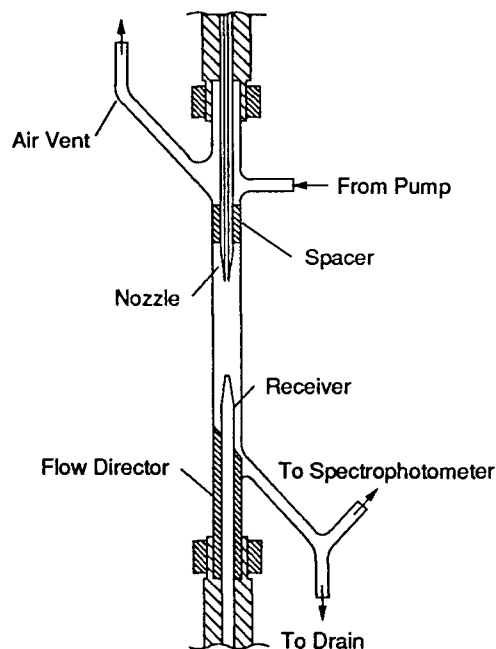


Figure 2.12 The inner portion of the Liquid-Jet Recycle Reactor (after Hanna and Noble<sup>[37]</sup>)

## 2.5 Rotating Diffusion Cell

In order to evaluate solvent extraction kinetics in a practical way, the interfacial area must be known and the contribution of diffusion must either be understood and taken account of or be eliminated. The rotating diffusion cell fulfills both of these criteria: the interfacial area can be measured and the thickness of the diffusion layers can be determined.

### 2.5.1 Apparatus

The rotating diffusion cell (RDC) technique was first developed by Albery *et al.*<sup>[43]</sup> as a method for studying interfacial reaction kinetics. The RDC, which is based on the rotating disc electrode, consists of a permeable filter mounted on a rotating hollow cylinder (see Figure 2.13). The hydrodynamics on both sides of the filter are well-defined, with the action of the rotating disk producing a uniform equivalent diffusion boundary layer across the surface of the disk. Furthermore, the thickness of the diffusion layers can be calculated if the rotational speed, kinematic viscosity, and diffusivity are known.

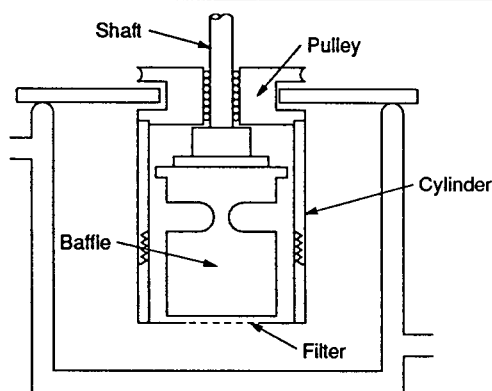


**Figure 2.13** The Rotating Diffusion Cell (after Albery *et al.*<sup>[43]</sup>)

When adapted to solvent extraction kinetic study, one compartment of the RDC is filled with a metal-bearing aqueous solution, and the other compartment is filled with the extractant-containing organic solution. A thin (~0.1mm) microporous filter of known area separates the two compartments. The speed of the rotating RDC cylinder is measured and a stationary baffle ensures that correct hydrodynamics are maintained in the inner compartment.

### 2.5.2 Theory

The rotating motion of the filter produces flow patterns which are well-defined according to rotating disk hydrodynamics. A cross-sectional view of the flow is shown in Figure 2.14a, and a view of the flow below the filter is shown in Figure 2.14b. Fluid in the inner cell is pulled down through the baffle to the surface of the filter, where it is radially thrown out in a circular motion. New fluid is pulled in through holes in the baffle - the gap between the baffle and the cylinder is sufficient to ensure no disruption in flow. On the underside of the filter, fluid circulates in a similar fashion.

Levich<sup>[45]</sup> solved the Navier-Stokes equations to give the velocity profiles for flow adjacent to a rotating disk. The convective-diffusion equation may then be solved if it is assumed that concentration only depends on the distance from the disk (i.e. radial and tangential symmetry) and there are no chemical reactions in the diffusion layer. Once the mass flux has been determined, an equation may be developed which describes the thickness of the equivalent diffusion layer, i.e.

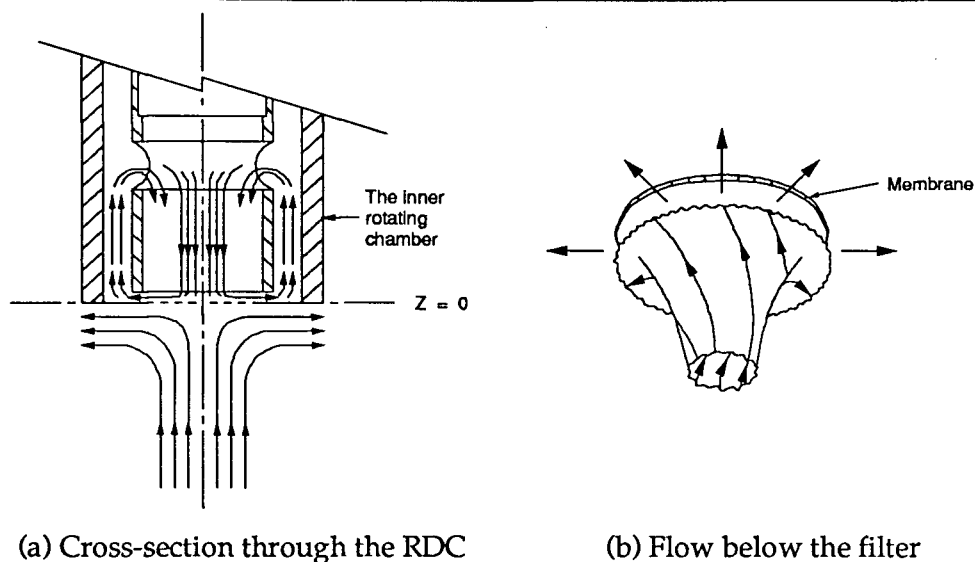


**Figure 2.14** Fluid flow patterns near the Rotating Diffusion Cell  
(after Patel<sup>[44]</sup>)

$$z_D = 0.643 \omega^{-1/2} \nu^{1/6} D^{1/3} \quad [2-4]$$

where  $z_D$  is the equivalent diffusion layer thickness in m,  $\omega$  is the disk's angular velocity in radians/second,  $\nu$  is the kinematic viscosity in  $\text{m}^2/\text{s}$ , and  $D$  is the diffusion coefficient in  $\text{m}^2/\text{s}$ .

If the interfacial flux is measured and plotted with respect to  $\omega^{-1/2}$ , the intercept is equal to the flux at infinite angular velocity. According to the Levich equation, at infinite velocity the thickness of the diffusion layer is equal to zero. At this point, the measured flux contains only the mass transfer resistances of diffusion through the filter and interfacial chemical reactions. The mass transfer resistance through the membrane may be calculated and subtracted, leaving only the interfacial chemical reaction.

### 2.5.3 Previous Work using the RDC

The RDC has been used to study interfacial transfer mechanisms in pharmaceutical systems, since by impregnating the filter with certain organic compounds it can effectively simulate drug absorption through biological membranes, especially skin.<sup>[46,47]</sup> More recently, the RDC has been applied to hydrometallurgical systems by several researchers in an attempt to study solvent extraction kinetics.

Albery and Fisk<sup>[48]</sup> examined copper extraction and stripping with Acorga P50, and determined rate constants for both the forward and reverse reactions. Albery *et al.*<sup>[27]</sup> placed a ring electrode on the RDC membrane surface in order to follow the rate of copper stripping. Using this method, the copper flux was determined by measuring the electrode current.

Dreisinger and Cooper<sup>[32]</sup> studied the extraction of cobalt and nickel with HEHEHP and found that a simplified MTWCR model adequately fit their results. The fitted parameters in the model indicated that both systems were operating in the mixed regime. Dreisinger and Cooper<sup>[33]</sup> later expanded on their earlier work by examining zinc, cobalt and nickel extraction from perchlorate solutions using D2EHPA in heptane. The effect of metal concentration, extractant concentration, pH and temperature on the extraction rate were examined in an attempt to determine the rate controlling steps. As indicated earlier, they found that the MTWCR model was able to fit the data for cobalt extraction, but nickel extraction was too slow to be adequately modelled. The extraction of zinc was fast enough that mass transfer became the rate limiting step; at low zinc concentrations aqueous mass transfer was rate limiting, while at higher zinc concentrations the rate limiting step became extractant transfer in the organic phase.

Most recently, Dreisinger *et al.*<sup>[49]</sup> examined the extraction of cobalt and nickel with D2EHPA. A baseline study involving the extraction of cobalt from sulphate media was carried out, and then the coextraction of cobalt and nickel from perchlorate solution was examined. In addition, the effect of buffering interfacial pH with a weak acid was examined with cobalt extraction from perchlorate solution.

Patel<sup>[44]</sup> examined the extraction of zinc, cobalt, copper, and nickel from sulphate solutions by either D2EHPA or D2EHDTPA in n-heptane using the RDC. He first conducted a series of experiments for all four metals, in which he varied the concentration of D2EHPA from 0.015M to 0.4M; the results of this experiment are shown in Figure 2.15. Under identical conditions, the reaction rate increases in the order Ni < Co < Cu < Zn. He then examined the effect of varying the metal concentration, pH, and D2EHPA concentration over a wider range for cobalt. Finally, he fitted all of his experimental results to a modified MTWCR model; estimated rate constants calculated by the model are given in Table 2.3.

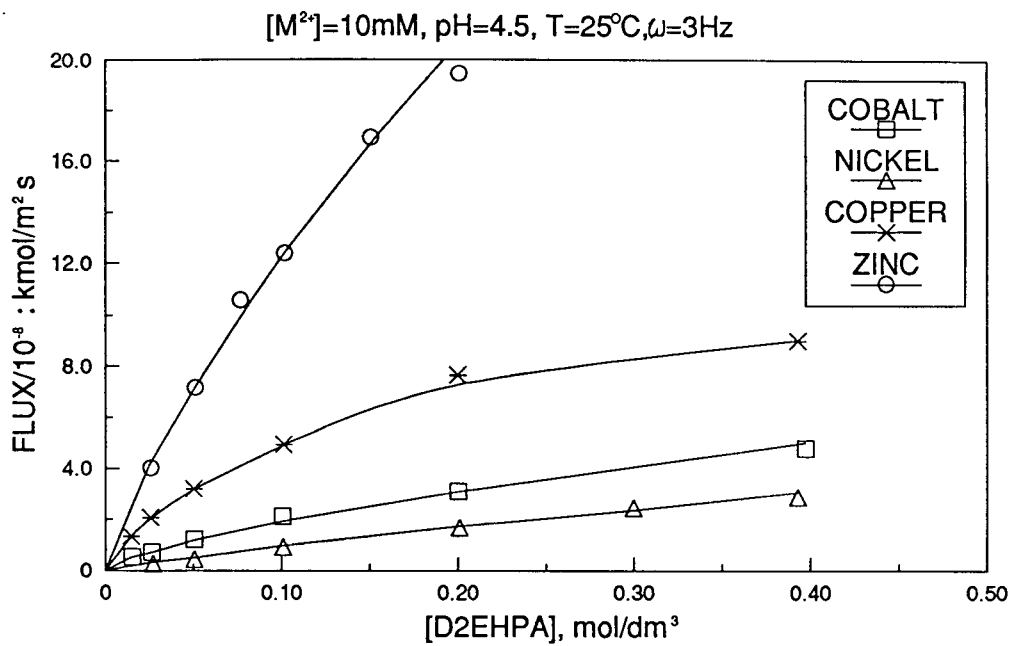


Figure 2.15 The extraction of Co, Ni, Cu and Zn by D2EHPA (after Patel<sup>[44]</sup>)

Table 2.3 Results of Patel's study of Ni, Co, Cu, and Zn extraction [44]

Metal	Measured Flux ( kmol m <sup>-2</sup> s <sup>-1</sup> )	Second Order Rate Constant $k_R$ ( m <sup>3</sup> kmol <sup>-1</sup> s <sup>-1</sup> )	$\delta_r$ ( $\mu$ m)
Nickel	$9.674 \times 10^{-9}$	$1.325 \times 10^7$	8.02
Cobalt	$2.110 \times 10^{-8}$	$9.460 \times 10^7$	3.56
Copper	$4.936 \times 10^{-8}$	$1.213 \times 10^8$	1.39
Zinc	$1.247 \times 10^{-7}$	$2.436 \times 10^9$	0.42

Using parameters calculated by the MTWCR model, Patel estimated the thickness of the reaction zone near the interface. Values of  $\delta_r$  for each metal are shown in Table 2.3; the thickness of the RDC aqueous diffusion layer ( $\delta_{aq}$ ) was estimated to be 32.59  $\mu$ m. For zinc,  $\delta_r \ll \delta_{aq}$ ; thus, as an approximation it can be assumed that the reaction occurs at the interface.

## 2.5.4 Summary

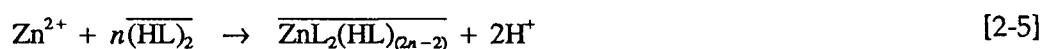
A number of different techniques for the study of solvent extraction kinetics have been examined. There is some uncertainty in the nature of diffusion barriers in the Lewis cell, and the interfacial contact area in the highly stirred AKUFVE cell is unknown. The single drop technique is useful for studying the behaviour of individual drops, but there is some uncertainty surrounding the hydrodynamics of the drop and mixing in its interior. The growing drop also has complex hydrodynamics, although claims have been made that at least partial solutions have been obtained. Finally, the laminar liquid jet can only be operated under certain conditions if jet stability is to be maintained, limiting its usefulness for studying a wide range of systems.

The rotating diffusion cell appears to be useful for the study of solvent extraction kinetics due to the well-defined interfacial area and its ability to eliminate diffusional contributions. Therefore, it was selected as the contactor of choice for this study.

## 2.6 Zn-D2EHPA equilibrium and kinetics

### 2.6.1 Zn-D2EHPA equilibrium

The stoichiometry of zinc extraction by D2EHPA can be expressed by an equation of the form:



where the value of  $n$  varies depending on the nature of the organic solvent and the aqueous media. For example, Huang and Juang<sup>[50]</sup> have shown that the extracted species (in kerosene at low metal loadings) has one associated D2EHPA monomer (i.e.  $n=1.5$ ). Li *et al.*<sup>[51]</sup> have demonstrated that as the organic phase becomes more fully loaded, viscosity increases, suggesting the formation of metal-extractant polymers.

The equilibria of the above reaction have been examined by different researchers<sup>[7,8,22,50-58]</sup> under various experimental conditions. Their results are summarized in Table 2.4. In general, the composition of the extracted species was found to be  $\text{ZnR}_2\cdot\text{HR}$  (i.e.  $n=1.5$ ) for aliphatic diluents, and  $\text{ZnR}_2\cdot(\text{HR})_2$  ( $n=2$ ) for aromatic diluents. Exceptions are the studies by Grimm and Kolarík<sup>[55]</sup> in  $\text{NO}_3/\text{n-dodecane}$ , Sato *et al.*<sup>[52]</sup> in  $\text{Cl}/\text{kerosene}$ , and

**Table 2.4** Survey of Equilibrium Studies using Zinc and D2EHPA

aqueous phase	diluent	composition of extracted species	$K_{ex}$	source
(Na,H)SO <sub>4</sub>	Shellsol T	ZnR <sub>2</sub> ·(HR) <sub>2</sub>	N/A	Rice and Smith [8]
(Na,H)SO <sub>4</sub>	n-heptane	ZnR <sub>2</sub> ·HR	7.35 x 10 <sup>-3</sup>	Ajawin <i>et al.</i> [22]
(Na,H)SO <sub>4</sub>	n-heptane	ZnR <sub>2</sub> ·HR	2.6 x 10 <sup>-3</sup>	Ajawin <i>et al.</i> [84]
(Na,H)SO <sub>4</sub>	kerosene	ZnR <sub>2</sub> ·HR	9.5 x 10 <sup>-3</sup>	Huang and Juang [50]
(Na,H)Cl	kerosene	ZnR <sub>2</sub> ·(HR) <sub>2</sub>	N/A	Sato <i>et al.</i> [52]
(Na,H)NO <sub>3</sub>	n-hexane	ZnR <sub>2</sub> ·HR	8.0 x 10 <sup>-2</sup>	Smelov <i>et al.</i> [53]
(Na,H)NO <sub>3</sub>	n-heptane	ZnR <sub>2</sub> ·HR	6.3 x 10 <sup>-2</sup>	Teramoto <i>et al.</i> [54]
(Na,H)NO <sub>3</sub>	n-octane	ZnR <sub>2</sub> ·HR	8.5 x 10 <sup>-2</sup>	Smelov <i>et al.</i> [53]
(Na,H)NO <sub>3</sub>	n-decane	ZnR <sub>2</sub> ·HR	9.0 x 10 <sup>-2</sup>	Smelov <i>et al.</i> [53]
(Na,H)NO <sub>3</sub>	n-dodecane	ZnR <sub>2</sub> ·HR & ZnR <sub>2</sub> ·(HR) <sub>2</sub>	N/A	Grimm and Kolarík [55]
(Na,H)NO <sub>3</sub>	benzene	ZnR <sub>2</sub> ·(HR) <sub>2</sub>	5.0 x 10 <sup>-2</sup>	Smelov <i>et al.</i> [56]
(Na,H)ClO <sub>4</sub>	Isopar-H <sup>†</sup>	ZnR <sub>2</sub> ·HR & ZnR <sub>2</sub> ·(HR) <sub>2</sub>	4.9 x 10 <sup>-2</sup> 7.6 x 10 <sup>-2</sup>	Sastre and Muhammed [57]
(Na,H)ClO <sub>4</sub>	Escaid 100 <sup>‡</sup>	ZnR <sub>2</sub> ·HR	10.1 x 10 <sup>-1</sup>	Li <i>et al.</i> [51]

<sup>†</sup>Isopar-H is odourless aliphatic kerosene (ESSO).

<sup>‡</sup>Escaid 100 is an aliphatic diluent which contains 19wt% aromatics (ESSO).

Sastre and Muhammed<sup>[57]</sup> in ClO<sub>4</sub>/Isopar-H. Sato *et al.* found that the dominant species was ZnR<sub>2</sub>·(HR)<sub>2</sub>, while Grimm and Kolarík and Sastre and Muhammed concluded that the extracted species was a mixture of ZnR<sub>2</sub>·HR and ZnR<sub>2</sub>·(HR)<sub>2</sub>.

Grimm and Kolarík<sup>[55]</sup> found that the log  $D$  vs. log [(HL)<sub>2</sub>] plot curved as the concentration of extractant increased. Li *et al.*<sup>[51]</sup> suggested that this was due to the co-extraction of sodium (present to maintain the aqueous phase at constant ionic strength). If this is indeed the case, then a higher value of  $n$  would be measured, erroneously implying that the extracted species was mixed. Another possibility is non-ideal behaviour of D2EHPA at high extractant concentrations (c.f. Section 2.2.2).

Trends may be observed with respect to the effects of changes in diluent and aqueous phase on the value of the extraction equilibrium constant,  $K_{ex}$ . From Table 2.4,  $K_{ex}$  decreases with increasing tendency for complex formation in the aqueous phase (complexing ability is in the order  $\text{ClO}_4 < \text{NO}_3 < \text{Cl} < \text{SO}_4$ ). Thus, the largest values for  $K_{ex}$  are found with species which have little or no aqueous complexing ability (nitrate and perchlorate). Also, at moderate to high ionic strengths, the ionic environment can have a significant effect on the activities of aqueous species, changing  $K_{ex}$ . The data in Table 2.4 also suggest that aromatic diluents tend to lower  $K_{ex}$ .

### 2.6.2 Zn-D2EHPA Kinetics

As implied earlier, the kinetics of zinc extraction by D2EHPA have been studied by many different researchers using many different types of kinetic contactors. Some relevant results are summarized in Table 2.5.

**Table 2.5** Survey of Kinetic Studies using Zinc and D2EHPA

Aqueous / Diluent	Contactor	Rate Controlling Mechanism	Source
(Na,H)SO <sub>4</sub> / heptane	Lewis Cell	interfacial chemical reaction	Ajawin <i>et al.</i> [7,22]
(K,H)NO <sub>3</sub> / dodecane	Lewis Cell	interfacial reaction	Cianetti & Danesi [59]
(Na,H)SO <sub>4</sub> / heptane	Lewis Cell	mixed regime <sup>†</sup>	Ajawin <i>et al.</i> [60]
(Na,H)SO <sub>4</sub> / kerosene	Lewis Cell	interfacial 2-step chemical reaction	Huang & Juang [61]
(Na,H)SO <sub>4</sub> / heptane	Rotating Diffusion Cell	mass transfer with chemical reaction	Patel [44]
(Na,H)ClO <sub>4</sub> / Isopar-H <sup>‡</sup>	Lewis Cell	interfacial	Aparicio & Muhammed [62]
HClO <sub>4</sub> / heptane	Rotating Diffusion Cell	mass transfer	Dreisinger & Cooper [33]

<sup>†</sup>Note: intentional selection of parameters to provide mixed regime.

<sup>‡</sup>Isopar-H is odourless aliphatic kerosene (ESSO).

Ajawin *et al.*<sup>[7,22]</sup> attempted to evaluate the reaction kinetics of zinc extraction from sulphate solutions by D2EHPA in heptane using a modified Nitsch cell (a variant of the Lewis cell). As indicated in Section 2.3.1, they found that the rate controlling mechanism was an interfacial chemical reaction. They also found that increasing the temperature or decreasing the aqueous ionic strength increased the rate of chemical reaction. An expression using the Debye-Huckel equation was derived to predict the rate of reaction under different conditions of ionic strength and temperature. Although this equation gave a good general fit to experimental results, Hughes and Zhu<sup>[41]</sup> have questioned its theoretical validity since Ajawin used the simple form of the Debye-Huckel equation which is valid only for low ionic strengths. Hughes and Zhu also suggested that at the high extractant concentrations used in Ajawin's experiments, the interface would be saturated.

Cianetti and Danesi<sup>[59]</sup> studied the kinetics and reaction mechanism of zinc, cobalt, and nickel extraction from nitrate solutions by D2EHPA in n-dodecane using an ARMOLLEX cell (a Lewis Cell variant). After analyzing their experimental results in terms of both interfacial two-step chemical reaction and interfacial film diffusion mechanisms, they concluded that since the rate constants for reactions between either  $Zn^{2+}$ ,  $Co^{2+}$ , or  $Ni^{2+}$  and D2EHPA were very similar, it was unlikely that a chemical reaction was rate controlling since the water exchange rate constants for these three metals are quite dissimilar. It was therefore proposed that the rate of reaction was diffusion controlled. However, Cianetti and Danesi suggested that, although macroscopic interfacial film diffusion could not be completely excluded, it was more likely that the rate controlling step was the microscopic diffusion of the solvated metal ion through a structured water layer at the aqueous/organic interface.

Ajawin *et al.*<sup>[60]</sup> expanded on their earlier work by studying zinc extraction under mixed rate controlling conditions. The bulk aqueous zinc concentration was decreased so that the concentration gradient across the boundary layer would be much less, creating conditions where the rate of film diffusion was approximately equal to the chemical reaction rate. Using the reaction mechanisms found in their earlier paper<sup>[22]</sup>, a simple model was developed which

incorporated both diffusion and chemical reaction terms, and the effect of stirring speed on the rate of reaction was examined. Both the aqueous and organic mass transfer coefficients were found to be directly proportional to the stirring speed.

Huang and Juang<sup>[61]</sup> studied both the extraction and stripping of zinc in sulphate media by D2EHPA in a kerosene diluent. The constant interfacial area cell design used in their study appears to be rather simplistic, with no baffles or other modifications evident. This perhaps provides an explanation for the rather low mixing speeds used (the plateau region was between 90 and 120 rpm). They determined that the extraction reaction was interfacial and that increasing ionic strength caused a decrease in extraction rate at high sulphate concentrations. There was no corresponding effect during stripping. The initial extraction rate was predicted by the equation:

$$R = k [\text{Zn}^{2+}] [\overline{(\text{HR})}_2] [\text{H}^+]^{-2} (1 + 9.94[\text{SO}_4^{2-}]^{1.2})^{-1}$$

where the rate constant,  $k$ , is equal to  $3.21 \pm 0.20 \times 10^{-7} \text{ (mol/dm)}^3 \text{ s}^{-1}$ . The reaction sequence that they developed is the same as that developed by Ajawin<sup>[22]</sup> (c.f. Section 2.3.1), but instead they favoured reaction (iv) as the rate controlling step, i.e.



Patel<sup>[44]</sup> studied the extraction of Co, Ni, Cu, and Zn from sulphate solutions by D2EHPA in n-heptane using the rotating diffusion cell. He developed a MTWCR model which adequately described the extraction rate under different experimental conditions, although there were some discrepancies. In general, the model provided a fairly good fit under rate controlling conditions varying from almost completely chemical reaction controlled (Ni) to almost completely diffusion controlled (Zn).

Aparicio and Muhammed<sup>[62]</sup> examined the extraction of zinc from perchlorate solutions by D2EHPA in Isopar-H. A modified Lewis cell with baffles and screens near the interface allowed fast mixing speeds (plateau region in the range 450 - 575 rpm), while an automated sampling system was used to track the variation in zinc concentration during the test run. They used an interfacial two-step chemical reaction, and incorporated the formation of both  $\overline{\text{ZnR}_2 \cdot \text{HR}}$  and  $\overline{\text{ZnR}_2 \cdot (\text{HR})}_2$  by using a fast equilibrium at the interface. The results

reported in this study are questionable due to the very low zinc concentrations used (0.05 - 0.5mM), and it is entirely probable that, although cell mixing was rapid, the system may have been operating in the mixed regime.

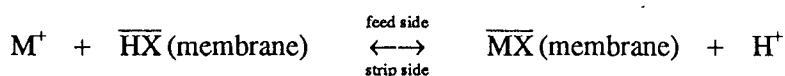
Finally, Dreisinger and Cooper<sup>[33]</sup> also studied the extraction kinetics of Zn, Co, and Ni from perchlorate solutions by D2EHPA in n-heptane using the rotating diffusion cell. They found that Zn extraction was controlled by interfacial film diffusion, and Co extraction could be modelled by a MTWCR model. However, as indicated in Section 2.3.3, Ni extraction was too slow to be modelled by either technique.

To summarize, different experimenters have used different types of apparatus under different experimental conditions in an attempt to elucidate the extraction mechanism of zinc from aqueous solutions by D2EHPA. At this point, it appears that the extraction of zinc is very rapid, and, when chemical reaction is the rate limiting step, it occurs as a multiple-step reaction either at or in a very narrow zone adjacent to the interface. However, due to the extremely fast ligand exchange rate of zinc, some experiments which have been interpreted as operating in the chemical control regime may have instead been operating in either a mixed or diffusional regime.

## 2.7 Supported Liquid Membranes

Supported liquid membranes (SLM's) have been proposed as an alternative process for the extraction of metals from dilute process streams. An extractant impregnated support is placed between two aqueous solutions. Metal is extracted from the feed solution into the membrane, migrates through the membrane, and is stripped into the second solution. SLM technology appears attractive when compared to conventional liquid-liquid extraction methods: possible advantages include lower capital and operating costs, lower energy costs, and higher separation factors. Also, since the amount of extractant used is small and since it is continuously regenerated in the SLM, very expensive extractants optimized for the particular metal system may be used.<sup>[1,63]</sup>

If we consider the case of metal extraction in a SLM system by an acidic extractant, then the reaction may be expressed by the following equilibria:



A general diagram of the transport and reaction processes in a SLM are shown in Figure 2.16. As shown in the figure, the extraction proceeds in four steps: metal extraction from the feed solution into the SLM, transport of the metal-extractant complex through the membrane, stripping of the metal into the strip solution and the corresponding regeneration of the extractant, and diffusion of the extractant back through the membrane to the feed side. An example of a simple hollow-fibre SLM module is shown in Figure 2.17.

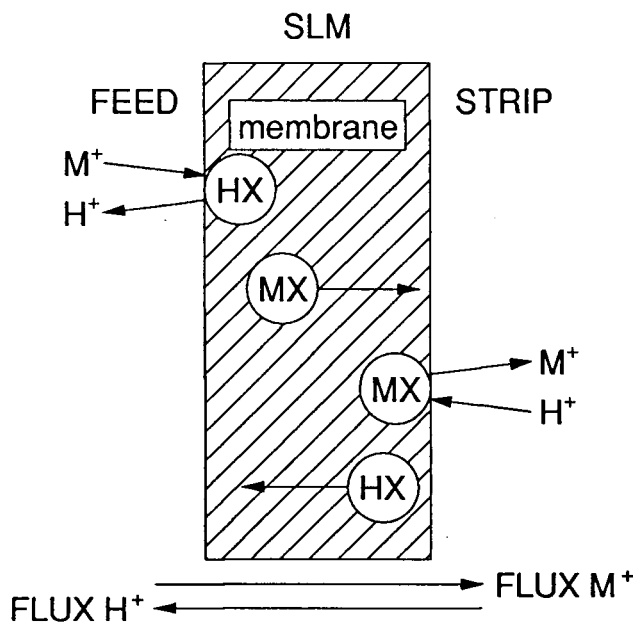


Figure 2.16 Extraction processes in a SLM (after Tavlarides *et al.*<sup>[21]</sup>)

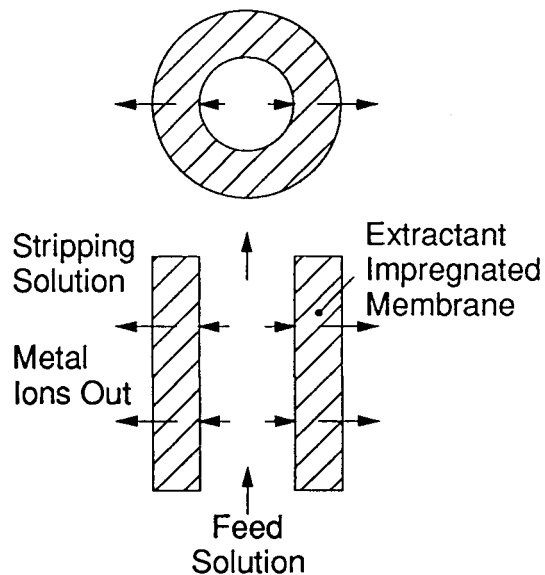


Figure 2.17 Axial and cross-sectional view of a hollow-fibre SLM module

Since in a SLM contactor the feed and strip phases are not particularly well agitated (they flow slowly past the membrane), the boundary layers are likely to be thick and therefore mass transfer may play a significant role in the overall reaction kinetics. In order to understand and effectively model the SLM system, it is therefore necessary to have a thorough understanding of not only the chemical reaction kinetics, but also mass transfer kinetics and transport processes through the membrane.

Fernandez *et al.*<sup>[64]</sup>, Teramoto *et al.*<sup>[54]</sup>, and Huang and Juang<sup>[65]</sup> have investigated the transport of zinc through a D2EHPA impregnated SLM.

Investigating zinc extraction from a sulphate system with a kerosene diluent, Huang and Juang<sup>[65]</sup> found that the rate controlling step was in most cases membrane diffusion. However, under certain circumstances (a combination of lower  $[M^{2+}]_{\text{feed}}$ , higher  $[(HR)_2]_{\text{total}}$  and lower  $[H^+]_{\text{feed}}$ ) aqueous film diffusion became either significant or dominant. Qualitatively, this is reasonable since when the metal concentration is low the concentration gradient is smaller so the total diffusion flux is less, while higher membrane extractant concentrations decrease the membrane resistance, which increases the possibility that aqueous film diffusion may have an influence on the reaction rate.

The work of Teramoto *et al.*<sup>[54]</sup> examined the extraction of zinc in a spiral SLM under industrial-type conditions. Experiments were performed with a n-dodecane diluent, a  $0.7 \text{ mol/dm}^3$   $(HL)_2$  concentration, an input pH of 5.6, and an input zinc concentration of 100 ppm. A long-term (1 month) test was performed to evaluate the behaviour of the SLM contactor with time. Output zinc concentration was  $\sim 1$  ppm, with some degradation in membrane performance after 32 days. The zinc concentration in the recirculated strip solution eventually reached a concentration of 40 gpl, at which point it was replaced; this value represents a concentration factor of  $\sim 40,000$ . Regeneration of the membrane was accomplished by passing the extractant phase and the strip solution through the strip side of the membrane - performance was restored without interrupting continuous operation. It was concluded that the rate determining step was zinc diffusion in the aqueous feed solution.

## 2.8 Summary

The understanding of reaction mechanisms and chemical reaction kinetics is essential for efficient process design and accurate modelling of existing industrial processes. In particular, the emerging technology of supported liquid membranes appears promising for the extraction of metals from dilute solution.

Initial attempts have been made to investigate the extraction of zinc in an SLM system with D2EHPA. One particular method for evaluating solvent extraction kinetics which is particularly well suited for this purpose is the rotating diffusion cell. The RDC operates under conditions

which are similar to SLM operating conditions, with the filter in the RDC in some circumstances simulating the SLM membrane. Thus, investigations of basic kinetic mechanisms by the RDC technique may be most helpful in measuring the rate controlling steps in SLM contactors.

---

## CHAPTER 3 - Experimental Methods

---

### 3.1 Reagents

All solutions were prepared from reagent grade chemicals with the exception of D2EHPA, which was purified by the technique outlined below (Section 3.1.1).

Zinc, cobalt, and nickel aqueous solutions were prepared by dissolving the required amount of the perchlorate salt in deionized water.

The NaOH solution used for pH stabilization during the RDC run was prepared by dissolving the required amount of NaOH in deionized water. The solution was then standardized (see Section 3.2).

D2EHPA/heptane stock solution was prepared by adding a weighted amount of purified D2EHPA to heptane. These solutions were not titrated.

#### 3.1.1 D2EHPA Purification

The D2EHPA supplied by Albright & Wilson was contaminated with small amounts of mono- and tri-(2-ethylhexyl) phosphoric acid and contained trace amounts of metals such as iron. Since the objective of this research project was to investigate the extraction kinetics of D2EHPA, the removal of impurities was necessary to ensure that the results obtained were correct. It was therefore purified by a modified version of Partridge and Jensen's copper salt method.<sup>[66]</sup>

Copper hydroxide (  $\text{Cu}(\text{OH})_2$  ) was prepared by adding a concentrated sodium hydroxide solution to a strong copper sulphate solution. The  $\text{Cu}(\text{OH})_2$ /water slurry produced was quite gelatinous, and filtration had to be done in several steps. The filter cake was washed several times, however, the final cake still had a significant water content. The  $\text{Cu}(\text{OH})_2$  filter cake was then added to a 1:1 mixture of impure D2EHPA and toluene. Since Cu (as hydroxide) was in excess, the result was an organic phase which was fully loaded with copper (i.e. all the free D2EHPA had combined with Cu to form  $\text{CuL}_2$ ). The three-phase mixture was placed in a separatory funnel and allowed to settle overnight, and the final

product was a solution containing three zones - a fully loaded D2EHPA-organic zone, a mixed organic/aqueous zone, and an aqueous zone containing suspended  $\text{Cu}(\text{OH})_2$  particles.

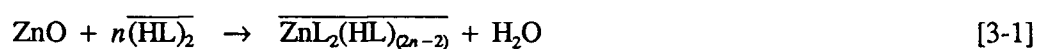
The organic solution was decanted and filtered with PS (phase separator) paper to remove any entrained water. The mixed organic/aqueous solution was centrifuged, and the organic phase was recovered and filtered. Acetone was then added to the Cu-D2EHPA/toluene mixture, precipitating Cu-D2EHPA salt. The solution was filtered, and the Cu-D2EHPA precipitate was washed with further acetone and then recovered. It was then re-dissolved in fresh toluene, and precipitated a second time with acetone. The final product was a virtually pure Cu-D2EHPA salt, with most of the impurities remaining in the toluene.

The pure Cu-D2EHPA salt was contacted twice with strong sulphuric acid, extracting the Cu into the aqueous phase as  $\text{CuSO}_4$ . Trace sulphuric acid was removed from the organic by repeated washing. The purified D2EHPA was then decanted and PS-paper filtered.

The final product was colourless, with no trace of the yellowish tinge that characterizes impure D2EHPA. The yield was ~55 percent, and a Gran Plot (see Section 3.2) gave a purity of 97.9% (the balance was assumed to be solvated water).

### 3.1.2 Preparation of Preloaded Zinc-D2EHPA

A bulk solution containing 0.205M D2EHPA in heptane was prepared for use in the preloading experiments. A first attempt to load the D2EHPA with zinc was made by contacting the D2EHPA-heptane solution with aqueous zinc perchlorate solutions. An addition of NaOH was required to maintain a high pH, however, this NaOH addition resulted in some sort of emulsion formation. After several attempts, this method was abandoned in favour of another, in which the D2EHPA-heptane solution was directly contacted with a stoichiometric amount of solid ZnO. The advantage of this method was that no NaOH addition was required to maintain a high pH, since the reaction proceeded according to the equation:



producing a very small amount of water. After stirring the D2EHPA-heptane/ZnO mixture on low heat for approximately 1/2 hour, it was filtered with PS-paper and the partially loaded Zn-D2EHPA solution was recovered.

### 3.2 Solution Analysis

As mentioned above, the NaOH solution was standardized by using potassium hydrogen phthalate (KHP) as a primary standard. Standardization was accomplished by titrating weighed amounts of KHP (dried for 3-4 hours at  $> 100^{\circ}\text{C}$ ) with the unknown NaOH solution. Phenolphthalein was used as an indicator.

The initial and final aqueous solutions for each RDC run were analyzed for zinc (and, where appropriate, for either nickel or cobalt) by diluting the unknown to a metal concentration appropriate for atomic absorption spectrophotometry. Each metal was analyzed for on its strongest characteristic wavelength: 213.9, 232.0, and 240.7 nm for Zn, Ni, and Co, respectively.

The final organic solution from each RDC run was stripped by three contacts with 0.5M  $\text{H}_2\text{SO}_4$ . The resulting strip solution was then analyzed by atomic absorption spectrophotometry as described above. The initial zinc content of the preloaded Zn-D2EHPA strip solutions was also determined by this method.

The Gran Plot method<sup>[67]</sup> was used to determine D2EHPA content, both to check the purity of the purified D2EHPA, and also to verify the loading of the preloaded Zn-D2EHPA strip solution. This method is effective since D2EHPA is a weak acid. An aliquot of the unknown organic sample was mixed with 2-propanol, and then titrated with a standardized 0.1M NaOH/75% 2-propanol solution. When the titration was near the equivalence point, the titrant was added dropwise, and the change in pH was recorded.

The plot of  $1/\Delta \text{pH}$  vs. Number of Drops has an inflection at the equivalence point, yielding the exact volume of titrant which was required to completely neutralize the D2EHPA. This type of plot is called a Gran plot; two sample plots are shown in Figures 3.1a and 3.2a. The D2EHPA concentration in the unknown solution could then be determined.

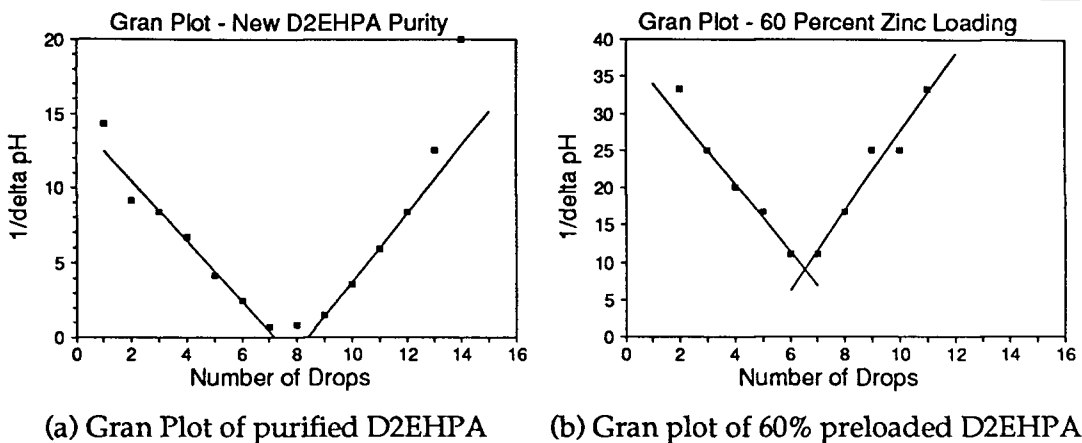


Figure 3.1 Sample Gran Plots

### 3.3 Rotating Diffusion Cell Apparatus

A diagram of the RDC apparatus used in this study is shown in Figure 3.2. The RDC was mounted on a lab stand anchored at each end to prevent vibration. The RDC was rotated by a pulley connected to a variable speed motor, and the rotational speed of the RDC was measured by an optical sensor (see Appendix A for details).

The thermostatted beaker below the RDC was filled with the aqueous solution, while the inner compartment of the cell was filled with the organic solution. A lid with holes for the RDC, a pH probe, a gas purge, and titrant addition was attached to the beaker; nitrogen was injected into the aqueous chamber above the solution level to prevent atmospheric  $\text{CO}_2$  from reacting with the aqueous solution and changing the pH.

The beaker assembly was mounted on a labjack so that the height of the beaker could be adjusted so that at all times the net flux due to hydrostatic pressure differences through the filter would be equal to zero. A constant temperature circulator was used to pump water through the double-walled beaker, maintaining the aqueous phase (and organic phase by conduction) at the desired temperature.

An autotitration system consisting of a Radiometer PHM82 pH meter, ABU80 autoburette, and TTT80 titrator was used to keep the pH at a constant level during a RDC run. A pH electrode was inserted into the outer compartment through the hole in the lid, and the system was preset at the desired pH. The volume of titrant dispensed was recorded by connecting the chart recorder

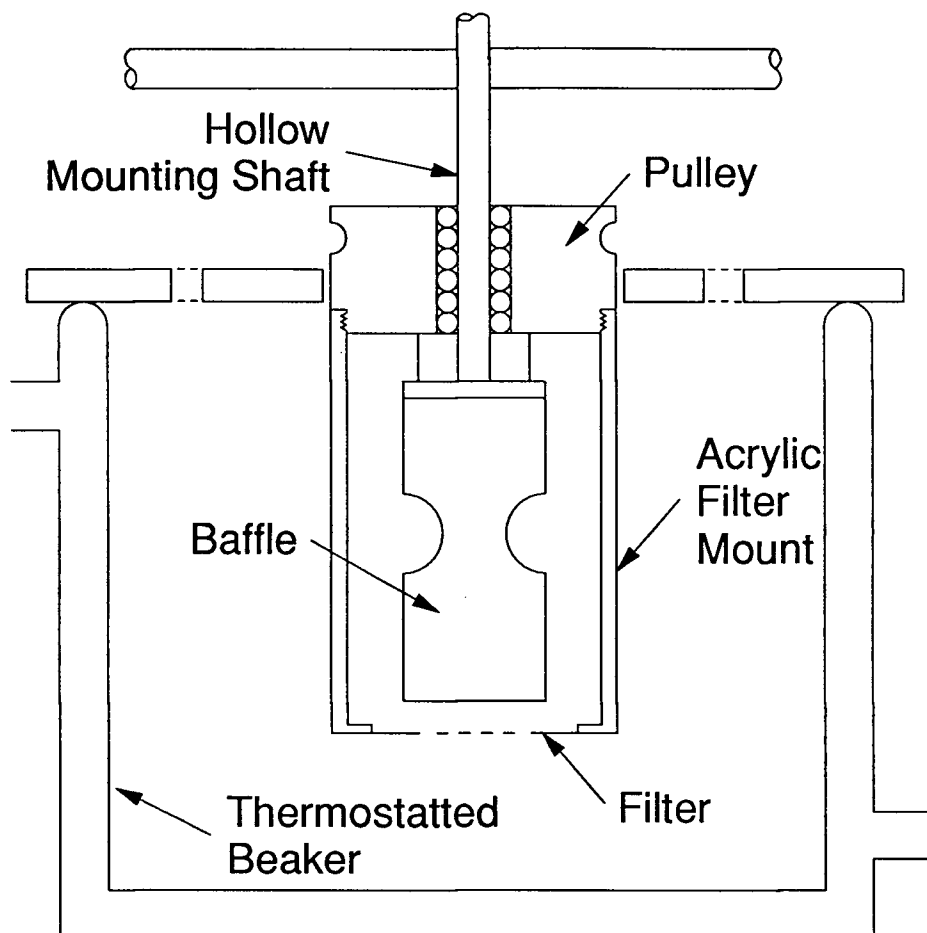


Figure 3.2 - The Rotating Diffusion Cell

output of the autoburette to a Data Translation DT2805 analog-to-digital converter which was attached to an IBM PC-XT. Existing data acquisition software was considered to be inadequate, so a Pascal computer program was written to record both the data from the autotitrator and the elapsed time. Program details and a flowchart are given in Appendix B.

### 3.4 Filter Preparation

The filter used for the majority of the RDC runs was a Millipore cellulose-acetate / cellulose-nitrate membrane filter with a pore size of  $0.45\mu\text{m}$ . The acrylic RDC cylinder was prepared for mounting by sanding with fine sandpaper, and then washing to remove any acrylic particles. It was then allowed to dry thoroughly. The filter was then mounted on the cylinder by using an acrylic cement which was prepared by dissolving scrap acrylic in chloroform. A good

bond between the filter and the cylinder was achieved by applying pressure with a small piece of acrylic sheeting; sticking was avoided by using a sheet of Teflon between the two pieces. The filter was allowed to dry thoroughly before "clearing".

The process of defining the interface surface, or clearing, requires the application of a solvent to the filter surface. The solvent partially dissolves the filter, collapsing the pores and rendering the affected area impermeable. This solvent, or clearing solution, consists of a mixture of equal parts of 1,4-dioxane, 1,2-dichloroethane, and hexanes. The mounted filter was rotated at approximately 200 rpm and the clearing solution was applied using a brush, starting at the outer edge and moving towards the center. A region approximately 12 mm in diameter was left uncleared; across this area metal transfer occurred during the RDC test. Once the filter had dried, the cleared area was transparent while the active filter area remained opaque.

The active filter area was then determined by measuring the diameter of the uncleared circle and calculating the area.

### 3.5 Experimental Procedure

In a typical RDC run, heptane was pipetted through the hollow mounting rod (shown in Figure 3.2), wetting the filter and allowing the organic/aqueous interface to form on the aqueous side of the filter. The cell was then lowered into the aqueous solution until the organic solution level was just below the aqueous solution level. Additional heptane was pipetted into the interior of the cell, and the height of the cell was adjusted to the vertical position where there is no net convective flow due to hydrostatic forces. A pH electrode was placed in the solution and the pH of the solution was adjusted by adding dilute NaOH until the pH reached the desired value. A volume of heptane containing the extractant (D2EHPA) was pipetted into the inner compartment and the data acquisition system and the pH-stat were started. A time-NaOH addition profile was recorded by the data acquisition system since the pH of the system was maintained at a constant value. Since NaOH titrant of known concentration was added to the system to maintain the pH, and since the rate of  $H^+$  release is directly proportional (2:1 ratio) to the amount of zinc extracted (c.f. reaction stoichiometry), the rate of zinc extraction could be determined.

A single test run consisted of operating the RDC at a certain rotational speed until steady-state had been attained and enough data had been recorded. This usually took only a few minutes since zinc extraction was quite rapid. The rotational speed was then changed and data collection occurred again. Six rotational speeds were tested in random order: 60, 100, 150, 200, 250, and 300 rpm.

After the experiment had been concluded, the raw datafile was analyzed to determine the steady-state extraction rate at each rotational speed. Since the diffusion boundary layer is proportional to the inverse square root of the rotational speed (according to equation 2-4), a RDC plot, normalized with respect to interfacial area could be constructed. A sample RDC plot is shown in Figure 3.3.

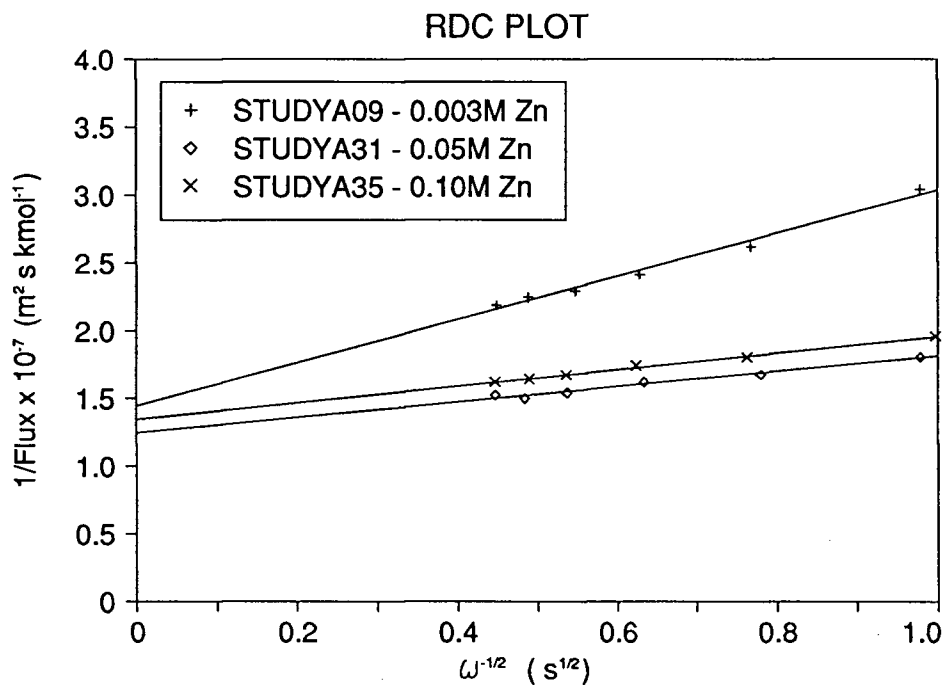


Figure 3.3 - A Sample RDC Plot showing lines from three different experiments  
Formal [D2EHPA] = 0.05 M, pH = 4.5, T = 25°C, filter = 0.45µm

As well as furnishing the flux of the system containing only chemical reaction resistances and diffusional resistance through the membrane, the RDC plot also provides qualitative information about the relative importance of diffusion and chemical reaction. For a system which

is operating completely in the chemical reaction regime the slope of the line will be equal to zero. As mass transfer processes in the aqueous and organic phases become more important, the slope increases, with a steep slope signifying strong mass transfer control.

In general, the extraction rate (flux) for a particular set of test conditions was characterized by the flux at a rotational speed of 1.67 Hz, i.e. 100 rpm. Plots which examined the variation in the rate of metal extraction under different conditions could then be drawn.

---

## **CHAPTER 4 - Results and Discussion**

---

This discussion of the results of the experimental program will take the following form. First the raw data from the system characterization studies will be presented, with some discussion of errors. Next the mass transfer mathematical model which was formulated to describe and predict extraction in the RDC system will be introduced, with a full theoretical derivation of relevant equations. The results of the major kinetic studies will then be shown, along with results from the mathematical model. The second mathematical model which was produced to describe the results from the preloading tests will then be introduced, again with theoretical derivations. The results of the preload experiments and model predictions will then be shown and discussed. The effect of temperature on extraction will be analyzed, although no model was developed which examined this parameter. Finally, results of the experiments which were conducted to examine the properties of the filters used in the RDC will be presented and discussed.

### **4.1 Initial Data from Test Runs**

The initial work involved developing a "standard condition" baseline against which subsequent experiments could be compared. A series of experiments in which the basic system parameters (zinc concentration, D2EHPA concentration, pH, and temperature) were varied were then performed. A summary of the baseline conditions and the range of parameters examined is given in Table 4.1. Figures 4.1 through 4.4 show the experimental data collected for the four parameters. For each parameter, representative figures were constructed for a RDC rotational speed of 100 rpm.

The effect of zinc concentration on the zinc flux is shown in Figure 4.1. The flux is highly dependent on the zinc concentration at low zinc concentrations, and is independent of bulk aqueous zinc concentration at higher concentrations. This suggests that the rate controlling step at low aqueous zinc concentrations may be mass transfer of zinc from the aqueous bulk to the interface, whereas at higher zinc concentrations some other step is rate controlling.

---

**Table 4.1** Experimental Conditions

Baseline RDC conditions

0.05M  $\text{Zn}(\text{ClO}_4)_2$

0.05F D2EHPA

Bulk pH = 4.5

T = 25°C

0.45 $\mu\text{m}$  Millipore filter

Parameters examined:

[ $\text{Zn}(\text{ClO}_4)_2$ ]: 0.001 - 0.20M

[D2EHPA]: 0.0025 - 0.10F

Bulk pH: 3.25 - 5.5

temperature: 15 - 50°C

---

In Figure 4.2 the effect of D2EHPA concentration on the zinc flux is examined. The rate of zinc extraction is approximately proportional to the formal D2EHPA concentration, which again suggests a mass transfer mechanism. However, in this case the rate controlling mechanism may be the transfer of D2EHPA from the organic bulk to the interface.

There is little dependence of zinc flux on pH as shown in Figure 4.3, indicating that this parameter is not particularly significant under the conditions examined. It is likely that the system is rate controlled by the flux of D2EHPA to the interface under all pH conditions, so changes in the bulk pH (and thus the resulting  $\text{H}^+$  concentration gradient) would have little effect on the flux until a critical value was reached.

As expected, the extraction rate increases with temperature, as shown in Figure 4.4. The increase in rate may be due to enhanced chemical reaction kinetics, or the increase in temperature may change solution properties so that resistances to mass transfer decrease. These results will be analyzed at a later time.

As can be seen in Figures 4.1 through 4.4, there is some scatter in the experimental data. Although it is difficult to make an accurate estimation of the errors involved, an examination of the results obtained from various tests of the standard conditions baseline indicated that in seven trials the average flux was  $5.49 \times 10^{-8} \text{ kmol/m}^2/\text{sec}$ , with a sample standard deviation of  $0.32 \times 10^{-8}$ .

Possible sources of error are numerous. Although attempts were made to maintain the concentrations of all reagents at constant values, it was necessary to prepare new batches of stock solutions. The sodium hydroxide used for acid neutralization was prepared on a biweekly basis to avoid errors due to the absorption of atmospheric CO<sub>2</sub>. Many batches of zinc perchlorate stock solution were used; in addition the zinc perchlorate source was changed. Finally, a new batch of purified D2EHPA was prepared when the stock of previously purified D2EHPA was consumed.

One of the major sources of error had to do with the measurement of the area of the cleared filter. Although a simple optical system was used, this method alone had a high systematic error; a measurement error of approximately 3 percent could be attributed to this step. Also, some of the cleared filters were not exactly circular; as much as possible these filters were eliminated.

Finally, a random source of error is the consistency of the filter membrane. The type of filter used in this study is a cellulose acetate-nitrate membrane which is typically used in microbiological applications. As with any manufactured product, it is likely that there is some variation in the porosity and filter thickness from filter to filter, which would cause changes in the flux. Also, the pore size distribution is not a "spike", but rather a normal distribution with some pores larger than the specified value and some pores smaller.

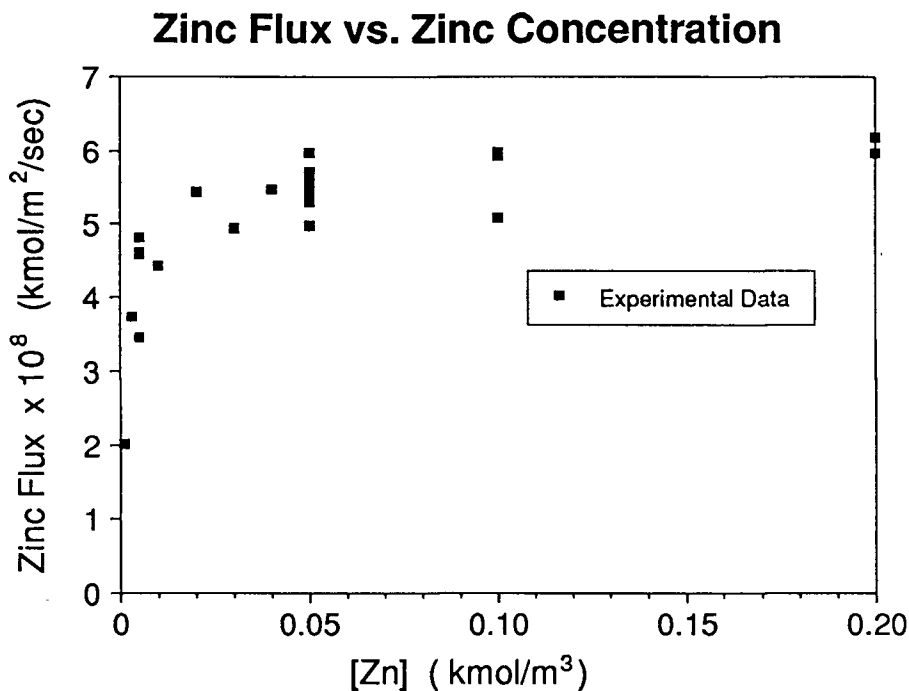


**Figure 4.1** Effect of changing bulk zinc concentration on zinc flux : Formal [D2EHPA] = 0.05 M, pH = 4.5, T = 25°C, filter = 0.45µm, ω = 100 rpm

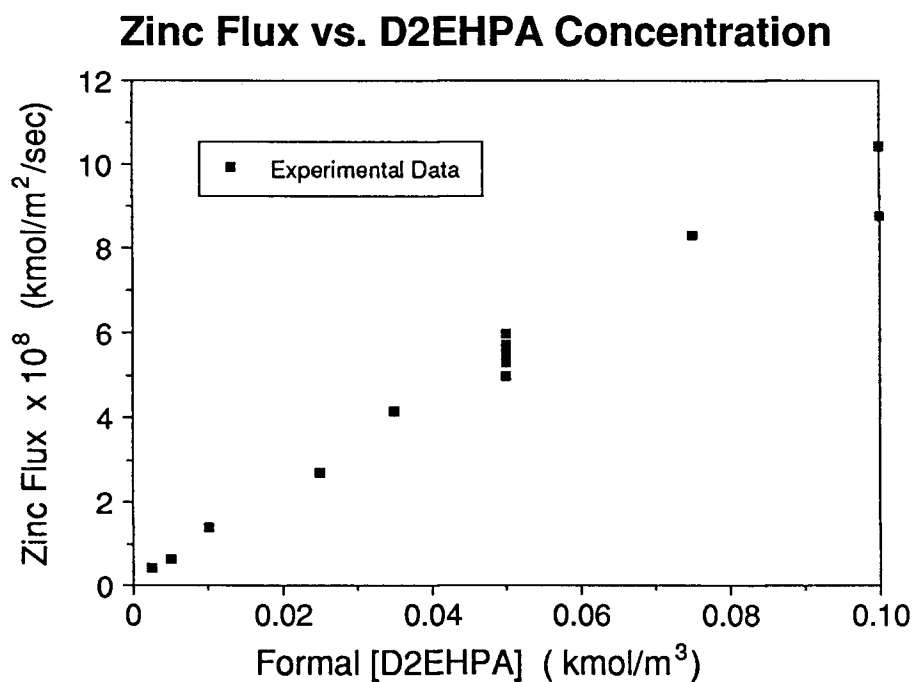


**Figure 4.2** Effect of changing D2EHPA concentration on zinc flux : [Zn] = 0.05 M, pH = 4.5, T = 25°C, filter = 0.45µm, ω = 100 rpm

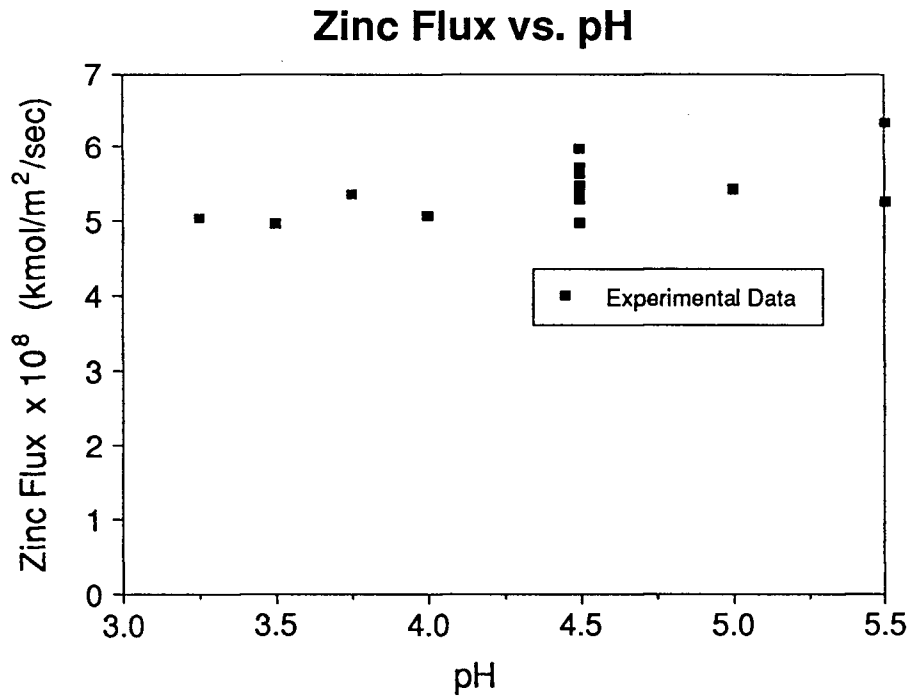


**Figure 4.3** Effect of changing bulk pH on zinc flux : [Zn] = 0.05M, Formal [D2EHPA] = 0.05 M, T = 25°C, filter = 0.45 $\mu$ m,  $\omega$  = 100 rpm

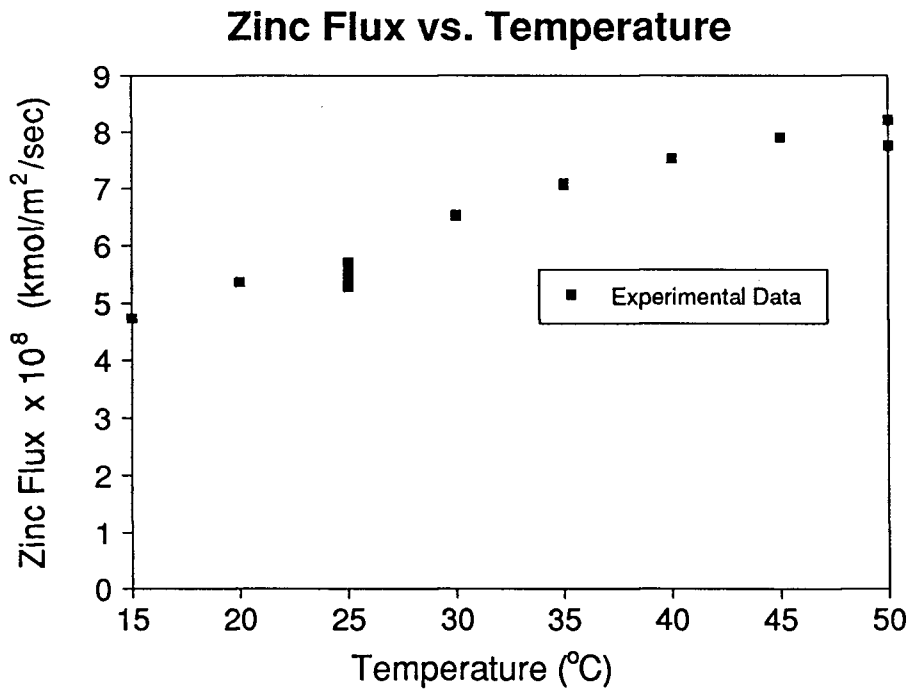
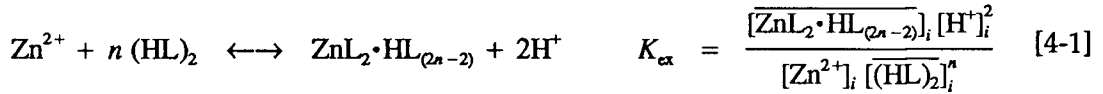


**Figure 4.4** Effect of changing temperature on zinc flux : [Zn] = 0.05 M, Formal [D2EHPA] = 0.05 M, pH = 4.5, filter = 0.45 $\mu$ m,  $\omega$  = 100 rpm

## 4.2 Basic Mathematical Model

A mathematical model was developed to predict the rate of extraction with changes in bulk zinc concentration, bulk D2EHPA concentration, and pH. In order to evaluate the relative importance of mass transfer as opposed to chemical reaction, initial calculations were made of the maximum flux (virtual maximum rate, or VMR) allowed by the system conditions.

An initial estimation of the effect of mass transfer on zinc extraction was made by considering the extreme cases in which either aqueous phase mass transfer (of  $Zn^{2+}$  to the interface) or organic phase mass transfer (of D2EHPA to the interface) is dominant. Since it is likely that over the range of concentrations examined the extracted species exists as both  $ZnL_2 \cdot HL$  (i.e.  $n=1.5$ ) and  $ZnL_2 \cdot (HL)_2$  ( $n=2$ )<sup>(2)</sup>, VMR rates for both species will be calculated. The association factor,  $n$ , is defined as the ratio of D2EHPA dimer to extracted zinc. For the general extraction equilibrium



with equilibrium constant  $K_{ex}$ , the fluxes of  $Zn^{2+}$  and  $(HL)_2$  may be related by a simple mass balance, i.e.

$$J_{Zn^{2+}} = \frac{1}{n} J_{(HL)_2} \quad [4-2]$$

Note that the fluxes are defined as shown in Figure 4.5.

The aqueous mass transfer rate limited flux can be directly determined from Fick's first law, i.e.

$$J_{Zn^{2+}} = k_{Zn^{2+}} [C_{Zn^{2+}}^{bulk} - C_{Zn^{2+}}^i] \quad [4-3]$$

where  $C_{Zn^{2+}}^i$  and  $C_{Zn^{2+}}^{bulk}$  are the interfacial and bulk concentrations of  $Zn^{2+}$ , respectively. The mass transfer coefficient,  $k_{Zn^{2+}}$ , is defined by the equation

$$k_{Zn^{2+}} = \frac{D_{Zn^{2+}}}{z_{D, aq}} \quad [4-4]$$

---

2 It is unlikely that there would be much  $ZnL_2$  present under standard operating conditions, and therefore this species was not considered.

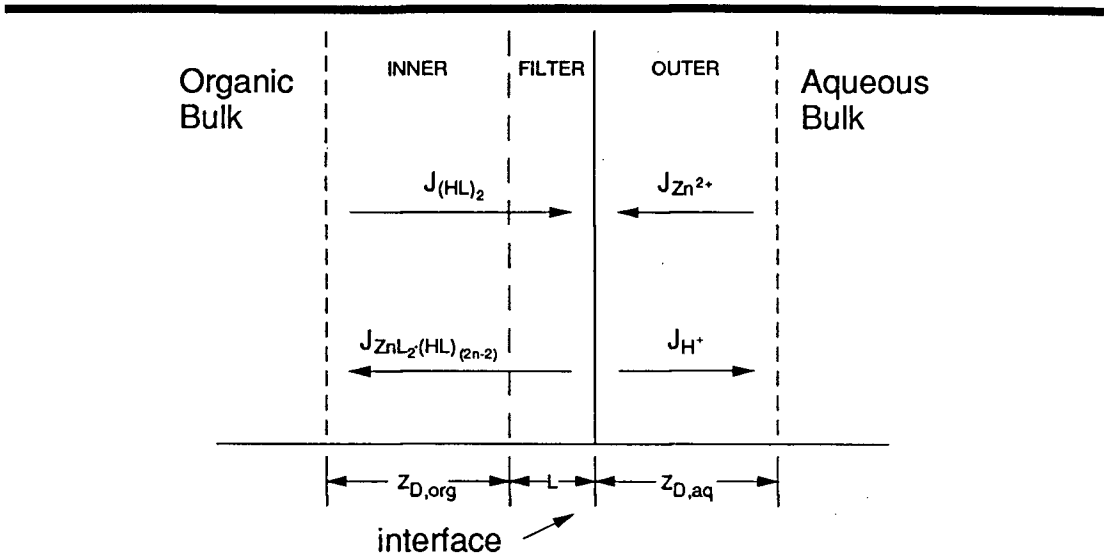


**Figure 4.5** Diagram of species and flux direction definitions for the VMR model

where  $D_{Zn^{2+}}$  is the aqueous diffusion coefficient of  $Zn^{2+}$ , and  $z_{D,aq}$  is the diffusion boundary layer thickness as given by the Levich equation,

$$z_D = 0.643 \omega^{-1/2} \nu^{1/6} D^{1/3} \quad [4-5]$$

The organic mass transfer rate limited flux can be similarly derived from Fick's first law, i.e.

$$J_{(HL)_2} = k_{(HL)_2} [c_{(HL)_2}^{bulk} - c_{(HL)_2}^i] \quad [4-6]$$

where  $c_{(HL)_2}^i$  and  $c_{(HL)_2}^{bulk}$  are the interfacial and bulk concentrations of  $(HL)_2$ , respectively. Note that in this derivation,  $C$  denotes an aqueous species, and  $c$  denotes an organic species. Furthermore, the superscript  $i$  indicates an interfacial species, while either  $b$  or  $bulk$  indicates a species in the bulk phase. The mass transfer coefficient,  $k_{(HL)_2}$ , is defined by the equation<sup>[33]</sup>

$$k_{(HL)_2} = \frac{D_{(HL)_2}}{z_{D,org} + L/\alpha} \quad [4-7]$$

where  $D_{(HL)_2}$  is the organic diffusion coefficient of  $(HL)_2$ ,  $z_{D,org}$  is the diffusion boundary layer thickness as given by equation [4-5],  $L$  is the effective filter length, and  $\alpha$  is the filter porosity. The

additional term  $L/\alpha$  is due to the resistance of the filter to diffusion; this term is only present for organic phase species since it has been established that the aqueous/organic interface exists on the aqueous side of the filter surface.

The virtual maximum rates of  $Zn^{2+}$  transport (aqueous phase mass transfer control) and  $(HL)_2$  transport (organic phase mass transfer control) may be calculated from equations [4-3] and [4-7]. The results were overlaid on the experimental plots for zinc flux vs. zinc concentration, and zinc flux vs. D2EHPA concentration, as shown in Figures 4.6 and 4.7.

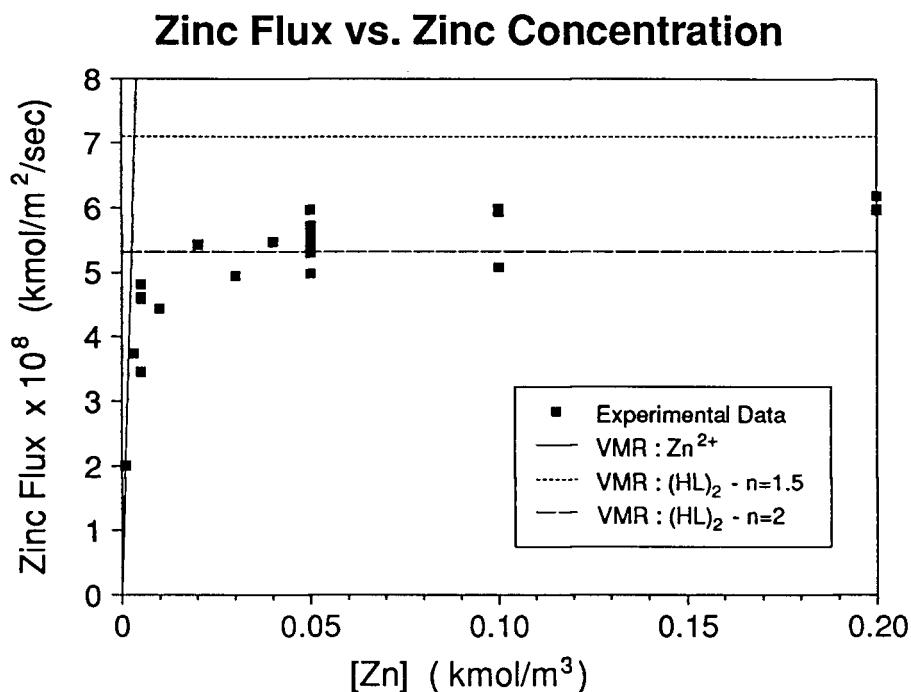
In Figure 4.6, for low zinc concentrations, it can be seen that zinc transport to the interface appears to be rate controlling. At higher zinc concentrations, the rate controlling step appears to become the transport of D2EHPA to the interface. If a value of  $n=1.5$  is used, the VMR is greater than the observed flux; for  $n=2$ , the VMR is lower than the observed results. Therefore, it is probable that the value of  $n$  is neither 1.5 nor 2, but rather extraction of both species occurs simultaneously.

Figure 4.7, showing VMR plots for flux vs. D2EHPA concentration, implies that the association factor is near 1.5 at low D2EHPA concentrations, and increases as the concentration of D2EHPA increases. This is reasonable, since the amount of additional D2EHPA associated with an extracted zinc-extractant molecule is governed by an equilibrium which favours higher values of  $n$  with increasing D2EHPA concentration. From the plot, it appears that the assumption that the rate controlling step at moderate to high D2EHPA concentrations is mass transfer of D2EHPA to the interface is correct.

The VMR calculations imply that the chemical reactions occur fast enough that the system can be simulated by a simple mass transfer model. The following discussion will focus on describing the theoretical basis for the mathematical model; source code is given in Appendix D.

For the aqueous zinc flux and the hydrogen ion flux only two species were assumed to be present:  $Zn^{2+}$  and  $H^+$ . It was assumed that there were no chemical reactions in the boundary layer, and therefore diffusion profiles were linear as stated by Fick's first law.

All D2EHPA present in the organic bulk was assumed to be dimeric, and the extractant diffusing to the interface was also assumed to be entirely in the dimeric form. Once at the interface, the partition between monomeric and dimeric D2EHPA was computed based on the total D2EHPA concentration at the interface. The zinc-extractant complex formed at the interface was assumed



**Figure 4.6** VMR predictions and experimental data for changes in bulk zinc concentration : Formal [D2EHPA] = 0.05 M, pH = 4.5, T = 25 °C, filter = 0.45µm, ω = 100 rpm

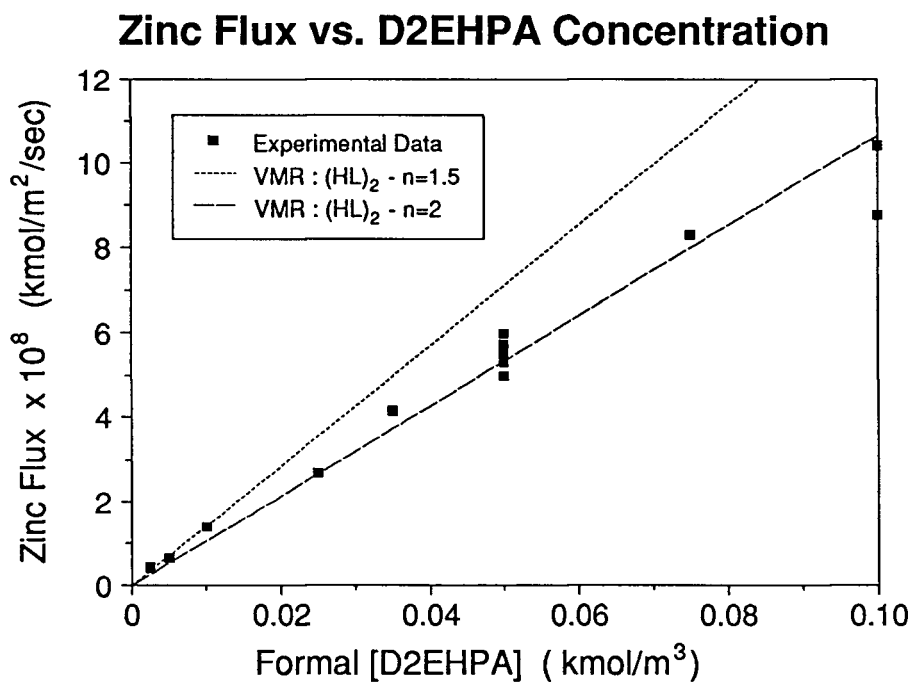


**Figure 4.7** VMR predictions and experimental data for changes in bulk D2EHPA concentration : [Zn] = 0.05 M, pH = 4.5, T = 25 °C, filter = 0.45µm, ω = 100 rpm

to exist as  $ZnL_2 \cdot HL$  and  $ZnL_2 \cdot (HL)_2$ , and no zinc-extractant complex was present in the organic bulk. It was assumed that for the  $HL$ ,  $(HL)_2$ ,  $ZnL_2 \cdot HL$  and  $ZnL_2 \cdot (HL)_2$  species that reactions occurred only at the interface and in the bulk phase, and that no speciation adjustment occurred in the boundary layer.

The activity coefficients of all species were assumed to be constant. The viscosity of the D2EHPA/heptane mixture was assumed to be equal to the viscosity of pure heptane; this will probably result in the computed diffusion coefficients for the organic species being too large. Since viscosity is also a parameter in the Levich equation, the viscosity term will cause a small increase in the equivalent boundary layer thickness; however, the increase will not be enough to offset the error in the diffusion coefficient.

The extraction stoichiometry for zinc reacting with monomeric D2EHPA to form a zinc-extractant complex with one or two associated D2EHPA molecules can be expressed as:



and



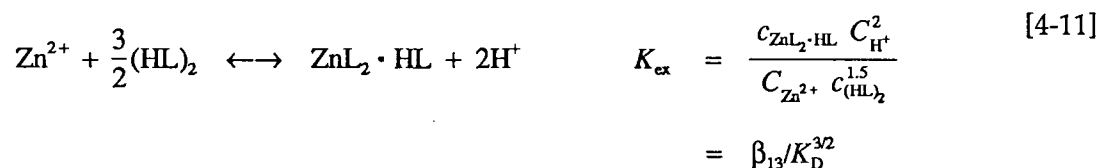
where  $\beta_{13}$  and  $\beta_{14}$  are the formation constants for the species  $ZnL_2 \cdot HL$  and  $ZnL_2 \cdot (HL)_2$  respectively.

A similar expression can be developed for the dimerization equilibrium between monomeric and dimeric D2EHPA:



where  $K_D$  is the dimerization constant for D2EHPA.

An expression for the extraction of zinc (as  $ZnL_2 \cdot HL$ ) by D2EHPA in the dimeric form can be developed by combining equations [4-8] and [4-10]:



From equations [4-8] and [4-9] the distribution of the two zinc species  $ZnL_2 \cdot HL$ , and  $ZnL_2 \cdot (HL)_2$  can be interrelated as follows:



The quotient  $\beta_{13}/\beta_{14}$  is equal to the stepwise formation constant  $K_4$ .

At any point in the organic, the monomeric and dimeric concentrations of D2EHPA are related by the following equations:

$$c_{(HL)_2, total} = \frac{1}{2}c_{HL} + c_{(HL)_2} \quad [4-13]$$

substituting from [4-10],

$$c_{(HL)_2, total} = \frac{1}{2}c_{HL} + K_D c_{HL}^2 \quad [4-14]$$

rearranging,

$$K_D c_{HL}^2 + \frac{1}{2}c_{HL} - c_{(HL)_2, total} = 0 \quad [4-15]$$

This can be solved using the quadratic equation if the total concentration of D2EHPA is known.

From equation [4-1], the fluxes of the aqueous and organic species diffusing to and from the interface may be related by a mass balance, i.e.

$$J_{Zn^{2+}} = \frac{1}{n} J_{(HL)_2} = J_{ZnL_2 \cdot (HL)_2, total} = 2J_{H^+} \quad [4-16]$$

Once again, the fluxes are defined as shown in Figure 4.5.

From Fick's first law,

$$J_{Zn^{2+}} = k_{Zn^{2+}} [C_{Zn^{2+}}^{bulk} - C_{Zn^{2+}}^i] \quad [4-17]$$

$$J_{H^+} = k_{H^+} [C_{H^+}^i - C_{H^+}^{bulk}] \quad [4-18]$$

$$J_{(HL)_2} = k_{(HL)_2} [c_{(HL)_2}^{bulk} - c_{(HL)_2}^i] \quad [4-19]$$

$$\begin{aligned}
J_{\text{ZnL}_2 \cdot (\text{HL})_x, \text{total}} &= J_{\text{ZnL}_2 \cdot \text{HL}} + J_{\text{ZnL}_2 \cdot (\text{HL})_2} & [4-20] \\
&= k_{\text{ZnL}_2 \cdot \text{HL}} \left[ c_{\text{ZnL}_2 \cdot \text{HL}}^i - c_{\text{ZnL}_2 \cdot \text{HL}}^{\text{bulk}} \right] + k_{\text{ZnL}_2 \cdot (\text{HL})_2} \left[ c_{\text{ZnL}_2 \cdot (\text{HL})_2}^i - c_{\text{ZnL}_2 \cdot (\text{HL})_2}^{\text{bulk}} \right]
\end{aligned}$$

where for aqueous species,

$$k_i = \frac{D_i}{z_{D, \text{aq}}} \quad [4-21]$$

and for organic species,

$$k_i = \frac{D_i}{z_{D, \text{org}} + L/\alpha} \quad [4-22]$$

By substituting  $c_{\text{ZnL}_2 \cdot (\text{HL})_2}$  from equation [4-12] into equation [4-20], and assuming that the bulk concentrations of  $\text{ZnL}_2 \cdot \text{HL}$  and  $\text{ZnL}_2 \cdot (\text{HL})_2$  are equal to zero, an expression for  $J_{\text{ZnL}_2 \cdot (\text{HL})_x, \text{total}}$  solely in terms of  $c_{\text{ZnL}_2 \cdot \text{HL}}^i$  may be developed, i.e.

$$J_{\text{ZnL}_2 \cdot (\text{HL})_x, \text{total}} = \left( k_{\text{ZnL}_2 \cdot \text{HL}} + k_{\text{ZnL}_2 \cdot (\text{HL})_2} \frac{c_{\text{HL}}^i}{\beta_{13}/\beta_{14}} \right) c_{\text{ZnL}_2 \cdot \text{HL}}^i \quad [4-23]$$

If a value is assumed for  $J_{\text{Zn}}$ , then the concentration of the interfacial species may be computed by using equations [4-16], [4-17], [4-18], [4-19], and [4-23]. The expression for  $K_{\text{ex}}$  (equation [4-11]) can be re-written as:

$$\frac{c_{\text{ZnL}_2 \cdot \text{HL}}^i c_{\text{H}^+}^i{}^2}{c_{\text{Zn}}^i c_{(\text{HL})_2}^i{}^{1.5}} - K_{\text{ex}} = f(J_{\text{Zn}}) \quad [4-24]$$

where  $f(J_{\text{Zn}})$  should equal 0.

If the concentrations of the four interfacial species are substituted into equation [4-24], then the correct value for the flux  $J_{\text{Zn}}$  can be determined by iterating  $J_{\text{Zn}}$  until  $f(J_{\text{Zn}})$  converges. A general flowchart showing the basic structure of the simple mathematical model is shown in Figure 4.8.

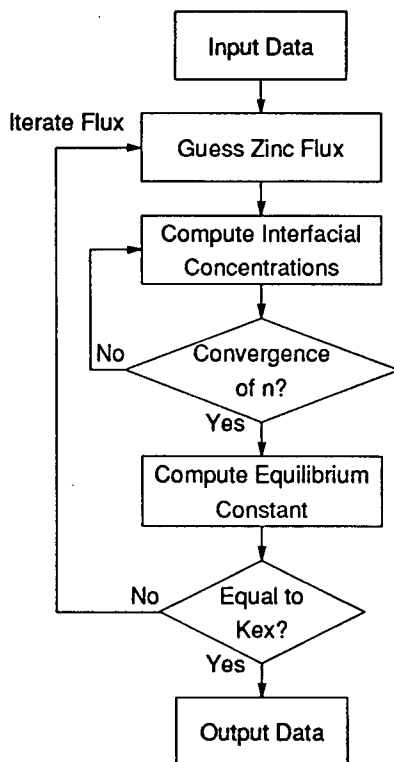


**Figure 4.8** Basic program structure of the simple mathematical model

## 4.3 Basic Model Predictions

### 4.3.1 Basic Model Verification

The basic mathematical model fits the results surprisingly well when the number of assumptions and the accuracy of some critical physiochemical parameters (including the diffusion coefficients of D2EHPA and zinc-D2EHPA species in heptane) are considered. Figures 4.9 through 4.14 show the measured rates of zinc flux and the model predictions for changes in aqueous zinc concentration, formal D2EHPA concentration, and bulk pH.

The model fits the very low zinc concentration regions of Figures 4.9 and 4.10 well, but overpredicts the zinc flux at higher zinc concentrations. Similarly, the fit of the model is good in Figures 4.11 and 4.12 at low D2EHPA concentrations, but again diverges at higher D2EHPA concentrations.

As shown in Figures 4.13 and 4.14, the model overpredicts the zinc flux for all values of pH examined. The model curve is fairly flat, indicating that pH has little to no effect on the zinc flux in the range examined; the predicted curve dips slightly around pH=3, indicating that at this point the effect of pH may start becoming significant.

The model compares well with experimental data only at low zinc concentrations, where the rate controlling step is not the diffusion of  $(HL)_2$  in the organic phase, but rather the diffusion of  $Zn^{2+}$  in the aqueous phase. At high zinc concentrations, moderate to high D2EHPA concentrations, and at all values of pH, the model overpredicts the rate of zinc extraction. This indicates that the inaccuracy in the model most likely lies on the organic side.

There are three likely explanations. The first is that since most of the physiochemical parameters for the organic species were not available as experimentally verified data, empirical correlations were used. The most critical values derived using correlations are the diffusion coefficients of  $(HL)_2$ ,  $ZnL_2 \cdot HL$ , and  $ZnL_2 \cdot (HL)_2$ . In particular, the model is most sensitive to the diffusion coefficient of  $(HL)_2$  since, under conditions of organic rate control, the diffusion of this species is rate controlling.

The second possibility for error is that the thickness and porosity of the filters used in this study are not as specified by the manufacturer.

The final possibility is that some of the assumptions incorporated in the model are not completely valid. The assumption that all D2EHPA present in the bulk organic is dimeric is valid at high D2EHPA concentrations; examination of the monomer/dimer equilibrium indicates that at a total D2EHPA concentration of 0.05 F, 98.6% of the D2EHPA would be in the dimeric form; even at a total D2EHPA concentration of 0.0005 F, 86.8% of the D2EHPA is dimeric. Thus, the assumption that all D2EHPA diffusing to the interface is dimeric is not too bad, although there is some error since HL diffuses faster than  $(HL)_2$ . The greatest error would be from the assumption that there is no readjustment of speciation as the zinc-extractant species migrate to the bulk. Under conditions where the system is  $(HL)_2$  mass transfer controlled, there would be very little free  $(HL)_2$  at the interface, resulting in a low value of  $n$  at the interface. However, as these low  $n$  zinc-extractant complexes migrate

through the boundary layer towards the bulk, the concentration of D2EHPA increases. If the chemical reactions are fast, some of the D2EHPA reacts and further solvates the zinc-extractant complexes, creating a non-linear  $(HL)_2$  diffusion profile.

To better understand the effect of different parameters on the model, a sensitivity analysis of the model was performed. The effect of three different parameters was examined: the organic side diffusion coefficients, the equilibrium constant  $K_{ex}$ , and the filter equivalent thickness  $L/\alpha$ .

Figures 4.15 and 4.16 show the effect of changing the organic species diffusion coefficients for different zinc and D2EHPA concentrations. For this analysis, all three diffusion coefficients (for  $(HL)_2$ ,  $ZnL_2 \cdot HL$ , and  $ZnL_2 \cdot (HL)_2$ ) were altered by up to  $\pm 20\%$ . As can be seen in these figures, small changes in the organic species diffusion coefficients can have a significant effect on the extraction rate.

The effect of changing the equilibrium constant,  $K_{ex}$ , was examined in Figures 4.17 and 4.18. Small changes of the order of 10 or 20 percent had little effect on the extraction rate, so larger steps were used in order that the effect of different  $K_{ex}$  values could be seen. For larger values of  $K_{ex}$ , the transition from one mass transfer regime to another occurs faster (c.f. Figure 4.17); smaller values cause the mass transfer limited rate to be approached more slowly (c.f. Figures 4.17 and 4.18).

The final parameter examined is the filter equivalent thickness  $L/\alpha$ ; plots are shown in Figures 4.19 and 4.20. Since the thickness of the filter is larger than the organic side diffusion boundary layer, increasing or decreasing the filter thickness has a significant effect on the flux if the system is in the organic mass transport controlled regime.

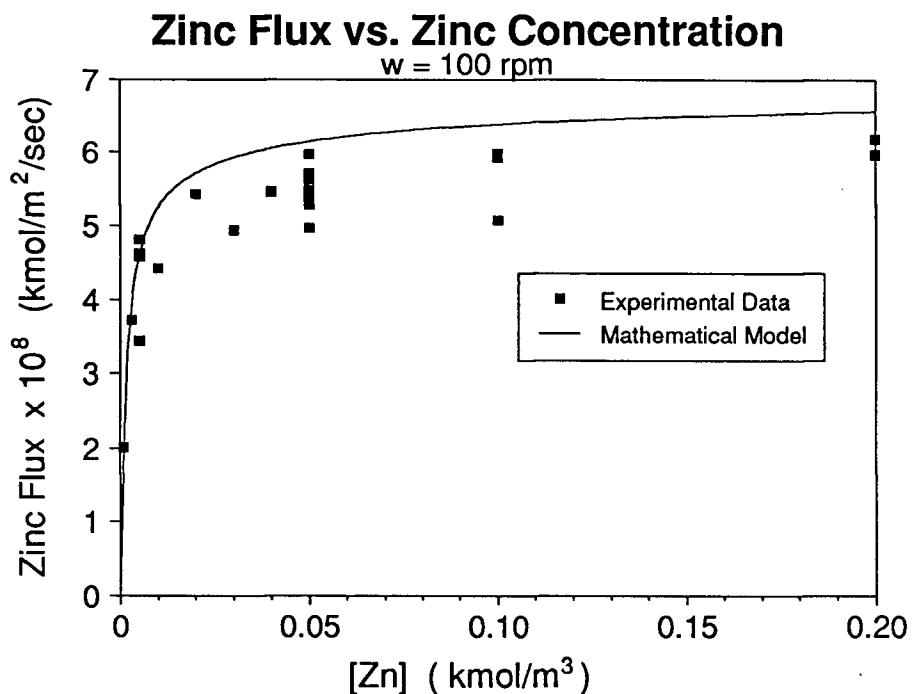


**Figure 4.9** Effect of changing bulk zinc concentration on zinc flux : Formal [D2EHPA] = 0.05 M, pH = 4.5, T = 25°C, filter = 0.45 $\mu$ m,  $\omega = 100 \text{ rpm}$

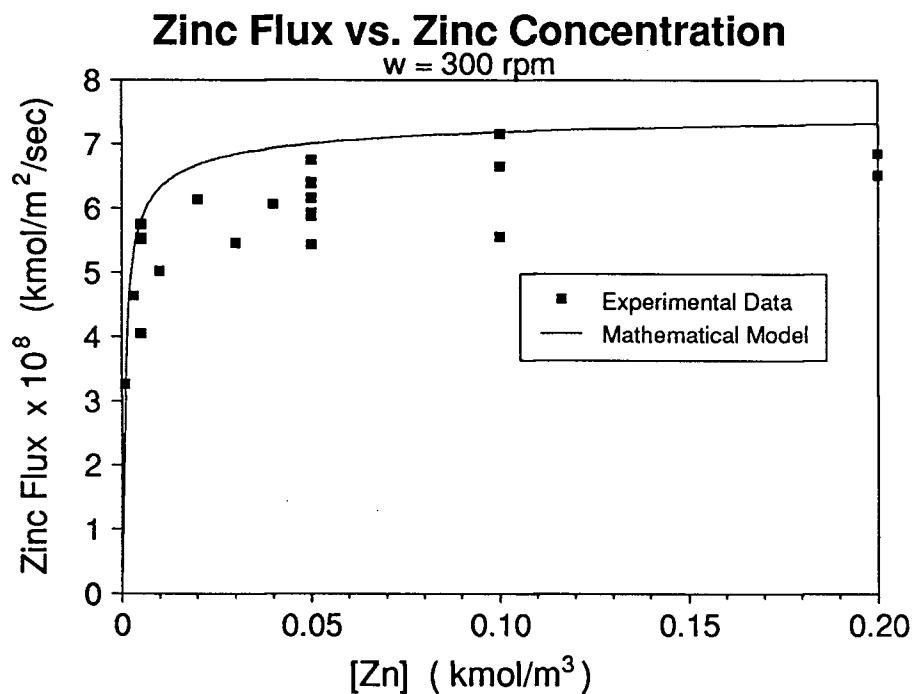


**Figure 4.10** Effect of changing bulk zinc concentration on zinc flux : Formal [D2EHPA] = 0.05 M, pH = 4.5, T = 25°C, filter = 0.45 $\mu$ m,  $\omega = 300 \text{ rpm}$

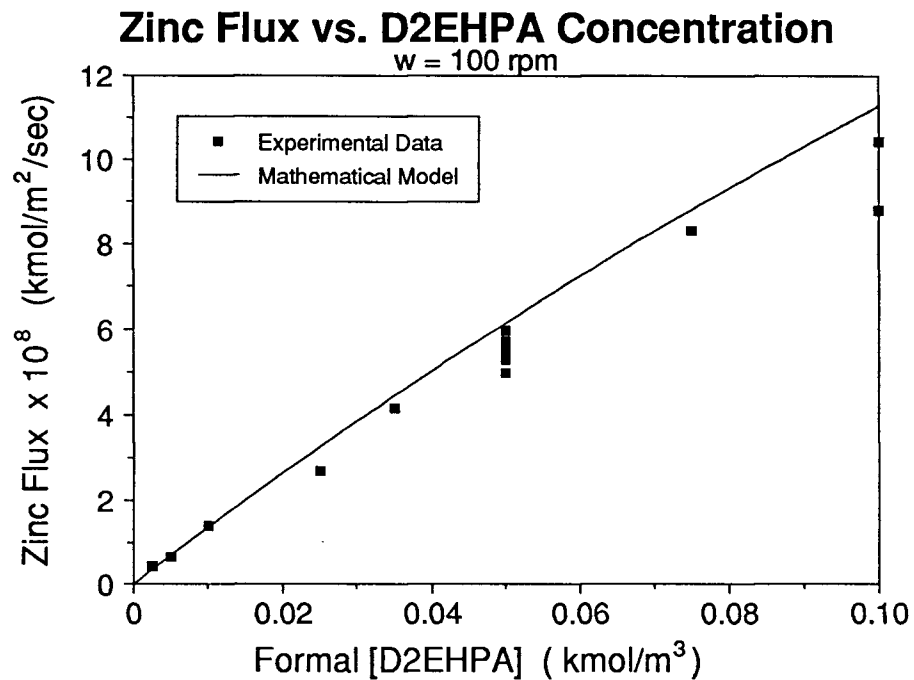


**Figure 4.11** Effect of changing D2EHPA concentration on zinc flux :  
 $[\text{Zn}] = 0.05\text{M}$ ,  $\text{pH} = 4.5$ ,  $T = 25^\circ\text{C}$ , filter =  $0.45\mu\text{m}$ ,  $\omega = 100 \text{ rpm}$

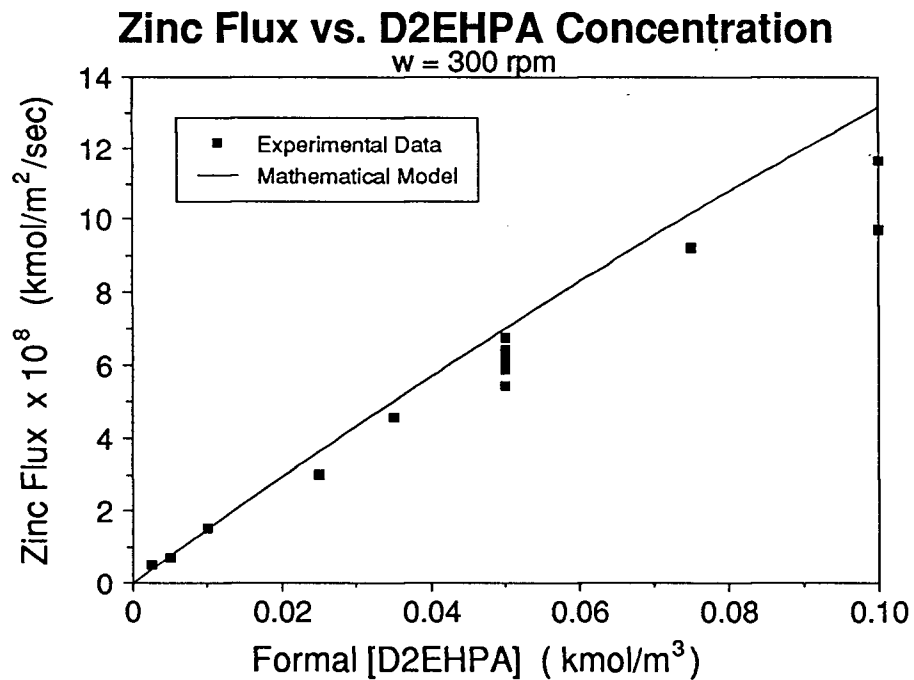


**Figure 4.12** Effect of changing D2EHPA concentration on zinc flux :  
 $[\text{Zn}] = 0.05\text{M}$ ,  $\text{pH} = 4.5$ ,  $T = 25^\circ\text{C}$ , filter =  $0.45\mu\text{m}$ ,  $\omega = 300 \text{ rpm}$

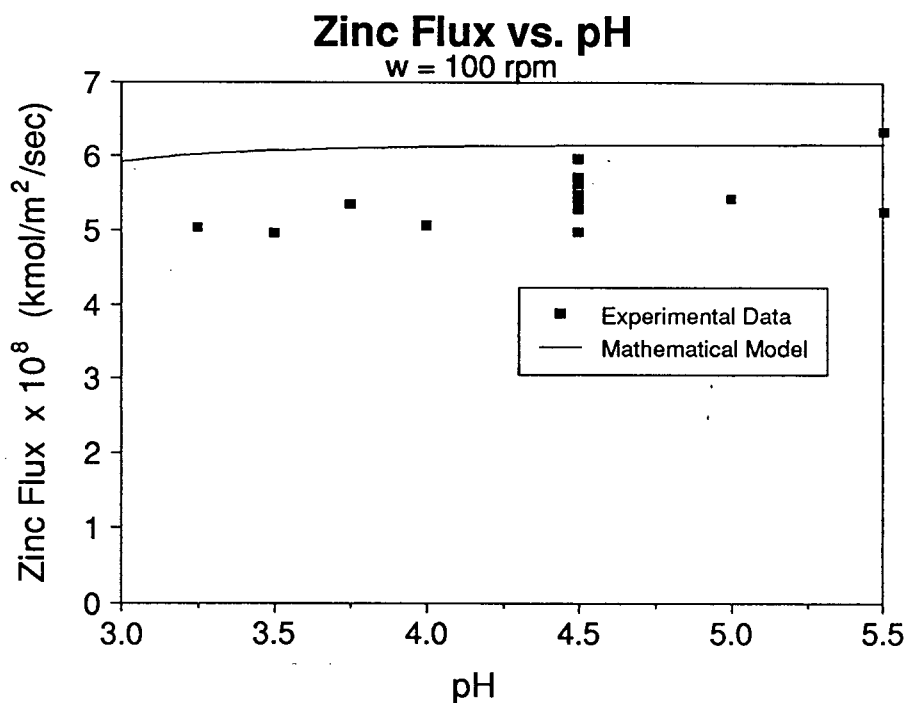


**Figure 4.13** Effect of changing bulk pH on zinc flux : [Zn] = 0.05M, Formal [D2EHPA] = 0.05 M, T = 25 °C, filter = 0.45 $\mu$ m,  $\omega$  = 100 rpm

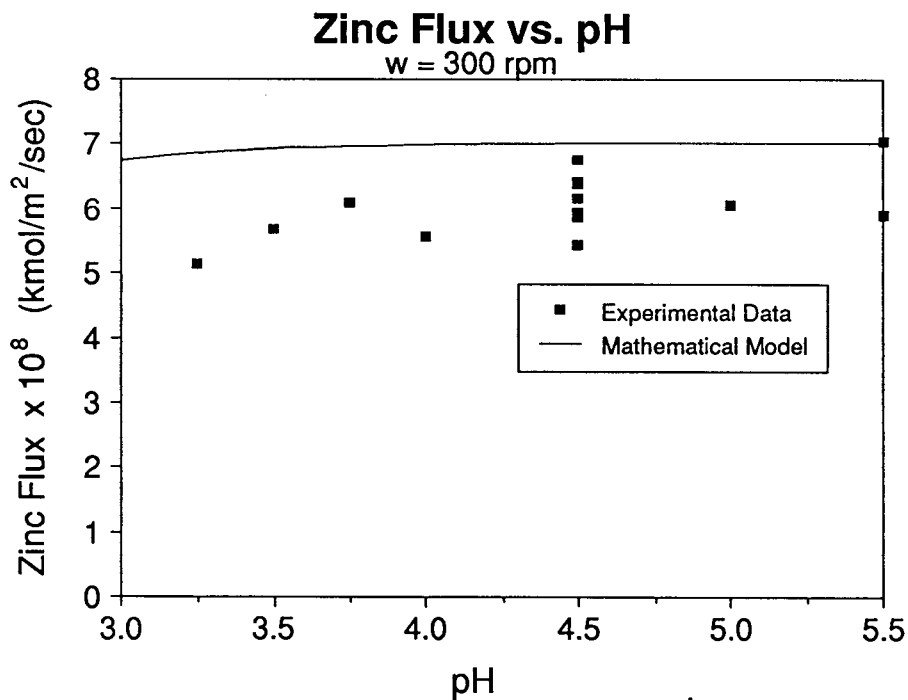


**Figure 4.14** Effect of changing bulk pH on zinc flux : [Zn] = 0.05M, Formal [D2EHPA] = 0.05 M, T = 25 °C, filter = 0.45 $\mu$ m,  $\omega$  = 300 rpm

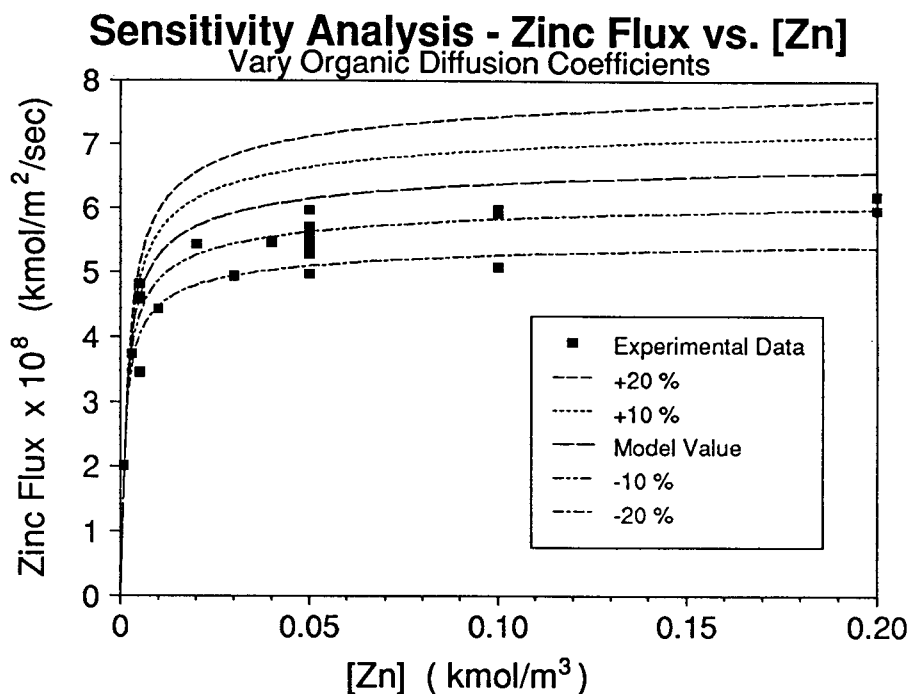


**Figure 4.15** Zinc flux vs. zinc concentration for changes in the organic species diffusion coefficients : Formal [D2EHPA] = 0.05 M, pH = 4.5, T = 25 °C, filter = 0.45 μm, ω = 100 rpm

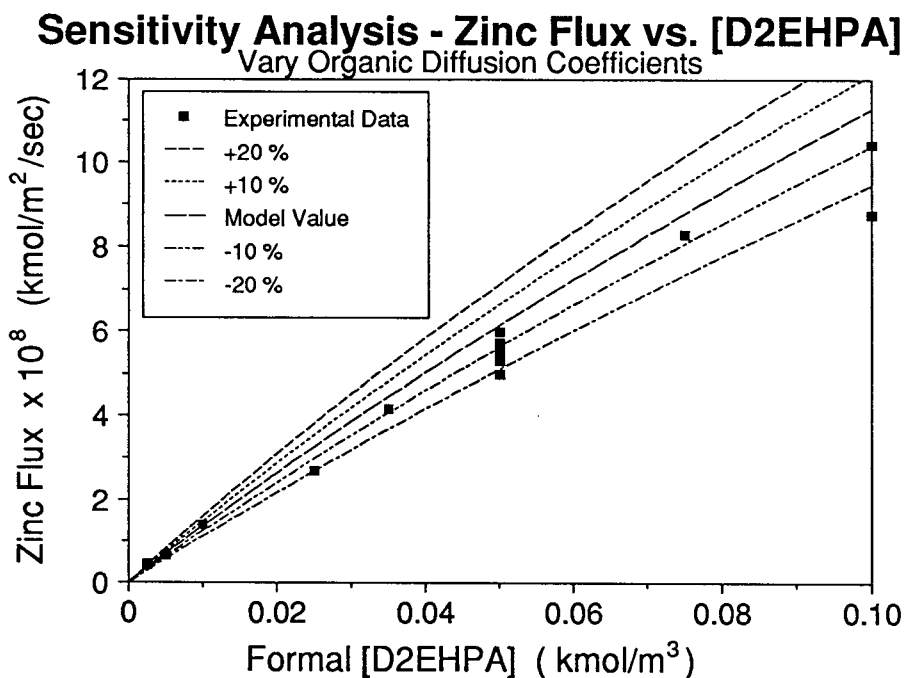


**Figure 4.16** Zinc flux vs. D2EHPA concentration for changes in the organic species diffusion coefficients : [Zn] = 0.05M, pH = 4.5, T = 25 °C, filter = 0.45 μm, ω = 100 rpm

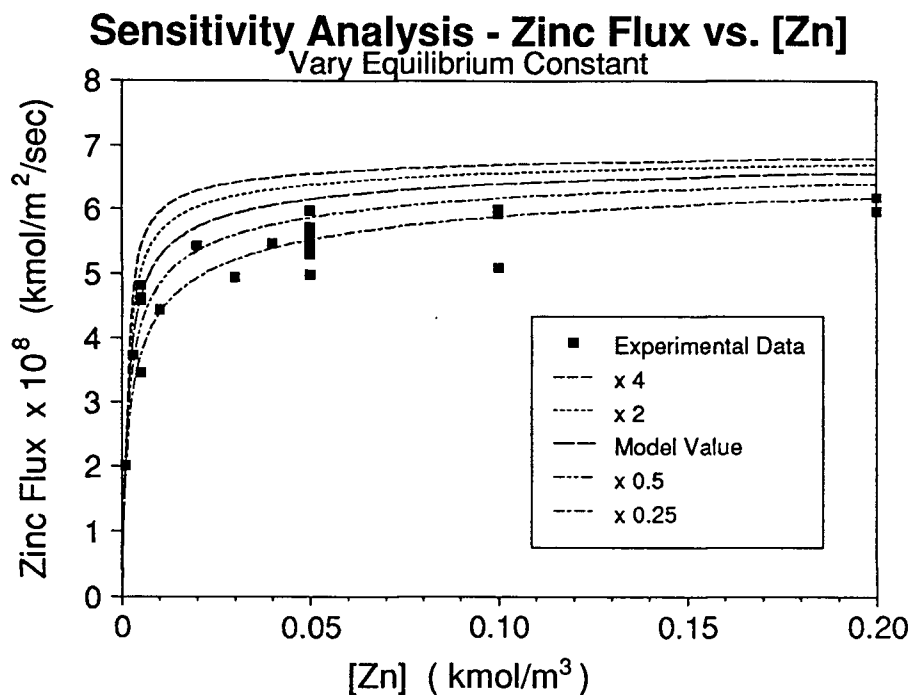


**Figure 4.17** Zinc flux vs. zinc concentration for changes in the equilibrium constant  $K_{eq}$  : Formal [D2EHPA] = 0.05 M, pH = 4.5, T = 25°C, filter = 0.45 $\mu$ m,  $\omega$  = 100 rpm

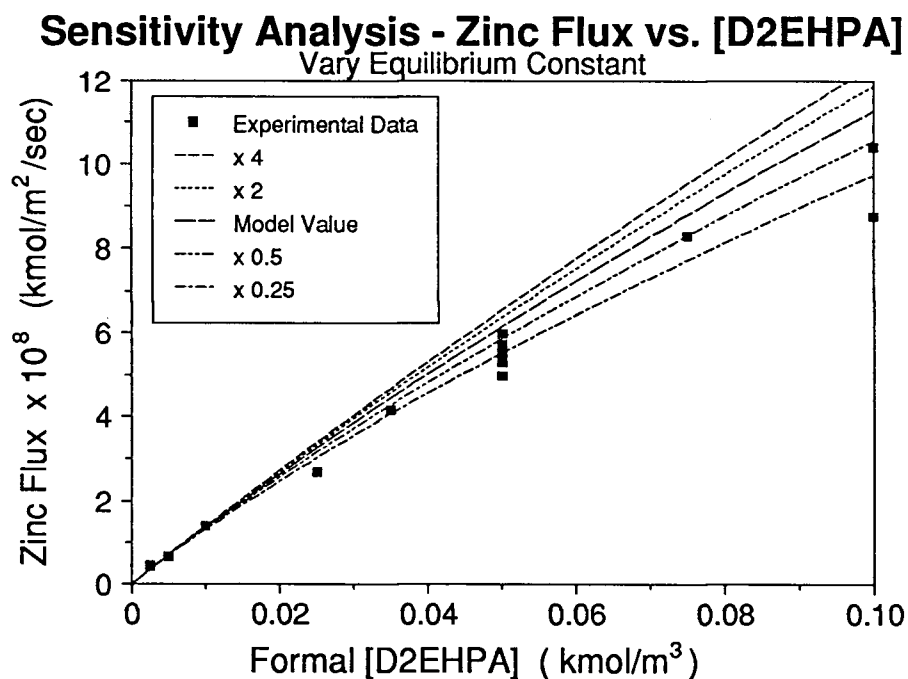


**Figure 4.18** Zinc flux vs. D2EHPA concentration for changes in the equilibrium constant  $K_{eq}$  : [Zn] = 0.05M, pH = 4.5, T = 25°C, filter = 0.45 $\mu$ m,  $\omega$  = 100 rpm

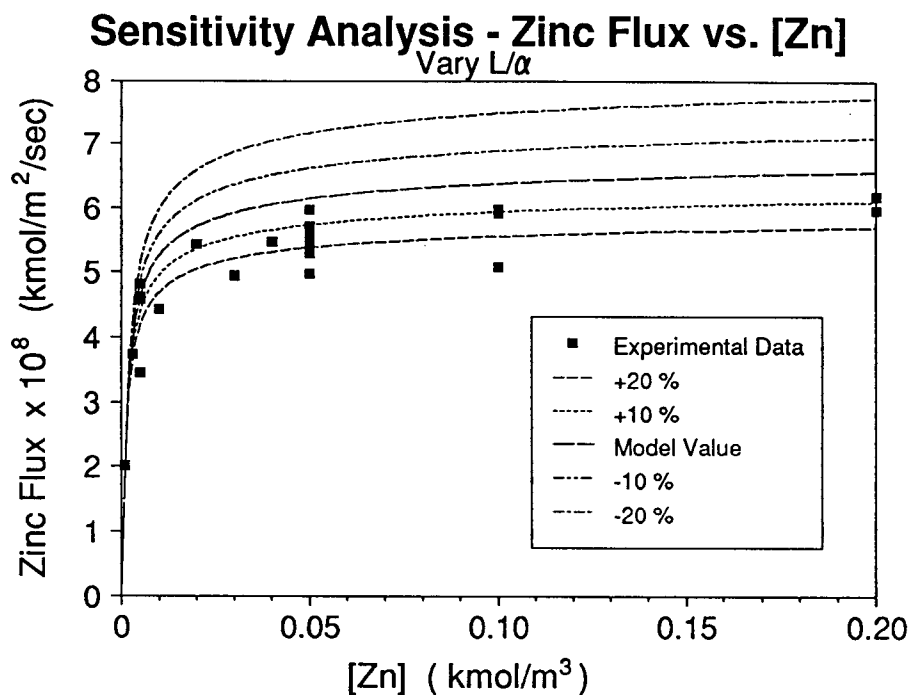


Figure 4.19 Zinc flux vs. zinc concentration for changes in the filter equivalent thickness  $L/\alpha$ : Formal [D2EHPA] = 0.05 M, pH = 4.5,  $T = 25^\circ\text{C}$ , filter =  $0.45\mu\text{m}$ ,  $\omega = 100 \text{ rpm}$

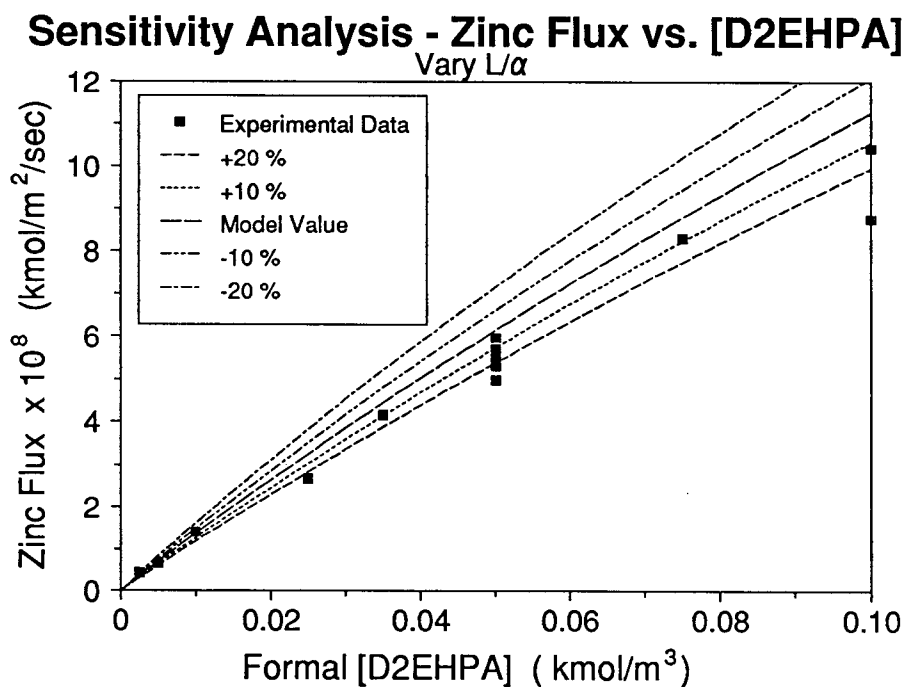


Figure 4.20 Zinc flux vs. D2EHPA concentration for changes in the filter equivalent thickness  $L/\alpha$ : [Zn] = 0.05M, pH = 4.5,  $T = 25^\circ\text{C}$ , filter =  $0.45\mu\text{m}$ ,  $\omega = 100 \text{ rpm}$

### 4.3.2 Basic Model Predictions

When the model was used to predict the zinc flux for any given set of conditions (bulk zinc concentration, formal bulk D2EHPA concentration, and bulk pH), the interfacial concentrations of the various species in the system were computed. In this section, some of the data produced by the model will be examined to see if they are consistent with the current understanding of the rate controlling processes.

Figures 4.21 - 4.24 examine the effect that bulk zinc concentration has on the association factor  $n$ , the interfacial pH, and the interfacial zinc and D2EHPA concentrations. At low bulk zinc concentrations aqueous mass transfer of  $Zn^{2+}$  is the rate controlling step, and as the zinc concentration increases the organic mass transfer of D2EHPA becomes rate controlling.

In Figure 4.21, at low bulk zinc concentrations the association factor is large, but it decreases rapidly as zinc concentration increases. This may be attributed to the transition from aqueous mass transfer of  $Zn^{2+}$  as the rate controlling step to organic mass transfer of D2EHPA. If D2EHPA transport is not rate controlling, then there exists an excess concentration of D2EHPA at the interface which is available for complexing zinc-extractant molecules.

Figure 4.22 examines the effect of zinc concentration on the interfacial pH. In the low zinc concentration region, where zinc transport is rate controlling, the flux increases with increasing zinc concentration, which causes the interfacial pH to decrease. Again, as the transition is made from zinc mass transfer control to D2EHPA mass transfer control, the zinc concentration has a decreasing effect on the flux, and therefore a decreasing effect on the interfacial pH.

When D2EHPA transport is rate controlling, only a small concentration gradient is required to maintain the zinc flux at the organic rate controlled limit. Thus, for concentrations above approximately  $0.01 \text{ kmol/m}^3$  (from Figure 4.23), the interfacial zinc concentration essentially remains at a fixed value below the bulk zinc concentration.

Figure 4.24 shows the predicted effect of bulk zinc concentration on the concentration of the various interfacial D2EHPA species. The D2EHPA concentration decreases with increasing zinc concentration, first rapidly, and then more slowly as D2EHPA mass transport becomes dominant.

Figures 4.25 - 4.28 examine the effect that bulk D2EHPA concentration has on the average association factor  $n_{avg}$ , the interfacial pH, and the interfacial zinc and D2EHPA concentrations. The average association factor,  $n_{avg}$ , is defined as the computed total flux of D2EHPA (expressed as dimer) divided by the computed zinc flux.

In Figure 4.25, the association factor increases with increasing D2EHPA concentration. This may be once again attributed to the amount of free D2EHPA available for complexation. In the entire concentration region examined, the rate controlling step is the organic mass transfer of D2EHPA. Thus, with increasing overall D2EHPA concentration there will be a small increase in the amount of free D2EHPA at the interface, resulting in some increase in the value of  $n_{avg}$ .

The decrease in interfacial pH with increasing D2EHPA concentration, as shown in Figure 4.26, is directly related to the increase in zinc flux. As the zinc flux increases, more  $H^+$  ions are generated at the interface, resulting in a larger concentration gradient across the aqueous boundary layer. The same mechanism results in a decrease in the interfacial zinc concentration, as seen in Figure 4.27, due to a faster rate of consumption of  $Zn^{2+}$  ions.

The decrease in interfacial  $Zn^{2+}$  concentration and the increase in interfacial  $H^+$  concentration with increasing bulk D2EHPA concentration result, for fixed equilibrium constant  $K_{ex}$ , in a larger interfacial D2EHPA concentration at equilibrium. Thus, although the zinc (and thus the D2EHPA) flux is increasing, the interfacial D2EHPA concentration also increases slightly to maintain equilibrium. This effect can be seen in Figure 4.28.

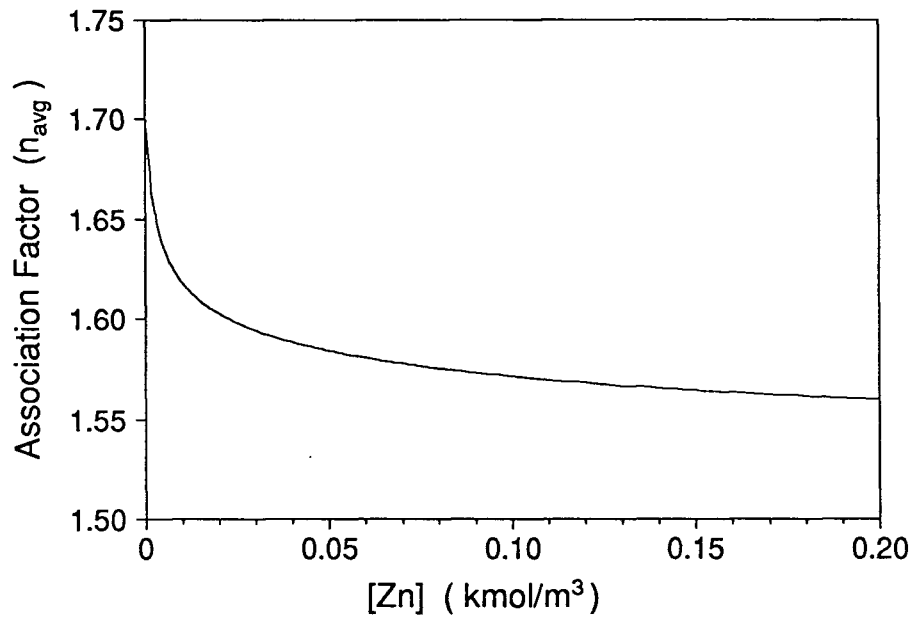
Figures 4.29 - 4.32 examine the effect that the bulk pH has on the association factor  $n_{avg}$ , the interfacial pH, and the interfacial zinc and D2EHPA concentrations. In the pH region examined, D2EHPA transport is the rate controlling step.

Figure 4.29 shows the effect of changes in pH on the value of  $n_{avg}$ . For low values of pH, the interfacial pH will decrease, resulting in a larger interfacial D2EHPA concentration, which will result in a slight increase in  $n_{avg}$ .

The interfacial pH increases slightly as the bulk pH is increased in order to keep the concentration gradient across the boundary layer at a relatively constant value (Figure 4.30). Since the flux is relatively constant across the entire pH range, there is little effect on either the interfacial zinc concentration or the interfacial D2EHPA concentration (Figures 4.31 and 4.32). The slight dip in flux at low pH values (c.f. Figure 4.13) is most likely caused by low interfacial pH values causing a shift in the extraction equilibrium.

---

### Association Factor ( $n_{avg}$ ) vs. Zinc Conc.



**Figure 4.21** Predicted change in association factor ( $n_{avg}$ ) with bulk zinc concentration : Formal  $[D2EHPA] = 0.05 \text{ M}$ ,  $\text{pH} = 4.5$ ,  $T = 25^\circ\text{C}$ , filter =  $0.45\mu\text{m}$ ,  $\omega = 100 \text{ rpm}$

---

### Interfacial pH vs. Zinc Concentration

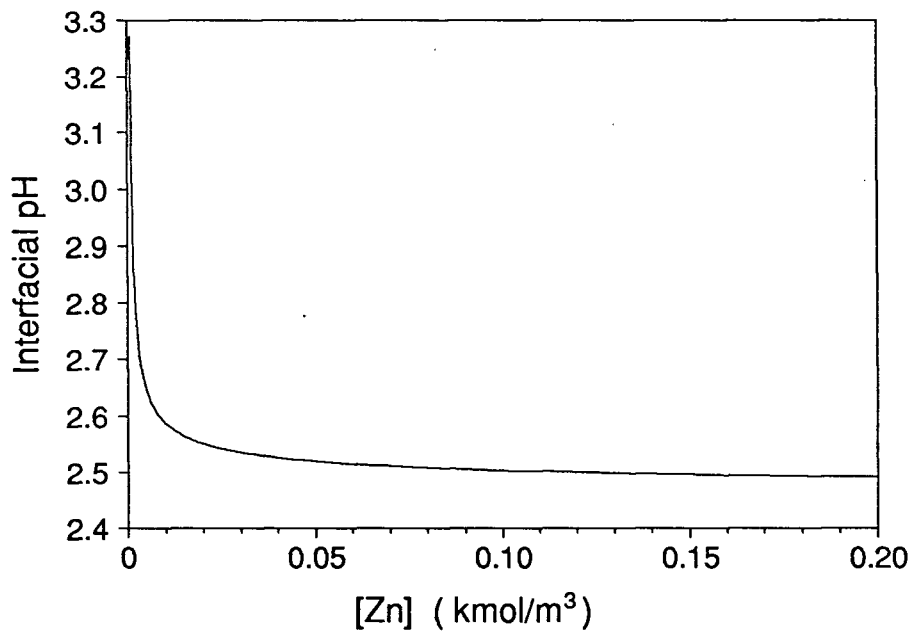


**Figure 4.22** Predicted change in interfacial pH with bulk zinc concentration : Formal  $[D2EHPA] = 0.05 \text{ M}$ ,  $\text{pH} = 4.5$ ,  $T = 25^\circ\text{C}$ , filter =  $0.45\mu\text{m}$ ,  $\omega = 100 \text{ rpm}$

---

---

### Interfacial Zinc Conc. vs. Bulk Zinc Conc.

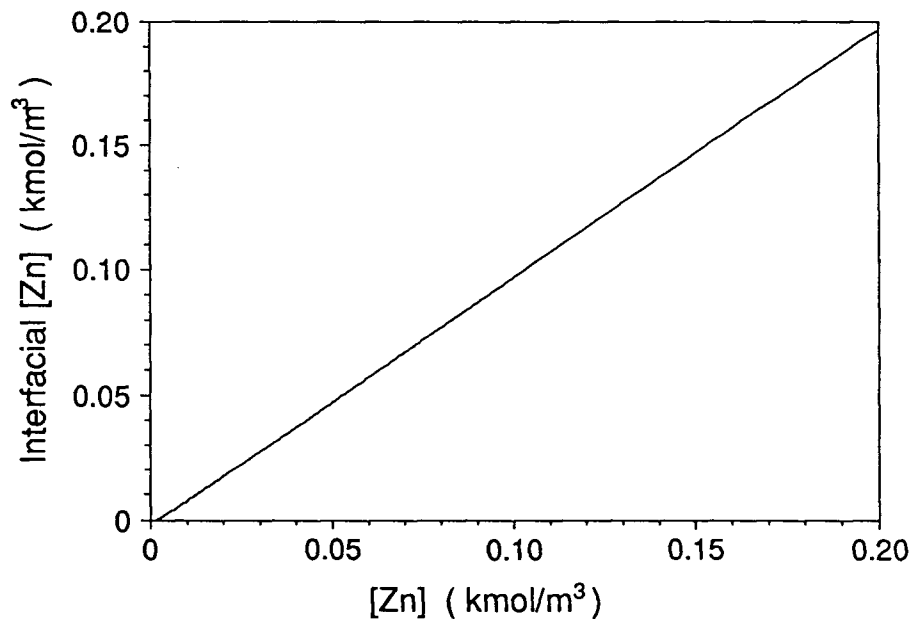


**Figure 4.23** Predicted change in interfacial zinc concentration with bulk zinc concentration : Formal [D2EHPA] = 0.05 M, pH = 4.5, T = 25°C, filter = 0.45 $\mu$ m,  $\omega$  = 100 rpm

---

### Interfacial D2EHPA Conc. vs. Zinc Conc.

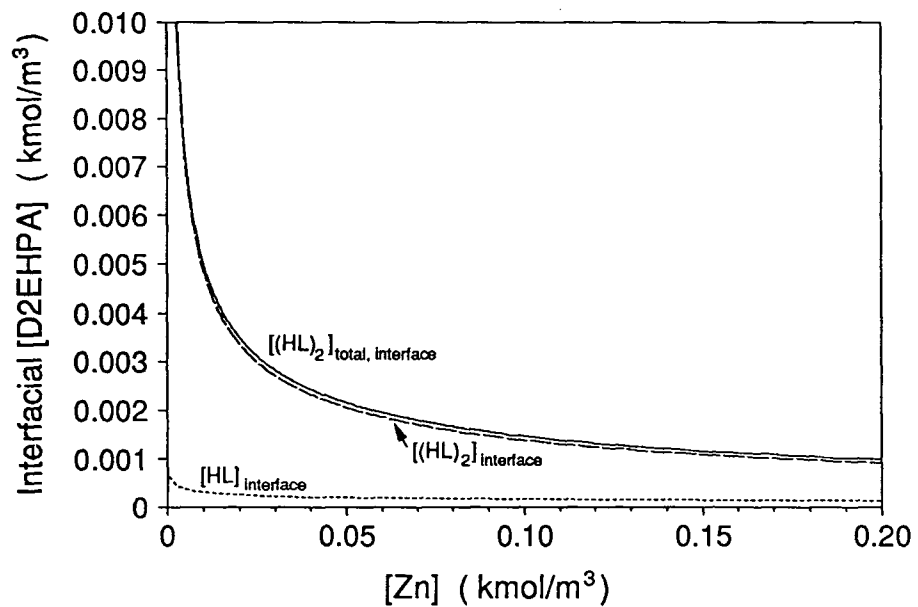


**Figure 4.24** Predicted change in interfacial D2EHPA concentration with bulk zinc concentration : Formal [D2EHPA] = 0.05 M, pH = 4.5, T = 25°C, filter = 0.45 $\mu$ m,  $\omega$  = 100 rpm

---

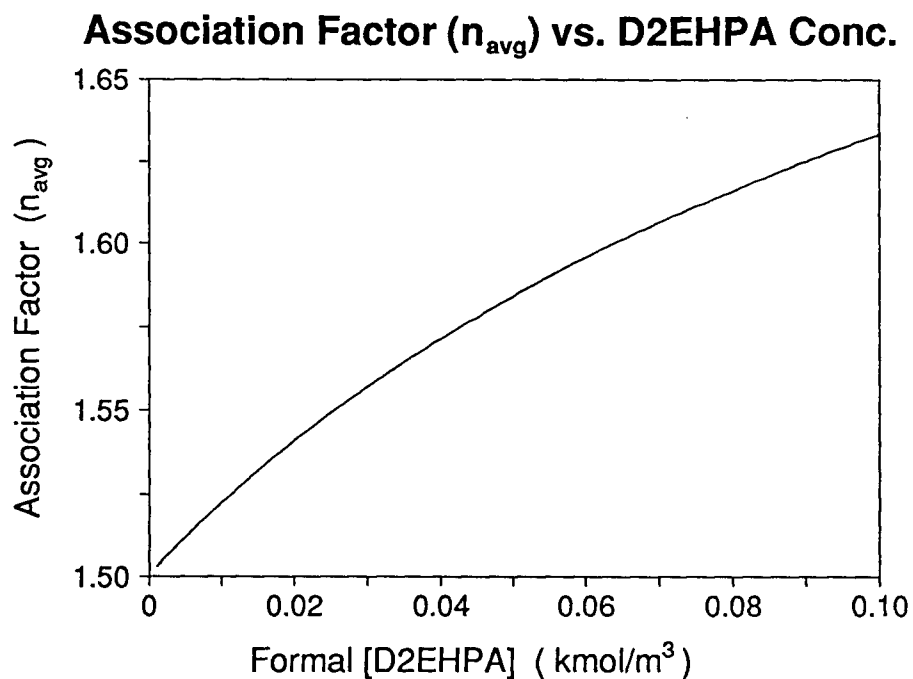


**Figure 4.25** Predicted change in association factor ( $n_{avg}$ ) with bulk D2EHPA concentration : [Zn] = 0.05M, pH = 4.5, T = 25°C, filter = 0.45 $\mu$ m,  $\omega$  = 100 rpm

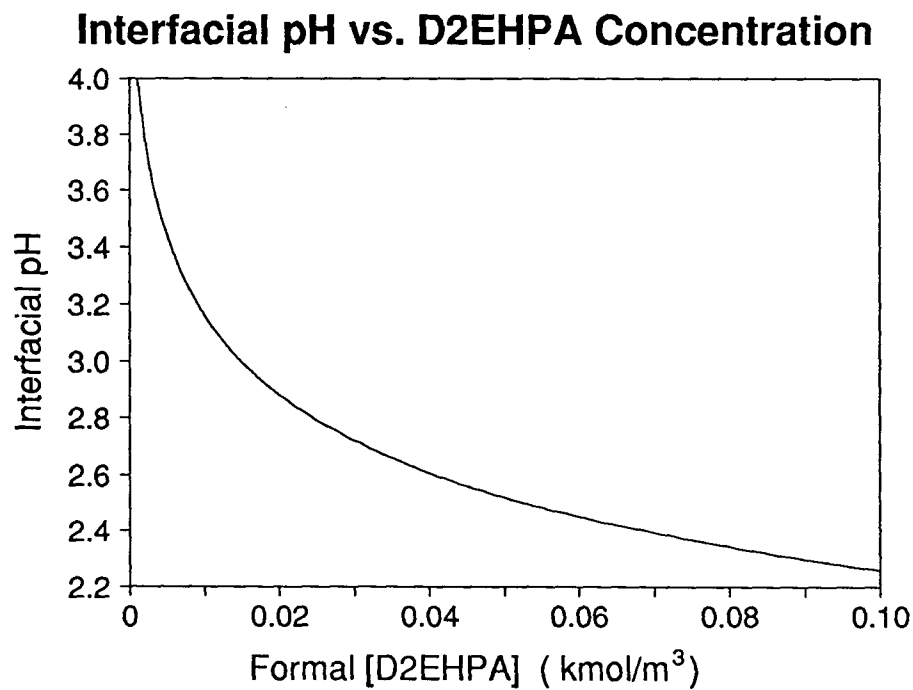


**Figure 4.26** Predicted change in interfacial pH with bulk D2EHPA concentration : [Zn] = 0.05M, pH = 4.5, T = 25°C, filter = 0.45 $\mu$ m,  $\omega$  = 100 rpm

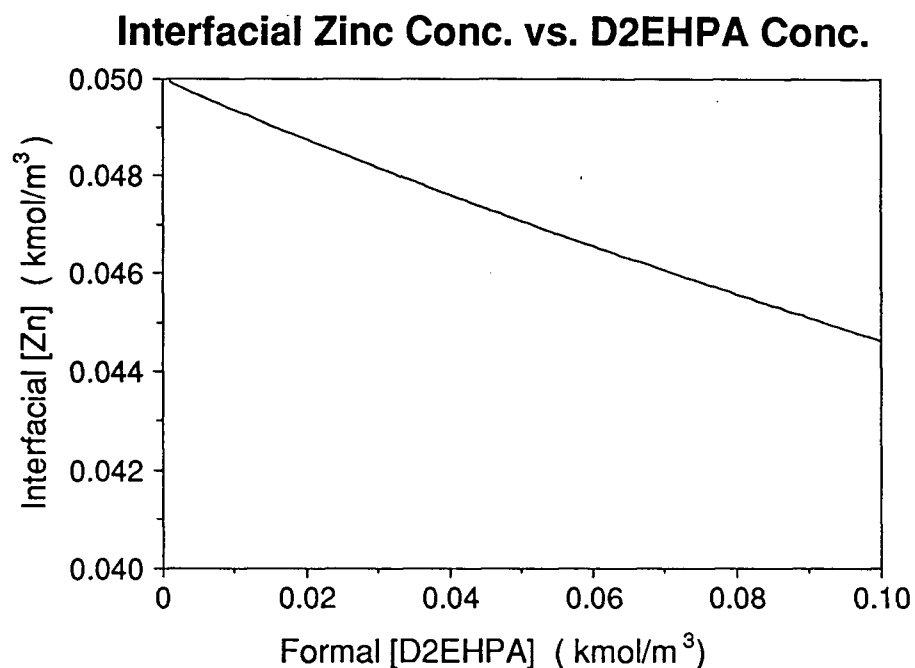


**Figure 4.27** Predicted change in interfacial zinc concentration with bulk D2EHPA concentration : [Zn] = 0.05M, pH = 4.5, T = 25°C, filter = 0.45 $\mu$ m,  $\omega$  = 100 rpm

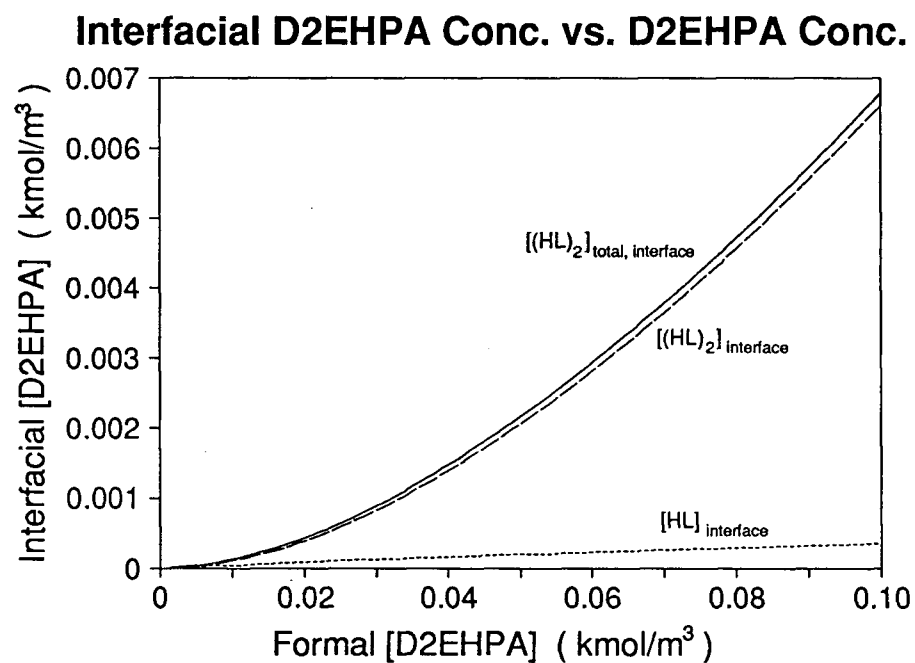


**Figure 4.28** Predicted change in interfacial D2EHPA concentration with bulk D2EHPA concentration : [Zn] = 0.05M, pH = 4.5, T = 25°C, filter = 0.45 $\mu$ m,  $\omega$  = 100 rpm

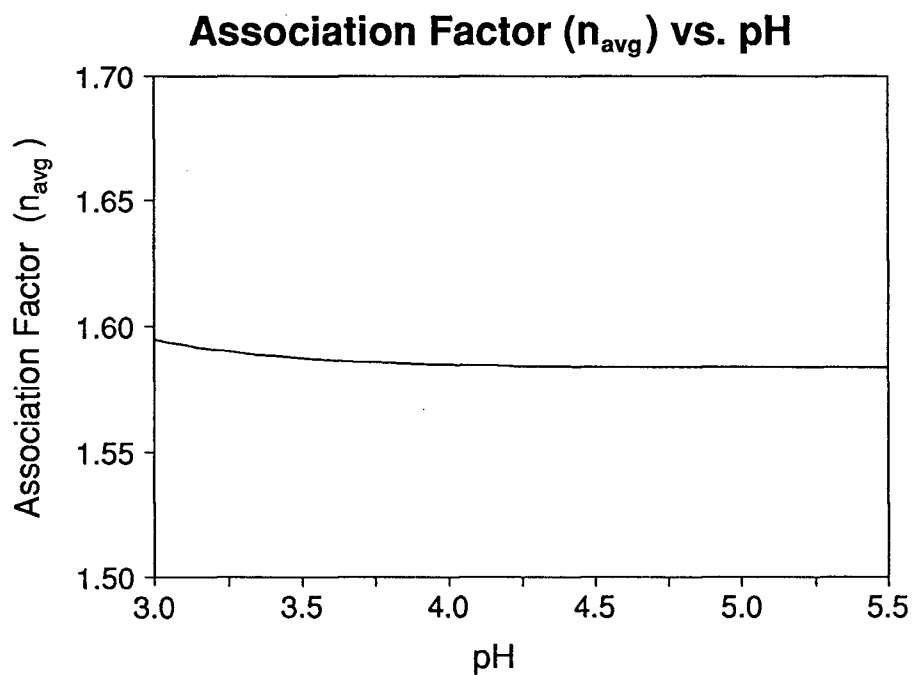


**Figure 4.29** Predicted change in association factor ( $n_{avg}$ ) with bulk pH :  
[Zn] = 0.05M, Formal [D2EHPA] = 0.05 M, T = 25 °C,  
filter = 0.45 $\mu$ m,  $\omega$  = 100 rpm

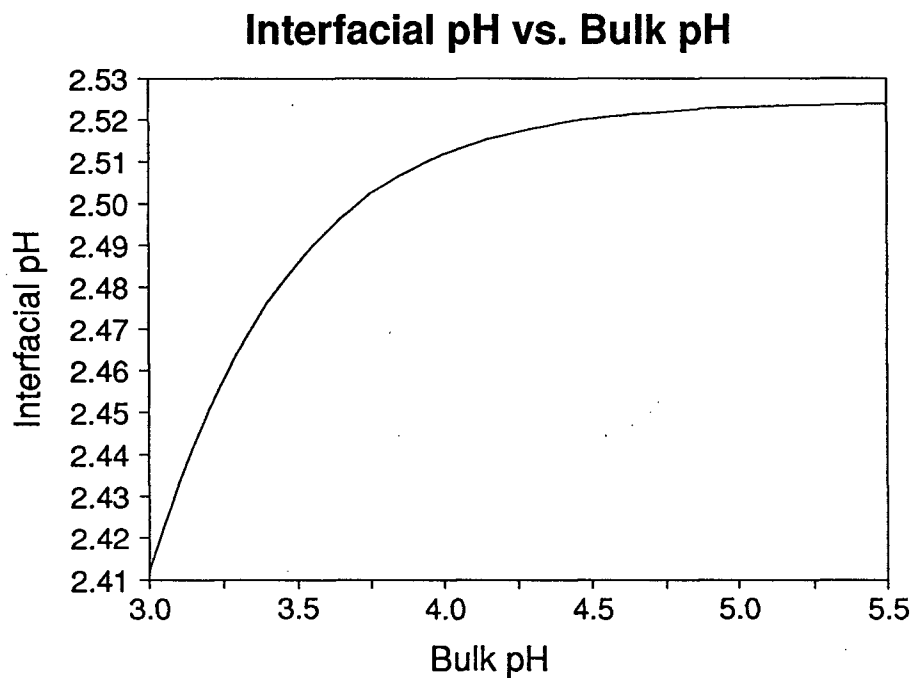


**Figure 4.30** Predicted change in interfacial pH with bulk pH : [Zn] = 0.05M,  
Formal [D2EHPA] = 0.05 M, T = 25 °C, filter = 0.45 $\mu$ m,  
 $\omega$  = 100 rpm

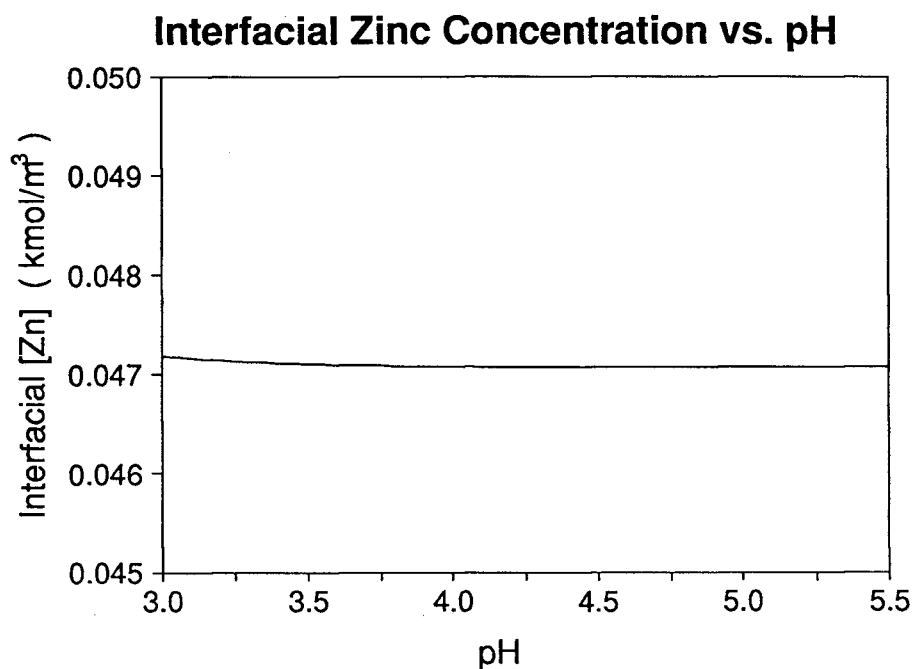


**Figure 4.31** Predicted change in interfacial zinc concentration with bulk pH :  
 [Zn] = 0.05M, Formal [D2EHPA] = 0.05 M, T = 25 °C,  
 filter = 0.45 $\mu$ m,  $\omega$  = 100 rpm

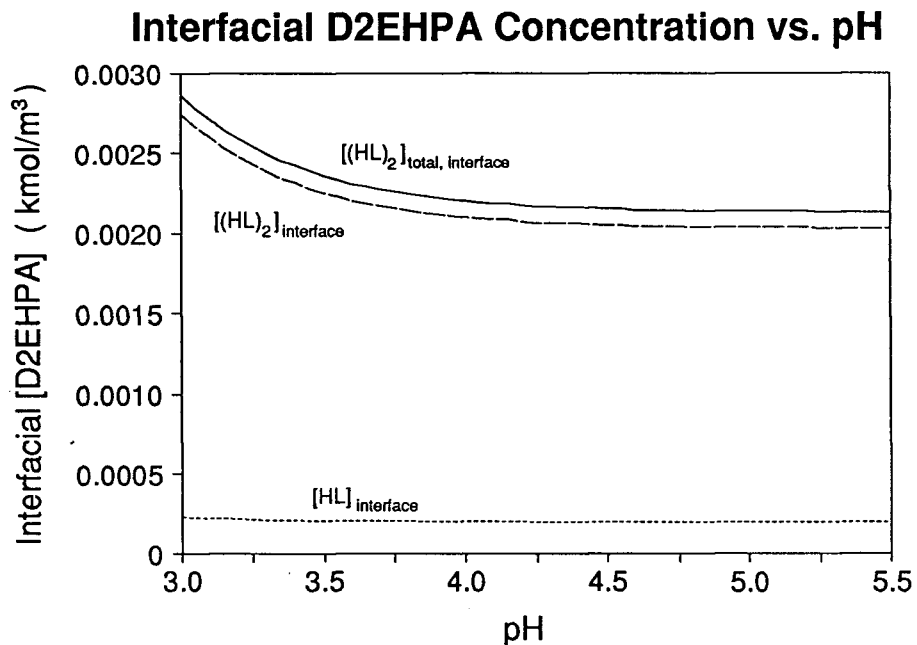


**Figure 4.32** Predicted change in interfacial D2EHPA concentration with bulk pH :  
 pH : [Zn] = 0.05M, Formal [D2EHPA] = 0.05 M, T = 25 °C,  
 filter = 0.45 $\mu$ m,  $\omega$  = 100 rpm

## 4.4 Extended Mathematical Model

The mathematical model presented in Section 4.2 was extended to incorporate the case where some of the extractant in the bulk organic phase is "tied up" with zinc. The amount of extractant tied up is defined by a percentage preload, where the preload is equal to the moles of zinc divided by the total molar content of D2EHPA (expressed as dimer). At low loadings, there will actually be less free D2EHPA than predicted by the preload, since the preload calculation assumes  $n=1$ , while  $n$  will be approximately equal to 1.7 at low loadings and only approach 1 near 100% preload.

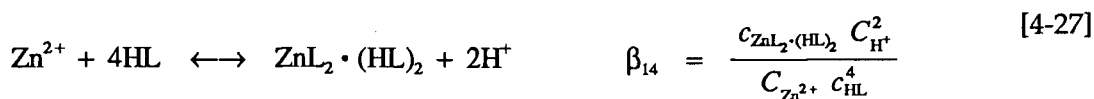
The conditions and equations for the aqueous phase are the same as those presented in Section 4.2.

In the organic phase, five possible species are now considered: HL, (HL)<sub>2</sub>, ZnL<sub>2</sub>, ZnL<sub>2</sub>·HL, and ZnL<sub>2</sub>·(HL)<sub>2</sub>. Each of these species exists both at the interface and in the organic bulk. Furthermore, at both the bulk and the interface, the concentrations of these five species are interrelated by a series of equilibria. The values input into the model are the total concentration of zinc in the organic bulk (expressed as preload) and the total concentration of D2EHPA in the bulk. The model must then compute the speciation of zinc and D2EHPA; the computation of the amount of free D2EHPA is particularly critical, since D2EHPA beyond the stoichiometric requirement is tied up with ZnL<sub>2</sub>·HL and ZnL<sub>2</sub>·(HL)<sub>2</sub>. It is still assumed that there is no redistribution of speciation across the boundary layer; however, this model accommodates the speciation and diffusion of both D2EHPA species.

The following derivation of the basic model equations will where necessary re-state those equations which are presented in Section 4.2 so that continuity of the derivation will be maintained. Again, the following discussion only focuses on the theoretical basis for the extended mathematical model; source code is given in Appendix E.

The extraction stoichiometry for zinc reacting with monomeric D2EHPA to form a zinc-extractant complex with zero to two associated D2EHPA ligands can be expressed as:





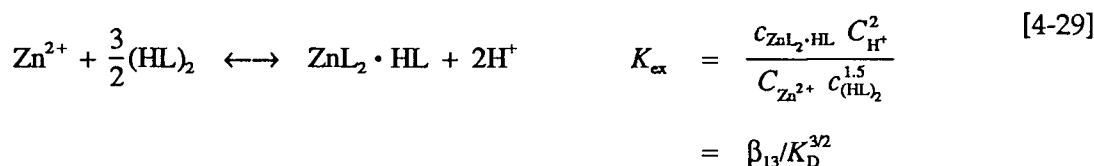
where  $\beta_{12}$ ,  $\beta_{13}$ , and  $\beta_{14}$  are the formation constants for the species  $\text{ZnL}_2$ ,  $\text{ZnL}_2 \cdot \text{HL}$ , and  $\text{ZnL}_2 \cdot (\text{HL})_2$  respectively.

A similar expression can be developed for the dimerization equilibrium between the monomeric and dimeric form of D2EHPA:



where  $K_D$  is the dimerization constant for D2EHPA. Using this expression, if either the concentration of monomeric or dimeric D2EHPA is known at any point in the organic, then the concentration of dimeric or monomeric D2EHPA, respectively, may be calculated.

An expression for the extraction of zinc (as  $\text{ZnL}_2 \cdot \text{HL}$ ) by D2EHPA in the dimeric form can be developed by combining equations [4-26] and [4-28]:



Equations can be developed from equations [4-25], [4-26], and [4-27] which interrelate the speciation of  $\text{ZnL}_2$ ,  $\text{ZnL}_2 \cdot \text{HL}$ , and  $\text{ZnL}_2 \cdot (\text{HL})_2$  as follows:



The quotient  $\beta_{1m}/\beta_{1(m+1)}$  is equal to the stepwise formation constant  $K_{m+1}$ .

At any point in the organic, the zinc species  $\text{ZnL}_2$ ,  $\text{ZnL}_2 \cdot \text{HL}$ , and  $\text{ZnL}_2 \cdot (\text{HL})_2$  are related by the following equations:

$$c_{\text{Zn, total}} = c_{\text{ZnL}_2} + c_{\text{ZnL}_2 \cdot \text{HL}} + c_{\text{ZnL}_2 \cdot (\text{HL})_2} \quad [4-32]$$

and

$$c_{ZnL_2} = \frac{c_{ZnL_2 \cdot HL} \beta_{12}/\beta_{13}}{c_{HL}} \quad [4-33]$$

$$c_{ZnL_2 \cdot (HL)_2} = \frac{c_{ZnL_2 \cdot HL} c_{HL}}{\beta_{13}/\beta_{14}} \quad [4-34]$$

Combining equations [4-32], [4-33], and [4-34],

$$c_{Zn,total} = \left[ \frac{c_{ZnL_2 \cdot HL} \beta_{12}/\beta_{13}}{c_{HL}} \right] + c_{ZnL_2 \cdot HL} + \left[ \frac{c_{ZnL_2 \cdot HL} c_{HL}}{\beta_{13}/\beta_{14}} \right] \quad [4-35]$$

$$\therefore c_{ZnL_2 \cdot HL} = \frac{c_{Zn,total}}{\frac{\beta_{12}/\beta_{13}}{c_{HL}} + 1 + \frac{c_{HL}}{\beta_{13}/\beta_{14}}} \quad [4-36]$$

Performing a mass balance over the entire organic/interface region for zinc and "L", for zinc,

$$-J_{Zn,total} + J_{ZnL_2} + J_{ZnL_2 \cdot HL} + J_{ZnL_2 \cdot (HL)_2} = 0 \quad [4-37]$$

$$J_{Zn,total} = J_{ZnL_2} + J_{ZnL_2 \cdot HL} + J_{ZnL_2 \cdot (HL)_2} \quad [4-38]$$

and for "L",

$$J_{HL} + 2J_{(HL)_2} + 2J_{ZnL_2} + 3J_{ZnL_2 \cdot HL} + 4J_{ZnL_2 \cdot (HL)_2} = 0 \quad [4-39]$$

Expanding equation [4-38],

$$J_{Zn,total} = -k_{ZnL_2} (c_{ZnL_2}^b - c_{ZnL_2}^i) - k_{ZnL_2 \cdot HL} (c_{ZnL_2 \cdot HL}^b - c_{ZnL_2 \cdot HL}^i) - k_{ZnL_2 \cdot (HL)_2} (c_{ZnL_2 \cdot (HL)_2}^b - c_{ZnL_2 \cdot (HL)_2}^i) \quad [4-40]$$

$$J_{Zn,total} = k_{ZnL_2} c_{ZnL_2}^i + k_{ZnL_2 \cdot HL} c_{ZnL_2 \cdot HL}^i + k_{ZnL_2 \cdot (HL)_2} c_{ZnL_2 \cdot (HL)_2}^i - \left( k_{ZnL_2} c_{ZnL_2}^b + k_{ZnL_2 \cdot HL} c_{ZnL_2 \cdot HL}^b + k_{ZnL_2 \cdot (HL)_2} c_{ZnL_2 \cdot (HL)_2}^b \right) \quad [4-41]$$

let

$$KCZnbulk = k_{ZnL_2} c_{ZnL_2}^b + k_{ZnL_2 \cdot HL} c_{ZnL_2 \cdot HL}^b + k_{ZnL_2 \cdot (HL)_2} c_{ZnL_2 \cdot (HL)_2}^b$$

$$\therefore J_{Zn,total} = k_{ZnL_2} c_{ZnL_2}^i + k_{ZnL_2 \cdot HL} c_{ZnL_2 \cdot HL}^i + k_{ZnL_2 \cdot (HL)_2} c_{ZnL_2 \cdot (HL)_2}^i - KCZnbulk \quad [4-42]$$

Substitute in values of  $c_{ZnL_2}$  and  $c_{ZnL_2 \cdot (HL)_2}$  from equations [4-33] and [4-34],

$$J_{Zn,total} = k_{ZnL_2} \left[ \frac{c_{ZnL_2 \cdot HL}^i \beta_{12}/\beta_{13}}{c_{HL}^i} \right] + k_{ZnL_2 \cdot HL} c_{ZnL_2 \cdot HL}^i \quad [4-43]$$

$$+ k_{ZnL_2 \cdot (HL)_2} \left[ \frac{c_{ZnL_2 \cdot HL}^i c_{HL}^i}{\beta_{13}/\beta_{14}} \right] - KCZnbulk$$

$$\therefore c_{ZnL_2 \cdot HL}^i = \frac{J_{Zn,total} + KCZnbulk}{k_{ZnL_2} \frac{\beta_{12}/\beta_{13}}{c_{HL}^i} + k_{ZnL_2 \cdot HL} + k_{ZnL_2 \cdot (HL)_2} \frac{c_{HL}^i}{\beta_{13}/\beta_{14}}} \quad [4-44]$$

Note that in this equation  $c_{ZnL_2 \cdot HL}^i$  is a function of  $J_{Zn,total}$ ,  $KCZnbulk$ , and  $c_{HL}^i$ .

Expanding equation [4-39],

$$k_{HL}(c_{HL}^i - c_{HL}^b) + 2k_{(HL)_2}(c_{(HL)_2}^i - c_{(HL)_2}^b) + 2k_{ZnL_2}(c_{ZnL_2}^i - c_{ZnL_2}^b) \quad [4-45]$$

$$+ 3k_{ZnL_2 \cdot HL}(c_{ZnL_2 \cdot HL}^i - c_{ZnL_2 \cdot HL}^b) + 4k_{ZnL_2 \cdot (HL)_2}(c_{ZnL_2 \cdot (HL)_2}^i - c_{ZnL_2 \cdot (HL)_2}^b) = 0$$

$$k_{HL}c_{HL}^i + 2k_{(HL)_2}c_{(HL)_2}^i + 2k_{ZnL_2}c_{ZnL_2}^i + 3k_{ZnL_2 \cdot HL}c_{ZnL_2 \cdot HL}^i + 4k_{ZnL_2 \cdot (HL)_2}c_{ZnL_2 \cdot (HL)_2}^i \quad [4-46]$$

$$- \left( k_{HL}c_{HL}^b + 2k_{(HL)_2}c_{(HL)_2}^b + 2k_{ZnL_2}c_{ZnL_2}^b + 3k_{ZnL_2 \cdot HL}c_{ZnL_2 \cdot HL}^b + 4k_{ZnL_2 \cdot (HL)_2}c_{ZnL_2 \cdot (HL)_2}^b \right) = 0$$

let

$$KCbulk = k_{HL}c_{HL}^b + 2k_{(HL)_2}c_{(HL)_2}^b + 2k_{ZnL_2}c_{ZnL_2}^b + 3k_{ZnL_2 \cdot HL}c_{ZnL_2 \cdot HL}^b + 4k_{ZnL_2 \cdot (HL)_2}c_{ZnL_2 \cdot (HL)_2}^b$$

$$\therefore k_{HL}c_{HL}^i + 2k_{(HL)_2}c_{(HL)_2}^i + 2k_{ZnL_2}c_{ZnL_2}^i + 3k_{ZnL_2 \cdot HL}c_{ZnL_2 \cdot HL}^i \quad [4-47]$$

$$+ 4k_{ZnL_2 \cdot (HL)_2}c_{ZnL_2 \cdot (HL)_2}^i - KCbulk = 0$$

From equations [4-28], [4-33], and [4-34], equation [4-47] can be rewritten as:

$$k_{HL}c_{HL}^i + 2k_{(HL)_2} \left[ K_D c_{HL}^i \right]^2 + 2k_{ZnL_2} \left[ \frac{c_{ZnL_2 \cdot HL}^i \beta_{12}/\beta_{13}}{c_{HL}^i} \right] \quad [4-48]$$

$$+ 3k_{ZnL_2 \cdot HL}c_{ZnL_2 \cdot HL}^i + 4k_{ZnL_2 \cdot (HL)_2} \left[ \frac{c_{ZnL_2 \cdot HL}^i c_{HL}^i}{\beta_{13}/\beta_{14}} \right] - KCbulk = 0$$

From equation [4-44], an expression has been developed for  $c_{ZnL_2 \cdot HL}^i$  as a function of  $c_{HL}^i$  and  $J_{Zn,total}$ .

If a value is assumed for  $J_{Zn,total}$  then equation [4-48] can be solved by iterating  $c_{HL}^i$ . The other

variables can then be solved for via equations [4-28], [4-44], [4-33], and [4-34]. The method of solution is then the same as in the simple mathematical model; the interfacial concentrations are substituted into expression for  $K_{ex}$  (equation [4-49]):

$$\frac{c_{ZnL_2 \cdot HL}^i C_{H^+}^{i 2}}{C_{Zn}^i c_{(HL)_2}^{i 1.5}} - K_{ex} = f(J_{Zn, total}) \quad [4-49]$$

where  $f(J_{Zn, total})$  should equal 0, and the correct value for the flux  $J_{Zn, total}$  can be determined by iterating  $J_{Zn, total}$  until  $f(J_{Zn, total})$  converges. A general flowchart showing the basic program structure of the extended mathematical model is shown in Figure 4.33.

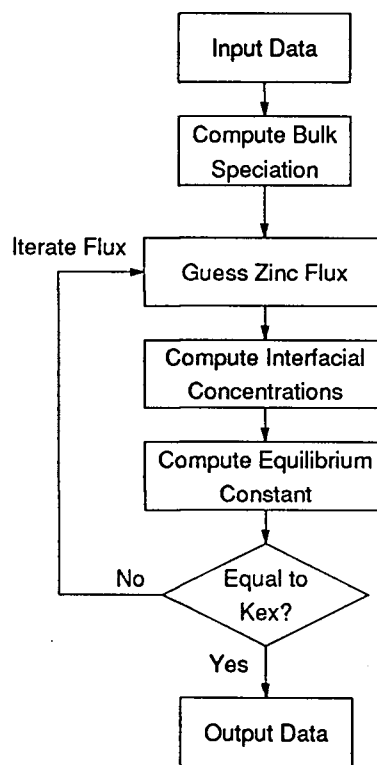


**Figure 4.33** Basic program structure of the extended mathematical model

## 4.5 Preload Results

An important part of this study was the examination of the effects that loading of the organic had on the overall extraction rate. Most academic studies of solvent extraction kinetics have used unloaded organic phases, producing values for the initial extraction rate. However, in industrial solvent extraction processes, circuits typically operate to high organic loadings. Extraction kinetics are likely quite different, since as loading increases the number of additional D2EHPA molecules complexing the species will change.

### 4.5.1 Extended Model Verification

In the preload experiments, the amount of zinc contained in the organic bulk was varied from 10% to 90% preload; total D2EHPA concentration was maintained at 0.05 F.

For the mathematical model, it was necessary to assume a value for the ratio of the formation constants of the  $ZnL_2$  and  $ZnL_2 \cdot HL$  species,  $\beta_{12}/\beta_{13}$ , as a suitable value could not be obtained from the literature. The best value of  $\beta_{12}/\beta_{13}$  was evaluated by substituting different values into the extended mathematical model; a graphical representation of the effects of different values of  $\beta_{12}/\beta_{13}$  are shown in Figure 4.34. For the purposes of evaluating the behaviour of the system,  $\beta_{12}/\beta_{13}$  was set equal to  $6 \times 10^{-5}$ , which gave a fairly good fit to the experimental results in the high preload range.

For any value of  $\beta_{12}/\beta_{13}$  selected, the model fit is rather poor over the preload range. A small value of  $\beta_{12}/\beta_{13}$  provides a fairly good fit at low preload values, but prevents significant amounts of the  $ZnL_2$  complex from forming at high preload values: A larger value of  $\beta_{12}/\beta_{13}$  fits better in the intermediate to high preload concentration range, but overpredicts the initial zinc flux. This effect is due to the predicted formation of a significant amount of  $ZnL_2$ , which has a higher diffusion coefficient than either  $ZnL_2 \cdot HL$  or  $ZnL_2 \cdot (HL)_2$ , and requires no additional HL molecules for complexation. Thus, in the case where the system is rate controlled by the diffusion of HL, the overall zinc flux will be higher.

No correction in the mathematical model is made for the change in viscosity which occurs as the extractant polymerizes at high loadings (c.f Figure 2.4). Since the diffusion

## Zinc Flux vs. Preload

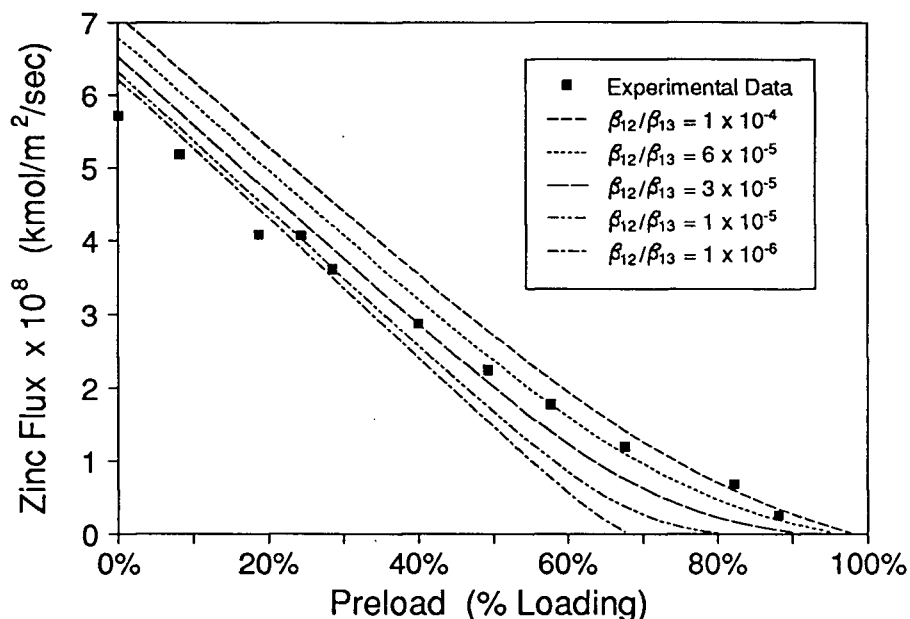


**Figure 4.34** Comparison of experimental data and extended model predictions for flux vs. preload for selected values of  $\beta_{12}/\beta_{13}$ :  
 $[\text{Zn}] = 0.05\text{M}$ , Formal  $[\text{D2EHPA}]_{\text{total}} = 0.05\text{ M}$ ,  $\text{pH} = 4.5$ ,  $T = 25^\circ\text{C}$ ,  
 filter =  $0.45\mu\text{m}$ ,  $\omega = 100\text{ rpm}$

coefficient is a function of the viscosity, it will also change, creating another source of error. Also, the assumption that there is no speciation redistribution in the boundary layer is highly suspect, as will be shown later.

The predicted zinc flux vs. preload is compared with experimental data in Figures 4.35 and 4.36. As outlined earlier, the model overpredicts the zinc flux at low preloads, and fits the data acceptably at high preloads for the given  $\beta_{12}/\beta_{13}$ .

The effect of different values of the organic side diffusion coefficients, the equilibrium constant  $K_{ex}$ , and the filter equivalent thickness  $L/\alpha$  on the predictions of the extended mathematical model were examined, with the results shown in Figures 4.37 through 4.39. Again, the extraction rate is quite sensitive to both the organic side diffusion coefficients and the filter equivalent thickness, but relatively insensitive to changes in  $K_{ex}$ .

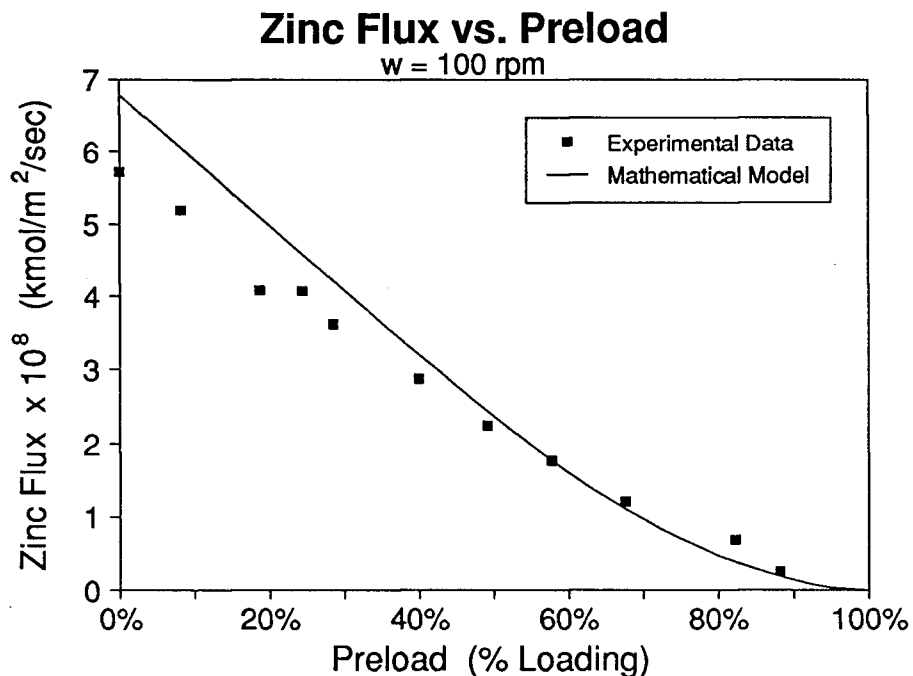


**Figure 4.35** Effect of preload on zinc flux :  $[\text{Zn}] = 0.05\text{M}$ , Formal  
 $[\text{D2EHPA}]_{\text{total}} = 0.05 \text{ M}$ ,  $\text{pH} = 4.5$ ,  $T = 25^\circ\text{C}$ , filter =  $0.45\mu\text{m}$ ,  
 $\omega = 100 \text{ rpm}$ ,  $\beta_{12}/\beta_{13} = 6 \times 10^{-5}$

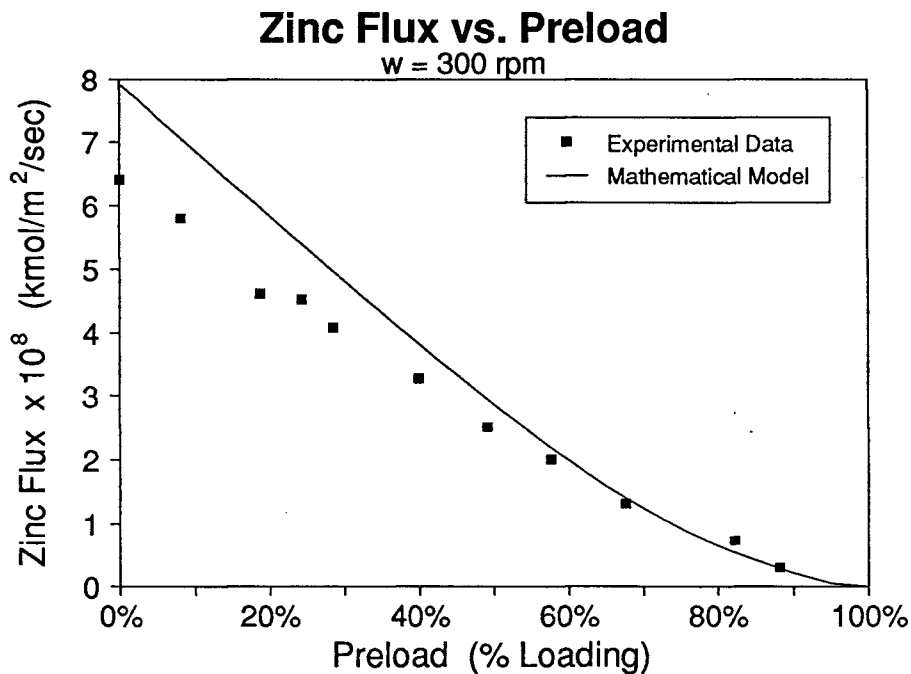


**Figure 4.36** Effect of preload on zinc flux :  $[\text{Zn}] = 0.05\text{M}$ , Formal  
 $[\text{D2EHPA}]_{\text{total}} = 0.05 \text{ M}$ ,  $\text{pH} = 4.5$ ,  $T = 25^\circ\text{C}$ , filter =  $0.45\mu\text{m}$ ,  
 $\omega = 300 \text{ rpm}$ ,  $\beta_{12}/\beta_{13} = 6 \times 10^{-5}$

### Sensitivity Analysis - Zinc Flux vs. Preload

Vary Organic Diffusion Coefficients

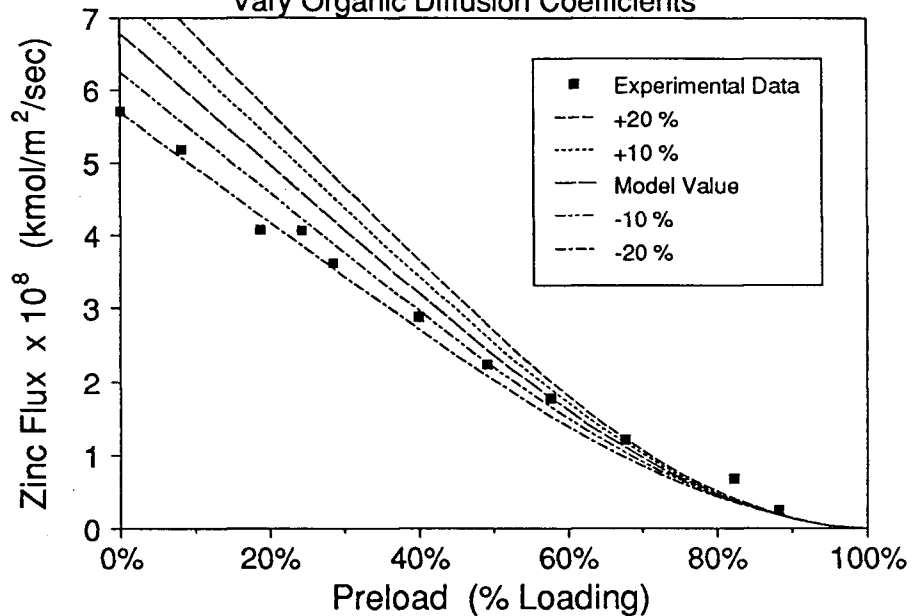


Figure 4.37 Zinc flux vs. preload for changes in the organic species diffusion coefficients :  $[Zn] = 0.05M$ , Formal  $[D2EHPA]_{total} = 0.05 M$ ,  $pH = 4.5$ ,  $T = 25^\circ C$ , filter =  $0.45\mu m$ ,  $\omega = 100 rpm$ ,  $\beta_{12}/\beta_{13} = 6 \times 10^{-5}$

### Sensitivity Analysis - Zinc Flux vs. Preload

Vary Equilibrium Constant

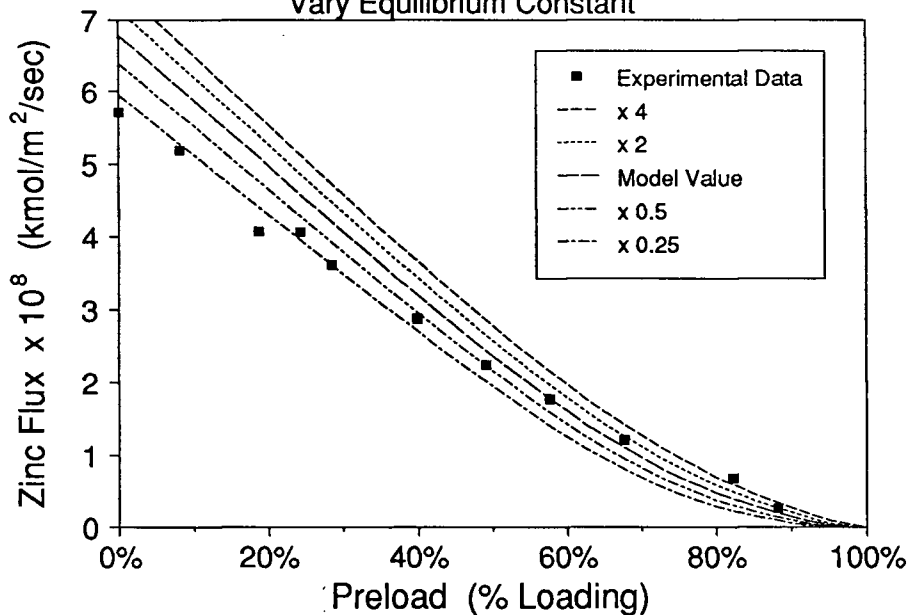
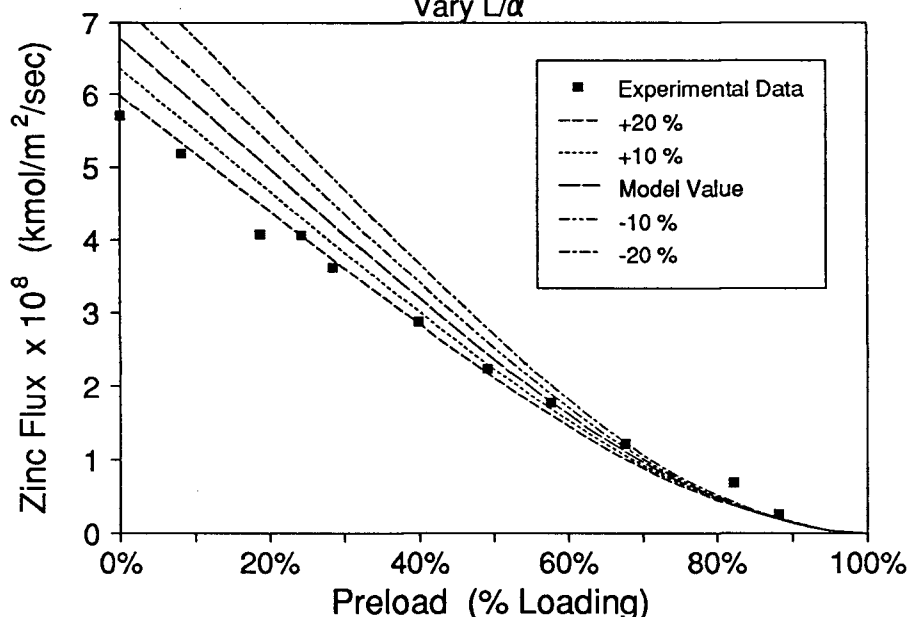


Figure 4.38 Zinc flux vs. preload for changes in the equilibrium constant  $K_{ex}$  :  $[Zn] = 0.05M$ , Formal  $[D2EHPA]_{total} = 0.05 M$ ,  $pH = 4.5$ ,  $T = 25^\circ C$ , filter =  $0.45\mu m$ ,  $\omega = 100 rpm$ ,  $\beta_{12}/\beta_{13} = 6 \times 10^{-5}$

## Sensitivity Analysis - Zinc Flux vs. Preload



**Figure 4.39** Zinc flux vs. preload for changes in the filter equivalent thickness  $L/\alpha$ :  $[\text{Zn}] = 0.05\text{M}$ , Formal  $[\text{D2EHPA}]_{\text{total}} = 0.05\text{ M}$ ,  $\text{pH} = 4.5$ ,  $T = 25^\circ\text{C}$ , filter =  $0.45\mu\text{m}$ ,  $\omega = 100\text{ rpm}$ ,  $\beta_{12}/\beta_{13} = 6 \times 10^{-5}$

### 4.5.2 Extended Model Predictions

Examination of the interfacial and bulk concentration values computed by the extended model provides some valuable insights into the nature of the reactions which are occurring at the interface and in the bulk phases.

The aqueous interfacial zinc concentration and the interfacial pH both increase as expected for increasing preload (Figures 4.40 and 4.41). As zinc flux decreases, less  $\text{Zn}^{2+}$  is required and fewer  $\text{H}^+$  ions are produced at the interface, resulting in a shallower concentration gradient for both species.

Due to the multiple species equilibrium in both the organic bulk and at the interface, the concentration of D2EHPA monomer was computed at both points. Thus, the total D2EHPA flux to the interface now included both D2EHPA monomer and dimer terms. The predicted concentration of the various D2EHPA species, including the total D2EHPA

concentration in both regions, is shown in Figures 4.42 and 4.43. Although the diffusion of both species was included in the model, no provision was made for the readjustment of speciation in the boundary layer.

The association factor, showing the average amount of complexation of organic zinc by  $(HL)_2$ , was computed in both the bulk organic and at the interface. As can be seen in Figure 4.44, the increase in free D2EHPA in the bulk phase causes a significant increase in the amount of additional HL associated with the zinc-D2EHPA species. Qualitatively, the difference between the two curves is a measure of the amount of readjustment of speciation which occurs across the boundary layer, and thus the deviation from linearity of the diffusion profile for the three zinc species. This deviation can be quite significant due to the difference in diffusion coefficients of the three species (c.f. Table 2.2).

The amount of each zinc species, expressed as a fraction of the total amount of zinc, is shown in Figure 4.45 for both the bulk phase and the interface. Figures 4.46 and 4.47 show the absolute concentrations of all organic zinc species and the total organic zinc concentration for the bulk and interface, respectively.

The total bulk zinc concentration, shown in Figure 4.46, is directly related to the preload, and thus increases with increasing preload. As preload increases, the amount of free D2EHPA in the bulk decreases, resulting in a shift from high  $n$  species ( $ZnL_2 \cdot (HL)_2$ ) to low  $n$  species ( $ZnL_2$ ). From low to intermediate preload, the increase in organic zinc concentration results in increased levels of all organic species; in this range the decrease in free HL has little effect. However, at intermediate preload values the amount of free HL becomes significant, and the formation of  $ZnL_2 \cdot (HL)_2$  is less favourable than the formation of  $ZnL_2 \cdot HL$ . Finally, for high preload values the amount of free D2EHPA becomes so low (c.f. Figure 4.42) that only the formation of  $ZnL_2$  is favoured.

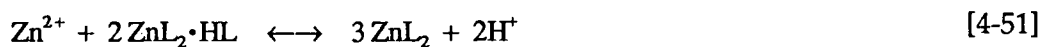
Increasing preload has little effect on the total organic zinc concentration at the interface (Figure 4.47). The decrease in the amount of free D2EHPA (c.f. Figure 4.43) causes a change in speciation, with lower  $n$  species favoured.

The concentration profiles of the interfacial and bulk species were overlaid in Figure 4.48. Initially, the bulk concentration of each zinc species is greater than that of its

interfacial counterpart, but as the preload increases the interfacial concentrations of first  $ZnL_2 \cdot (HL)_2$  and then  $ZnL_2 \cdot HL$  become greater than their bulk counterparts. Thus, the direction of zinc transport reverses for both  $ZnL_2 \cdot (HL)_2$  and  $ZnL_2 \cdot HL$ , and these two species diffuse to the interface where their additional complexed HL extracts  $Zn^{2+}$  and forms  $ZnL_2$  according to the equilibria:



and



The calculated fluxes for all the zinc species and the total D2EHPA flux are shown in Figure 4.49. Of particular interest is the upper preload range (>50%) where a significant fraction of the "L" supplied to the interface arrives as  $ZnL_2 \cdot (HL)_2$  and  $ZnL_2 \cdot HL$ ; at loadings greater than ~70%, free D2EHPA is no longer the major extractant.

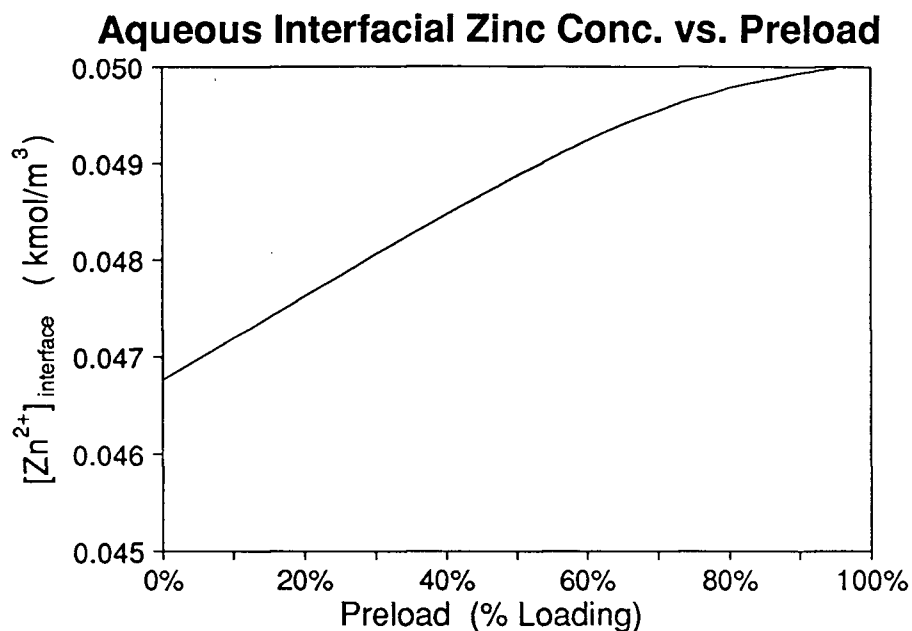


**Figure 4.40** Predicted change in interfacial zinc concentration (aqueous) with preload :  $[Zn] = 0.05M$ , Formal  $[D2EHPA]_{total} = 0.05 M$ ,  $pH = 4.5$ ,  $T = 25^{\circ}C$ , filter =  $0.45\mu m$ ,  $\omega = 100 rpm$ ,  $\beta_{12}/\beta_{13} = 6 \times 10^{-5}$

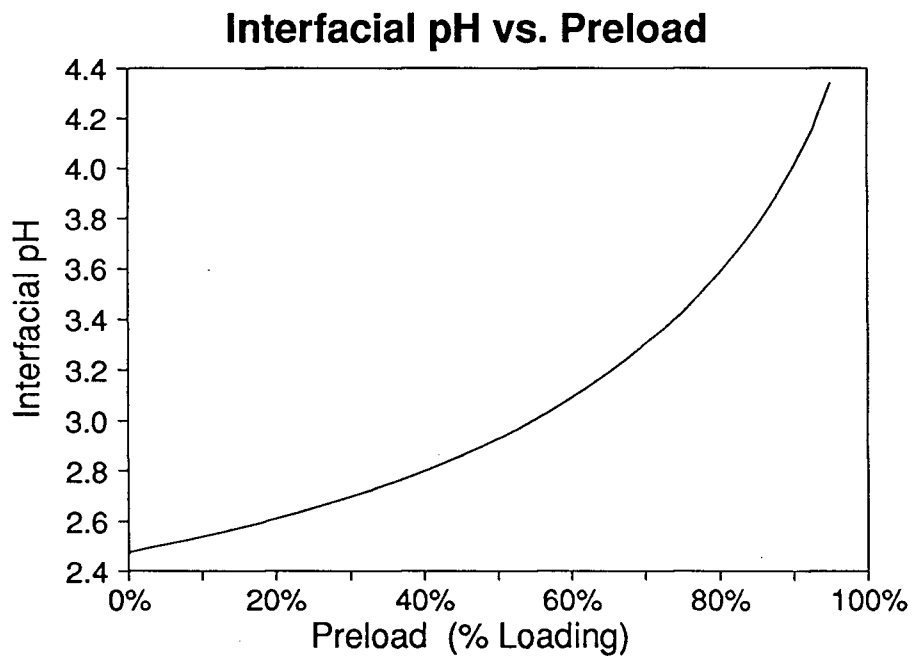


**Figure 4.41** Predicted change in interfacial pH with preload :  $[Zn] = 0.05M$ , Formal  $[D2EHPA]_{total} = 0.05 M$ ,  $pH = 4.5$ ,  $T = 25^{\circ}C$ , filter =  $0.45\mu m$ ,  $\omega = 100 rpm$ ,  $\beta_{12}/\beta_{13} = 6 \times 10^{-5}$

### Bulk D2EHPA Conc. vs. Preload

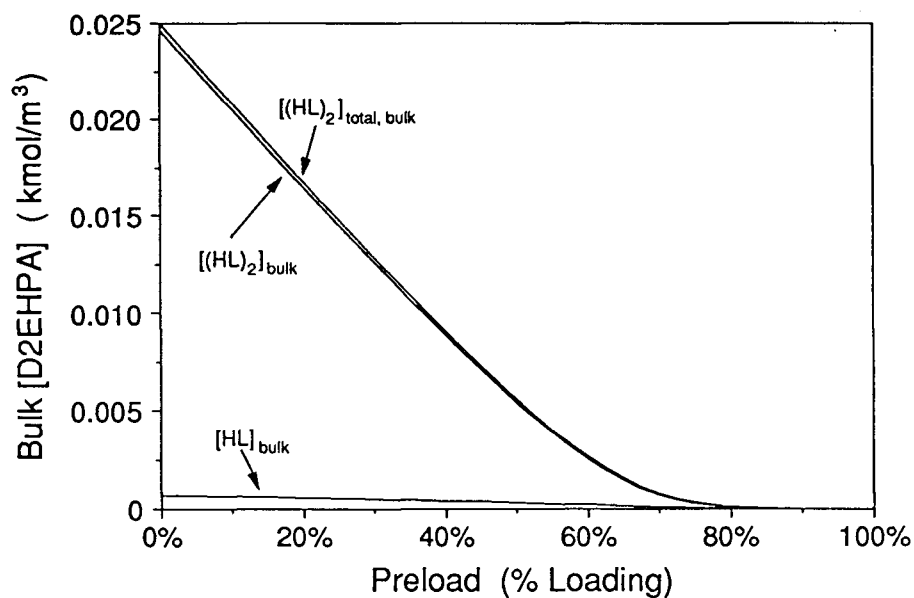


**Figure 4.42** Predicted change in bulk D2EHPA concentration with preload :  
 $[Zn] = 0.05M$ , Formal  $[D2EHPA]_{total} = 0.05 M$ ,  $pH = 4.5$ ,  $T = 25^\circ C$ ,  
 filter =  $0.45\mu m$ ,  $\omega = 100 rpm$ ,  $\beta_{12}/\beta_{13} = 6 \times 10^{-5}$

### Interfacial D2EHPA Conc. vs. Preload

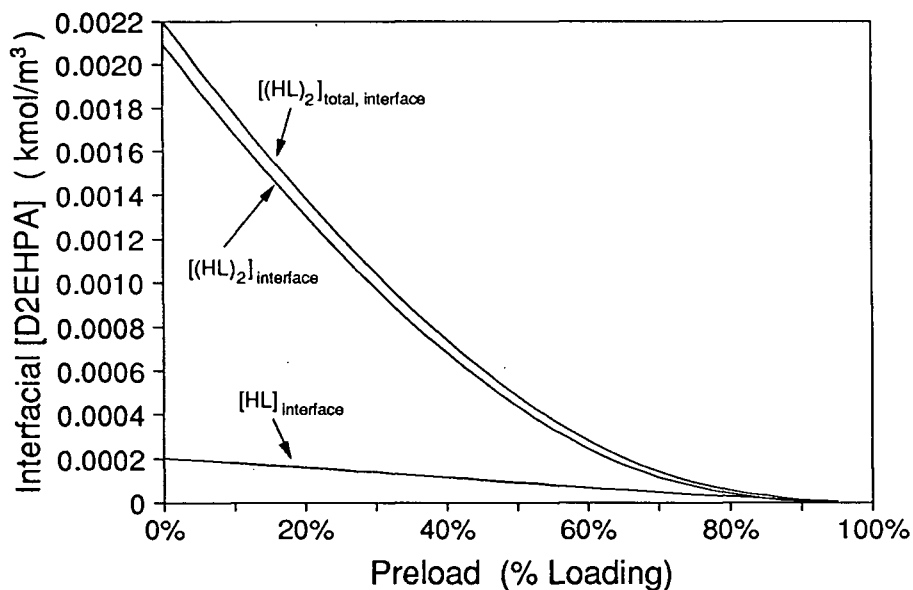


**Figure 4.43** Predicted change in interfacial D2EHPA concentration with  
 preload :  $[Zn] = 0.05M$ , Formal  $[D2EHPA]_{total} = 0.05 M$ ,  $pH = 4.5$ ,  
 $T = 25^\circ C$ , filter =  $0.45\mu m$ ,  $\omega = 100 rpm$ ,  $\beta_{12}/\beta_{13} = 6 \times 10^{-5}$

### Association Factor vs. Preload

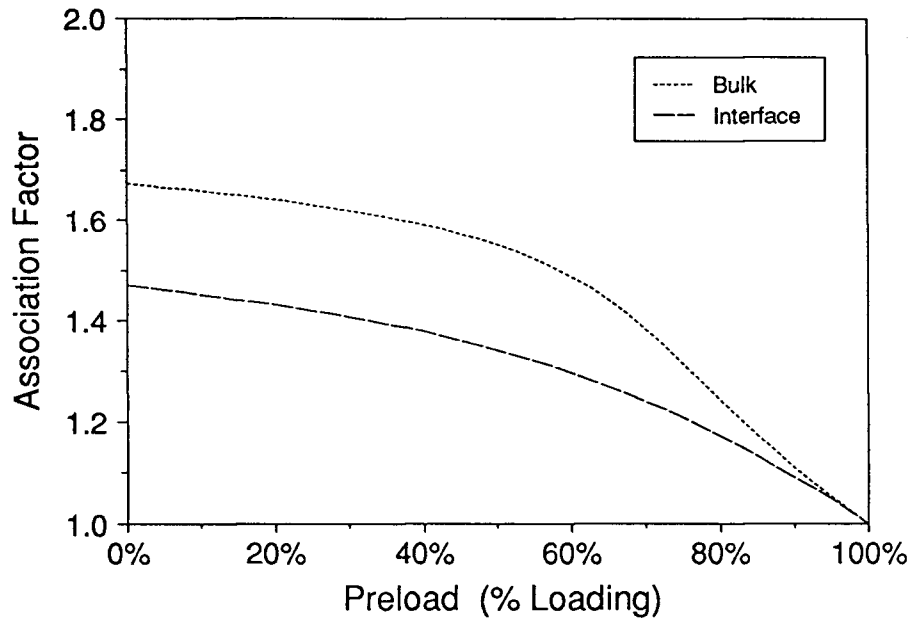


Figure 4.44 Predicted association factors vs. preload : [Zn] = 0.05M, Formal [D2EHPA]<sub>total</sub> = 0.05 M, pH = 4.5, T = 25 °C, filter = 0.45µm, ω = 100 rpm, β<sub>12</sub>/β<sub>13</sub> = 6 × 10<sup>-5</sup>

### Fractional Zinc Speciation vs. Preload

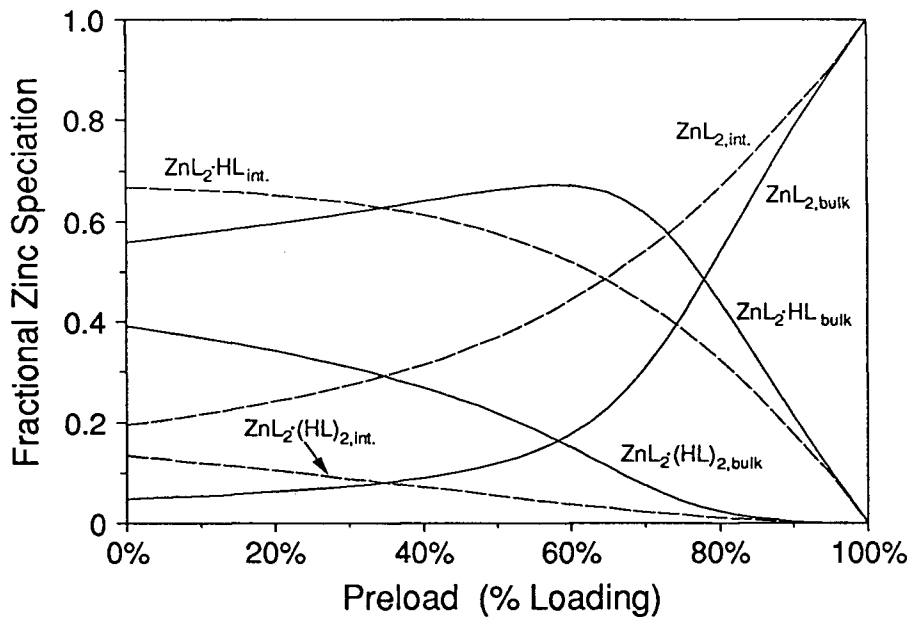
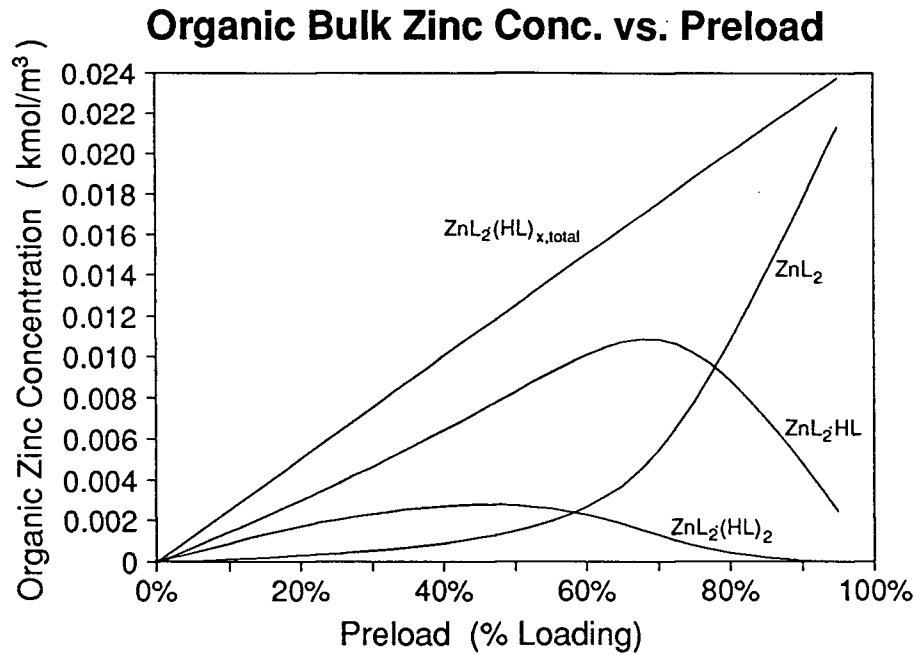
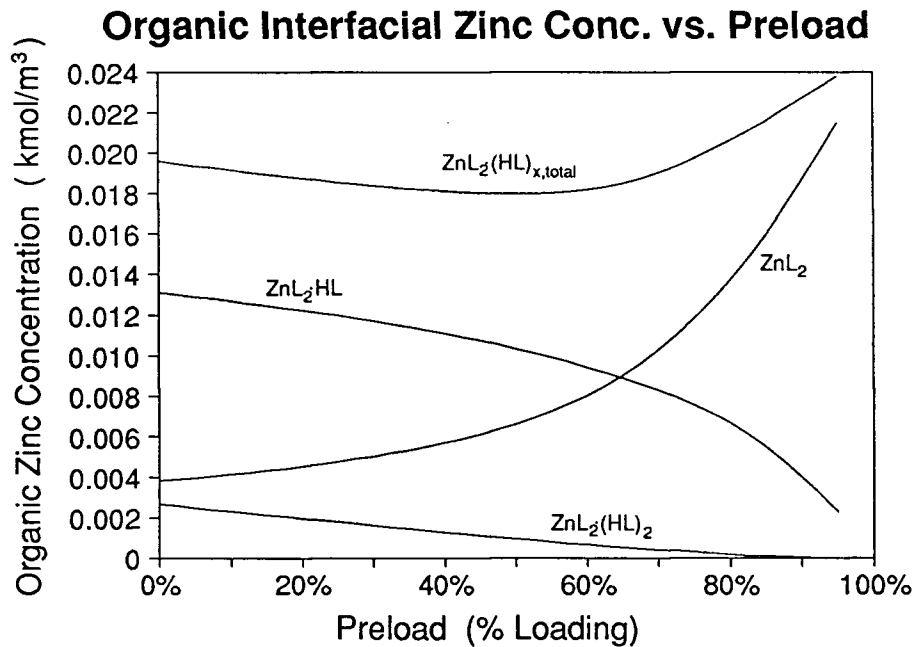


Figure 4.45 Predicted fractions of zinc species vs. preload : [Zn] = 0.05M, Formal [D2EHPA]<sub>total</sub> = 0.05 M, pH = 4.5, T = 25 °C, filter = 0.45µm, ω = 100 rpm, β<sub>12</sub>/β<sub>13</sub> = 6 × 10<sup>-5</sup>



**Figure 4.46** Predicted change in bulk zinc concentrations (organic) with preload :  $[Zn] = 0.05M$ , Formal  $[D2EHPA]_{total} = 0.05 M$ ,  $pH = 4.5$ ,  $T = 25^\circ C$ , filter =  $0.45\mu m$ ,  $\omega = 100 rpm$ ,  $\beta_{12}/\beta_{13} = 6 \times 10^{-5}$



**Figure 4.47** Predicted change in interfacial zinc concentrations (organic) with preload :  $[Zn] = 0.05M$ , Formal  $[D2EHPA]_{total} = 0.05 M$ ,  $pH = 4.5$ ,  $T = 25^\circ C$ , filter =  $0.45\mu m$ ,  $\omega = 100 rpm$ ,  $\beta_{12}/\beta_{13} = 6 \times 10^{-5}$

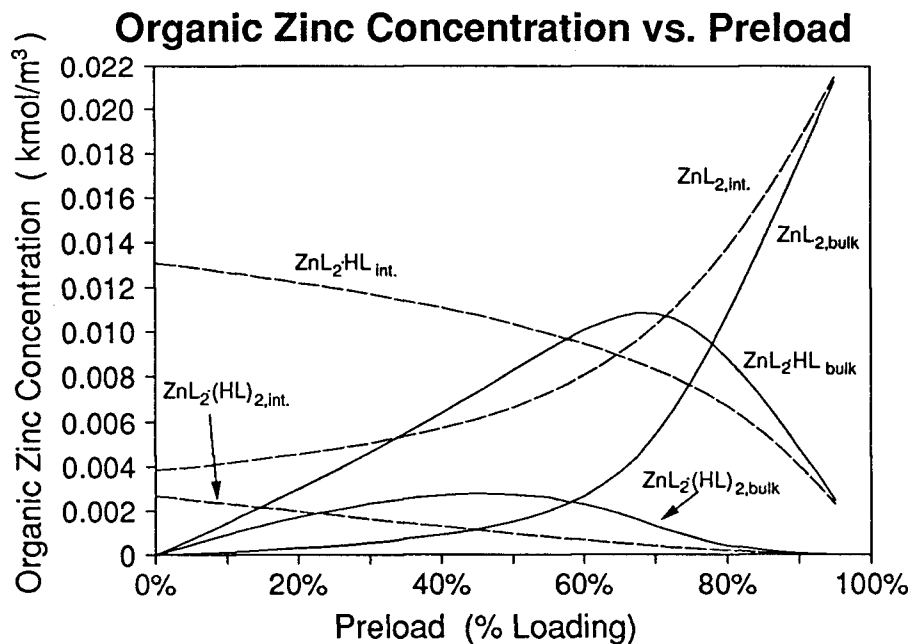


**Figure 4.48** Predicted change in organic zinc concentrations with preload :  
 $[Zn] = 0.05M$ , Formal  $[D2EHPA]_{total} = 0.05 M$ ,  $pH = 4.5$ ,  $T = 25^{\circ}C$ ,  
 filter =  $0.45\mu m$ ,  $\omega = 100 \text{ rpm}$ ,  $\beta_{12}/\beta_{13} = 6 \times 10^{-5}$

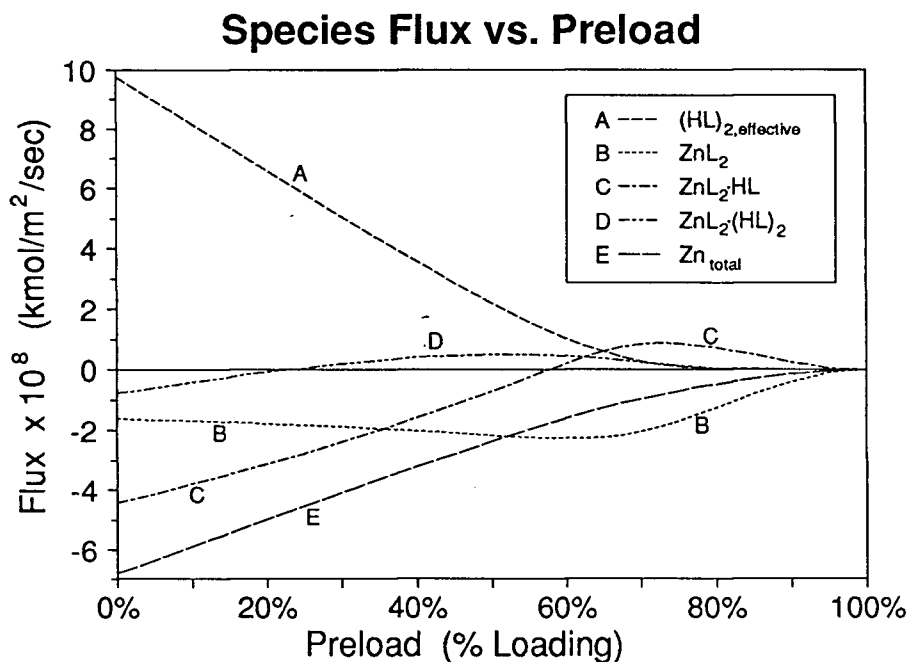


**Figure 4.49** Predicted flux of organic species with preload :  $[Zn] = 0.05M$ ,  
 Formal  $[D2EHPA]_{total} = 0.05 M$ ,  $pH = 4.5$ ,  $T = 25^{\circ}C$ ,  
 filter =  $0.45\mu m$ ,  $\omega = 100 \text{ rpm}$ ,  $\beta_{12}/\beta_{13} = 6 \times 10^{-5}$

## 4.6 Variable Temperature

Although no attempt was made to model the effect of temperature on the extraction processes, some preliminary work was done to investigate its effect. The zinc flux was measured over the temperature range 15 to 50 °C, and the observed rate was compared with a VMR model.

Assuming a mass transfer controlled system, a change in temperature will change such parameters as the diffusion coefficient of the various species and the viscosity of the organic and aqueous phases. An attempt was made to include these parameters by incorporating the temperature dependence of the viscosity of heptane into the VMR model. Since the diffusion coefficient calculated by the Wilke-Chang equation is a function of both temperature and viscosity (c.f. equation [2-3]), this method will probably give a reasonable estimation of the variation in diffusion coefficient over the moderate temperature range under consideration.

Data<sup>[20]</sup> were obtained for the viscosity of heptane at different temperatures, and the diffusion coefficients and Levich equivalent diffusion boundary layer thickness at each temperature were calculated. A VMR model was constructed for organic mass transfer control for both  $n=1.5$  and  $n=2$ . The model with experimental data for comparison is shown in Figure 4.50; the VMR curves appear to trace the general shape of the observed values.

An Arrhenius plot, shown in Figure 4.51, was constructed in order to determine the activation energy of the system. The points are generally linear, and the slope of the fitted line is -1497 K - this slope is equivalent to an activation energy  $E_a = 12.4$  kJ/mole. Activation energies of this magnitude are characteristic of diffusion controlled reactions.

### Zinc Flux vs. Temperature

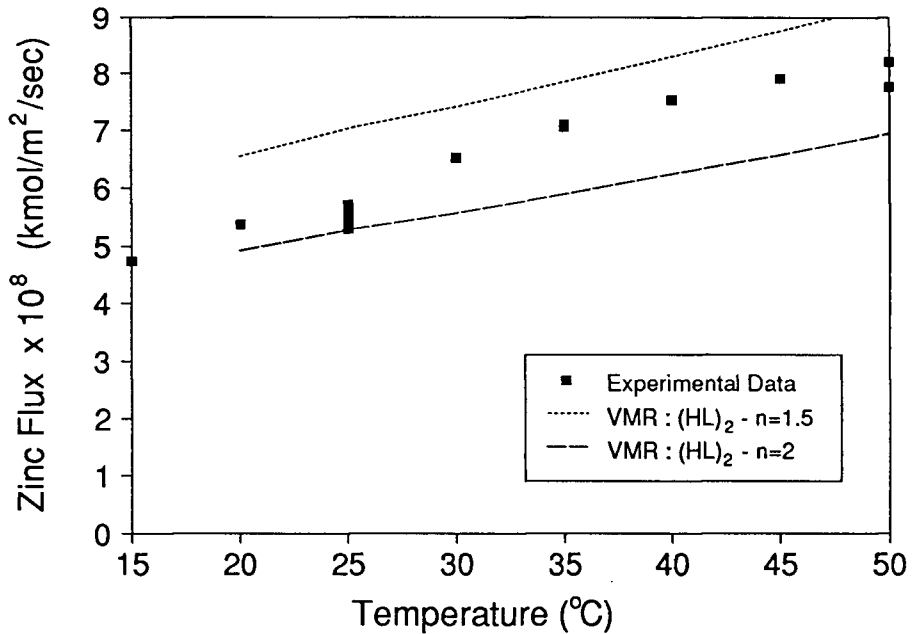


**Figure 4.50** VMR predictions and experimental data for changes in temperature :  
 [Zn] = 0.05M, Formal [D2EHPA] = 0.05 M, pH = 4.5, filter = 0.45 $\mu$ m,  
 $\omega$  = 100 rpm

### Arrhenius Plot - Ln flux vs 1/T

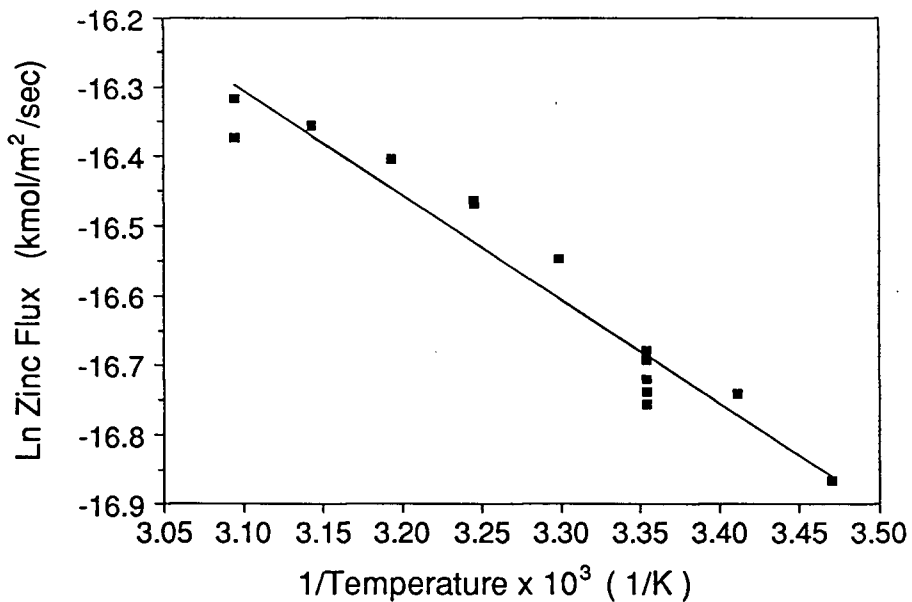


**Figure 4.51** Arrhenius Plot for experimental temperature data with linear regression fit : [Zn] = 0.05M, Formal [D2EHPA] = 0.05 M, pH = 4.5, filter = 0.45 $\mu$ m,  $\omega$  = 100 rpm

## 4.7 Filter Characterization

The effect of different filter pore sizes on the overall zinc extraction rate was examined. Three different filters were tested in addition to the standard 0.45 $\mu\text{m}$  Millipore filter; 0.05 $\mu\text{m}$ , 0.22 $\mu\text{m}$ , and 0.80 $\mu\text{m}$ . For the mathematical model, porosity and filter length values supplied by Millipore were used to compute the predicted flux at each discrete filter size.

---

**Table 4.2** Membrane Filter Characteristics

Average Pore Size ( $\mu\text{m}$ )	Filter Length, $L$ ( $\mu\text{m}$ )	Porosity, $\alpha$	$L/\alpha$ ( $\mu\text{m}$ )
0.05	150	0.72	208
0.22	150	0.75	200
0.45	150	0.79	190
0.80	150	0.82	183

---

As can be seen in Figures 4.52 and 4.53, there is only a slight decrease in zinc flux as the filter pore size is decreased from 0.80 $\mu\text{m}$  to 0.22 $\mu\text{m}$ ; however, there is a substantial drop in flux with the 0.05 $\mu\text{m}$  filter. The diameter of the  $(\text{HL})_2$  and  $\text{ZnL}_2$  molecules was estimated to be approximately 0.0014 $\mu\text{m}$ .<sup>63</sup> Thus, for the 0.05 $\mu\text{m}$  filter the  $(\text{HL})_2$  and  $\text{ZnL}_2$  molecules are only 35 times smaller than the filter pore size; it is likely that there is some interference between the filter and the organic "L" molecules which retards the flux.

It can therefore be concluded that for the filter pore size used in the baseline studies (0.45 $\mu\text{m}$ ), the filter has no effect on the rate of diffusion of the organic species.

---

3 The diameter of the molecules were calculated by computing the molecular volume at the normal boiling point using the method of Le Bas.<sup>[16]</sup> By assuming that the molecules are spherical, the diameter could then be determined. However, since the molecules are most likely elliptical, this method may have under-estimated the diameter of the  $(\text{HL})_2$  and  $\text{ZnL}_2$  molecules.

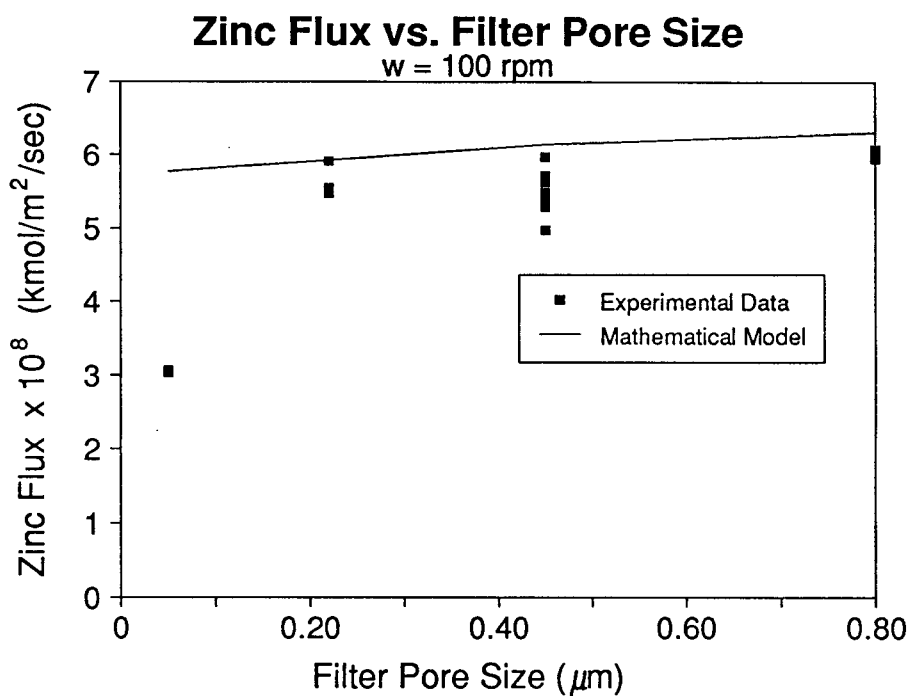


**Figure 4.52** Effect of changing filter pore size on zinc flux :  $[\text{Zn}] = 0.05\text{M}$ , Formal  $[\text{D2EHPA}] = 0.05 \text{ M}$ ,  $\text{pH} = 4.5$ ,  $T = 25^\circ\text{C}$ ,  $\omega = 100 \text{ rpm}$

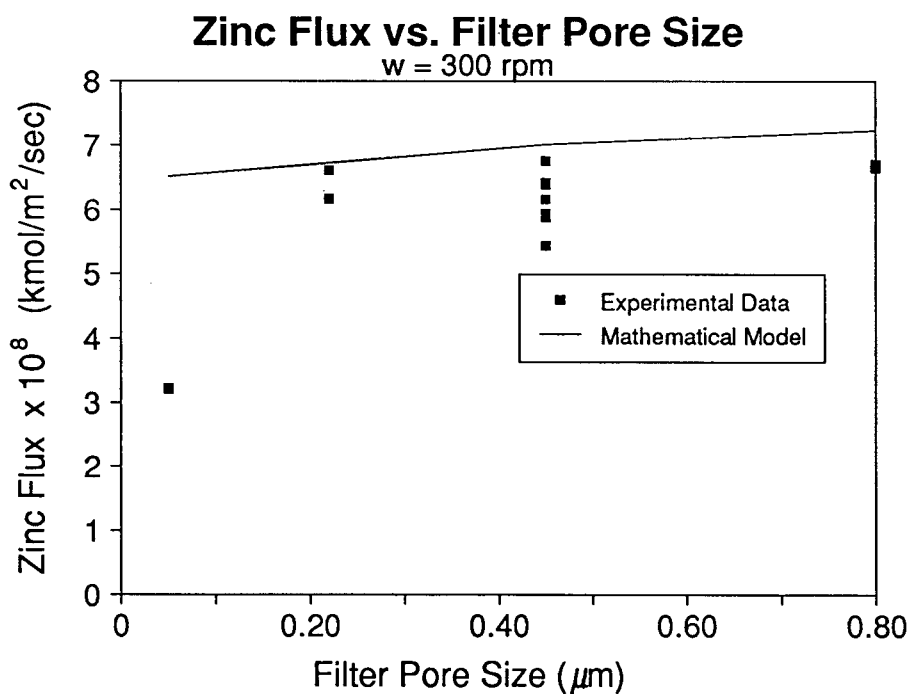


**Figure 4.53** Effect of changing filter pore size on zinc flux :  $[\text{Zn}] = 0.05\text{M}$ , Formal  $[\text{D2EHPA}] = 0.05 \text{ M}$ ,  $\text{pH} = 4.5$ ,  $T = 25^\circ\text{C}$ ,  $\omega = 300 \text{ rpm}$

## 4.8 SLM Applications

The results of this work have significant implications for the area of supported liquid membranes since the diffusion of extractant through the filter is analogous to the diffusion of extractant through the SLM. Some types of SLM's currently being investigated are similar to the membrane filter used in this study. For example, Huang and Juang<sup>[65]</sup> reported using Durapor microporous PVDF film with a thickness of  $125\mu\text{m}$ , a porosity of  $\sim 70\%$ , and an average pore size of  $0.45\mu\text{m}$ . This support is comparable to the Millipore membrane filter ( $L = 150\mu\text{m}$ ,  $\alpha = 79\%$ , and average pore size =  $0.45\mu\text{m}$ ). Also, since the average pore sizes are equal, the conclusion that the pore size has no effect on the extraction rate is valid.

The feed side interfacial behaviour in a SLM system will be very similar to that encountered in this study. Under most conditions, it is likely that aqueous mass transport of  $\text{Zn}^{2+}$  to the interface will not be rate controlling, and the feed side extraction will be governed by the diffusion of  $(\text{HL})_2$  through the membrane to the interface.

On the strip side of the SLM, it is probable that the situation will be similar to that encountered on the feed side. The chemical reaction will be fast, and since the only product diffusing through the aqueous to the interface would be  $\text{H}^+$ , it is likely that mass transport of extracted complex through the membrane to the interface would be the rate controlling step. Thus, the rate controlling steps in the SLM system would probably be the diffusion of  $(\text{HL})_2$  to the interface on the feed side, and perhaps the diffusion of  $\text{ZnL}_2 \cdot (\text{HL})_x$  to the interface on the strip side. This hypothesis must still be subjected to experimental verification.

---

## CHAPTER 5 - Conclusions

---

The extraction of zinc is controlled by the mass transfer of reactants ( $Zn^{2+}$  and  $(HL)_2$ ) to the interface. At low zinc concentrations, the system is controlled by the aqueous transport of  $Zn^{2+}$  to the interface; at higher zinc concentrations transport of D2EHPA becomes rate controlling. For the range of D2EHPA concentrations examined, the transport of D2EHPA was rate controlling. Bulk pH had a negligible effect, except perhaps at the lowest pH values examined, where there may be a slight decrease in extraction rate. This decrease can be most likely attributed to less favourable thermodynamics at low interfacial pH values. It appears that the chemical reaction rate is fast enough that it has a negligible effect on the overall extraction rate.

The basic mathematical model was adequate for predicting the extraction rate under variable conditions of zinc concentration, D2EHPA concentration, and pH. Although the model tends to overpredict the extraction rate, this effect is probably due to an error in one of the model parameters. The most likely sources of error are either the values for the organic diffusion coefficients or the filter equivalent thickness,  $L/\alpha$ .

The extraction of zinc with a partially loaded organic phase is also mass transfer controlled. The extended mathematical model predicts that the speciation of organic complexed zinc changes with increasing preload, and at high loadings the direction of  $ZnL_2 \cdot HL$  and  $ZnL_2 \cdot (HL)_2$  flux reverses, with these species providing extractant to the interface. At very high loadings,  $ZnL_2 \cdot HL$  provides almost all the extractant to the interface.

Experimental studies of the effect of temperature on the rate of zinc extraction resulted in a calculation of the activation energy,  $E_a$ , equal to 12.4 kJ/mole. This value is consistent with a diffusion mechanism:

Pore size had little effect on extraction rate, except for the 0.05 $\mu$ m filter, which caused a significant decrease in the extraction rate. It can therefore be concluded that the filter pores do not pose an additional resistance to mass transfer. This conclusion is important in SLM applications, because it shows that there is a minimum filter pore size below which the diffusion of species will be retarded.

---

## CHAPTER 6 - Recommendations for Further Work

---

The recommendations for further work can be divided into two sections: those that clarify some of the questions posed by this thesis, and others that continue the thrust of this work.

Experimental viscosity measurements of D2EHPA/heptane mixtures, and metal-loaded D2EHPA/heptane mixtures could be used by the Wilke-Chang relationship to determine more accurate organic species diffusion coefficients. Also, more extensive study could be done on the properties of the Millipore filter membranes, especially the filter thickness, tortuosity, and filter porosity. This information would result in more accurate predictions from the mathematical model. For the extended mathematical model, it would also be useful to determine an experimental value for the ratio of the formation constants  $\beta_{12}/\beta_{13}$ . Finally, the extended mathematical model could be re-written to accommodate changes in speciation across the organic boundary layer.

An investigation could be conducted into the properties of membranes being used for SLM applications. Determinations of thickness, tortuosity, and porosity could then be included in a mathematical model which could be used to optimize SLM design.

The techniques developed in this work could be used in the study of stripping reactions. By placing a loaded organic solution in the RDC inner compartment and an aqueous strip solution in the outer compartment, similar procedures could be used to determine the rate controlling steps.

The extraction behaviour of other metals could be studied, especially cobalt and nickel. Since the ligand exchange rates for these metals are slower, it is likely that the system would operate in either a mixed or chemical reaction regime. The mathematical model would have to be extended to accommodate a slow chemical reaction step.

Finally, by using a solvent impregnated filter membrane in the RDC, an aqueous feed solution in the outer compartment, and an aqueous strip solution in the inner compartment, a SLM-equivalent system could be studied.

---

## REFERENCES

---

1. *Developments in Solvent Extraction*, S. Alegret, ed., Ellis Horwood Ltd., Chichester, England, 1988.
2. Tavlarides, L.L., Bae, J.H., and Lee, C.K. Solvent extraction, membranes, and ion exchange in hydrometallurgical dilute metals separation. *Sep. Sci. Technol.*, **22** (2&3), pp. 581-617, 1987.
3. Ritcey, G.M. and Ashbrook, A.W. *Solvent Extraction: Principles and Applications to Process Metallurgy*, Part II, Elsevier Scientific Publishing Co., The Netherlands, 1979.
4. Brooks, C.S. Metal recovery from industrial wastes. *J. of Metals*, July 1986, pp. 50-57, 1986.
5. Wood, R. Processes in action - zinc recovery works in practice. *Process Eng.*, **8**, p. 6, 1977.
6. Nogueira, E.D., Regife, J.M. and Blythe, P.M. Zincex - the development of a secondary zinc process. *Chem. Ind.*, (2), pp. 63-67, 1980.
7. Ajawin, L.A., Pérez de Ortiz, E.S., and Sawistowski, H. Kinetics of extraction of zinc by di(2-ethylhexyl) phosphoric acid in n-heptane. *Proceedings of ISEC '80*, Paper 80-112, 1980.
8. Rice, N.M. and Smith, M.R. Recovery of zinc, cadmium and mercury (II) from chloride and sulphate media by solvent extraction. *J. appl. Chem. Biotechnol.*, **25**, pp. 379-402, 1975.
9. Flett, D.S. Solvent extraction in scrap and waste processing. *J. Chem. Tech. Biotechnol.*, **29**, pp. 258-272, 1979.
10. Reinhardt, H. Solvent extraction for recovery of metal waste. *Chem. Ind.*, 1 March, p. 210, 1975.
11. Peppard, D.F., Ferraro, J.R., and Mason, G.W. Hydrogen bonding in organophosphoric acids. *J. Inorg. Nucl. Chem.*, **7**, pp. 231-244, 1958.
12. Vandegrift, G.F. and Horwitz, E.P. Interfacial activity of liquid-liquid extraction reagents - I - dialkyl phosphorous based acids. *J. Inorg. Nucl. Chem.*, **42**, pp. 119-125, 1980.

13. Danesi, P.R. and Vandegrift, G.F. Activity coefficients of bis(2-ethylhexyl) phosphoric acid in n-dodecane. *Inorg. Nucl. Chem. Let.*, **17**, pp. 109-151, 1981.
14. Komasaawa, I., Otake, T., and Higaki, Y. Equilibrium studies of the extraction of divalent metals from nitrate media with di(2-ethylhexyl) phosphoric acid. *J. Inorg. Nucl. Chem.*, **43**, pp. 3351-3356, 1981.
15. Ul'yanov, V.S. and Sviridova, R.A. *Radiokhimiya*, **7**, p.538, 1969.
16. Perry, R.H. and Chilton, C.H. *Chemical Engineers Handbook, fifth edition*, McGraw-Hill Book Co., 1973.
17. Wilke, C.R. and Chang, P. Correlation of diffusion coefficients in dilute solutions. *A.I.Ch.E. Journal*, **1** (2), pp. 264-270, 1955.
18. Kolarik, Z. and Grimm, R. Acidic organophosphorous extractants - XXIV : the polymerization behaviour of Cu(II), Cd(II), Zn(II) and Co(II) complexes of di(2-ethylhexyl) phosphoric acid in fully loaded organic phases. *J. Inorg. Nucl. Chem.*, **38**, pp. 1721-1727, 1976.
19. Dreisinger, D.B. Ph.D. Thesis, Queen's University at Kingston, 1984.
20. *CRC Handbook of Chemistry and Physics, 62<sup>nd</sup> edition*, R.C. Weast, ed., CRC Press, Boca Raton, Florida, 1981.
21. Danesi, P.R. and Chiarizia, R. The kinetics of metal solvent extraction. *CRC Crit. Rev. Anal. Chem.*, **10** (1), pp. 1-126, 1980.
22. Ajawin, L.A., Pérez de Ortiz, E.S., and Sawistowski, H. Extraction of zinc by di(2-ethylhexyl) phosphoric acid. *Chem. Eng. Res. Des.*, **61**, pp. 62-66, 1983.
23. Hughes, M.A. and Rod, V. On the use of the constant interface stirred cell for kinetic studies. *Hydrometallurgy*, **12**, pp. 267-273, 1984.
24. Danesi, P.R., Vandegrift, G.F., Horwitz, E.P., and Chiarizia, R. Simulation of interfacial two-step consecutive reactions by diffusion in the mass-transfer kinetics of liquid-liquid extraction of metal cations. *J. Phys. Chem.*, **84**, pp. 3582-3587, 1980.
25. Roddy, J.W., Coleman, C.F, and Arai, S. Mechanism of the slow extraction of iron(III) from acid perchlorate solutions by di(2-ethylhexyl) phosphoric acid in n-octane. *J. Inorg. Nucl. Chem.*, **33**, pp. 1099-1118, 1971.

26. Komasaawa, I. and Otake, T. Kinetic studies of the extraction of divalent metals from nitrate media with bis(2-ethylhexyl) phosphoric acid. *Ind. Eng. Chem. Fundam.*, **22** (4), pp. 367-371, 1983.
27. Albery, W.J., Choudhery, R.A. and Fisk, P.R. Kinetics and mechanism of interfacial reactions in the solvent extraction of copper. *Faraday Discuss. Chem. Soc.*, **77**, pp. 53-65, 1984.
28. Danesi, P.R. and Vandegrift, G.F. Kinetics and mechanism of the interfacial mass transfer of  $\text{Eu}^{3+}$  and  $\text{Am}^{3+}$  in the system bis(2-ethylhexyl) phosphate-*n*-dodecane-NaCl-HCl-Water. *J. Phys. Chem.*, **85**, pp. 3646-3651, 1981.
29. Fleming, C.A., Nicol, M.J., Hancock, R.D., and Finkelstein, N.P. The kinetics of the extraction of copper by LIX65N and the catalytic role of LIX63 in this reaction. *J. appl. Chem. Biotechnol.*, **28**, pp. 443-452, 1978.
30. Miyake, Y., Matsuyama, H., Nishida, M., Nakai, M., Nagase, N., and Teramoto, M. Kinetics and mechanism of metal extraction with acidic organophosphorous extractants (I): Extraction rate limited by diffusion process. *Hydrometallurgy*, **23**, pp. 19-35, 1990.
31. Hughes, M.A. A general model to account for the liquid/liquid kinetics of extraction of metals by organic acids. *Faraday Discuss. Chem. Soc.*, **77**, paper 7, 1984.
32. Dreisinger, D.B. and Cooper, W.C. The kinetics of cobalt and nickel extraction using HEHEHP. *Solv. Ex. Ion Ex.*, **4** (2), pp. 317-344, 1986.
33. Dreisinger, D.B. and Cooper, W.C. The kinetics of zinc, cobalt and nickel extraction in the D2EHPA-heptane- $\text{HClO}_4$  system using the rotating diffusion cell technique. *Solv. Ex. Ion Ex.*, **7** (2), pp. 335-360, 1989.
34. Cotton, F.A. and Wilkinson, G. *Advanced Inorganic Chemistry, 4th edition*, John Wiley & Sons, Inc., 1980.
35. Brisk, M.L. and McManamey, W.J. Liquid extraction of metals from sulphate solutions by alkylphosphoric acids : II. Kinetics of the extraction of copper and cobalt with di(2-ethylhexyl) phosphoric acid. *J. Appl. Chem.*, **19**, pp. 109-114, 1969.
36. Tavlarides, L.L. Modelling and scaleup of dispersed phase liquid-liquid reactors. *Chem. Eng. Comm.*, **8**, pp. 133-164, 1981.

37. Hanna, G.J. and Noble, R.D. Measurement of liquid-liquid interfacial kinetics. *Chem. Rev.*, **85**, pp. 583-598, 1985.
38. Freiser, H. The role of the interface in the extraction of metal chelates. *Proceedings of ISEC '83*, ACS, pp. 4-5, 1983.
39. Hanson, C. Solvent extraction - where next?. Plenary lecture, *Proceedings of ISEC '80*, 1980.
40. Atwood, R.L., Thatcher, D.N., and Miller, J.D. Kinetics of copper extraction from nitrate solutions by LIX 64N. *Metall. Trans.*, **6B**, pp. 465-473, 1975.
41. Hughes, M.A. and Zhu, T. Rates of extraction of cobalt from an aqueous solution to D2EHPA in a growing drop cell. *Hydrometallurgy*, **13**, pp. 249-264, 1985.
42. Freeman, R.W. and Tavlarides, L.L. Study of interfacial kinetics for liquid-liquid systems-I: the liquid jet recycle reactor. *Chem. Eng. Sci.*, **35**, pp. 559-566, 1980.
43. Albery, W.J., Burke, J.F., Leffler, E.B., and Hadgraft, J. Interfacial transfer studied with a rotating diffusion cell. *J.C.S. Faraday Trans. I*, **72**, pp. 1618-1624, 1976.
44. Patel, H.V. The kinetics of liquid-liquid extraction of metals in a rotating diffusion cell. Ph.D. thesis, University of Bradford, 1988.
45. Levich, Veniamin G. *Physicochemical Hydrodynamics*, Prentice-Hall, Inc., Englewood Cliffs, N.J., 1962.
46. Guy, R.H. and Fleming, R. A novel method to study the permeability of a phospholipid barrier. *J. of Chem. Soc. (Chem Comm)*, **17**, pp. 727-30, 1979.
47. Albery, W.J. and Hadgraft, J. Percutaneous absorption: interfacial transfer kinetics. *J. Pharmacy Pharmacology*, **31**, pp. 65-68, 1979.
48. Albery, W.J. and Fisk, P.R. The kinetics of extraction of copper with Acorga P50 studied by a diffusion cell. *Proceedings of Hydrometallurgy '81*, IMM, Manchester, 1981.
49. Dreisinger, D.B., Cooper, W.C., and Distin, P.A. The kinetics of divalent metal extraction with HDEHP, HEHEHP and HDTMPP using the rotating diffusion cell. *Proceedings 2nd Int'l. Conf. Sep. Sci. Technol.*, C.S.Ch.E., Hamilton, Ontario, pp. 151-157, 1989.
50. Huang, T.C. and Juang, R.S. Extraction equilibrium of zinc from sulfate media with bis(2-ethylhexyl) phosphoric acid. *Ind. Eng. Chem. Fundam.*, **25** (4), pp. 752-757, 1986.

51. Li, Z.C., Fürst, W., and Renon, H. Extraction of zinc(II) from chloride and perchlorate aqueous solutions by di(2-ethylhexyl) phosphoric acid in Escaid 100: experimental equilibrium study. *Hydrometallurgy*, **16**, pp. 231-241, 1986.
52. Sato, T., Kawamura, M., Nakamura, T. and Ueda, M. The extraction of divalent manganese, iron, cobalt, nickel, copper and zinc from hydrochloric acid solutions by di(2-ethylhexyl) phosphoric acid. *J. appl. Chem. Biotechnol.*, **28**, pp. 85-94, 1978.
53. Smelov, V.S., Lanin, V.P., Smyk, Z.A., and Chubkov, V.V. *Radiokhimiya*, **14** (3), p.352, 1972.
54. Teramoto, M., Matsuyama, H., Takaya, H., and Asano, S. Development of spiral-type supported liquid membrane module for separation and concentration of metal ions. *Sep. Sci. Technol.*, **22** (11), pp. 2175-2201, 1987.
55. Grimm, R. and Kolarík, Z. Acidic organophosphorous extractants - XIX : extraction of Cu(II), Co(II), Ni(II), Zn(II), and Cd(II) by di(2-ethylhexyl) phosphoric acid. *J. Inorg. Nucl. Chem.*, **36**, pp. 189-192, 1974.
56. Smelov, V.S., Lanin, V.P., Smyk, Z.A., and Chubkov, V.V. *Sov. Radiochem.*, **14**, p.364, 1972.
57. Sastre, A.M. and Muhammed, M. The extraction of zinc(II) from sulphate and perchlorate solutions by di(2-ethylhexyl) phosphoric acid dissolved in Isopar-H. *Hydrometallurgy*, **12**, pp. 177-193, 1984.
58. Forrest, C. and Hughes, M.A. The separation of zinc from copper by di(2-ethylhexyl) phosphoric acid - an equilibrium study. *Hydrometallurgy*, **3**, pp. 327-342, 1978.
59. Cianetti, C. and Danesi, P.R. Kinetics and mechanism of the interfacial mass transfer of  $Zn^{2+}$ ,  $Co^{2+}$ , and  $Ni^{2+}$  in the system: bis(2-ethylhexyl) phosphoric acid, n-dodecane -  $KNO_3$ , water. *Solv. Ex. Ion Ex.*, **1** (1), pp. 9-26, 1983.
60. Ajawin, L.A., Demetron, J., Pérez de Ortiz, E.S., and Sawistowski, H. Effect of mass transfer parameters on zinc extraction by HDEHP. *Inst. Chem. Eng. Symp. Ser.*, **88**, pp. 183-191, 1985.
61. Huang, T.C. and Juang, R.S. Kinetics and mechanism of zinc extraction from sulfate medium with di(2-ethylhexyl) phosphoric acid. *J. Chem. Eng. Japan*, **19** (5), pp. 379-396, 1986.

62. Aparicio, J. and Muhammed, M. Extraction kinetics of zinc from aqueous perchlorate solution by D2EHPA dissolved in Isopar-H. *Hydrometallurgy*, **21**, pp. 385-399, 1989.
63. Danesi, P.R. Separation of metal species by supported liquid membranes. *Sep. Sci. Technol.*, **19** (11&12), pp. 857-894, 1984-85.
64. Fernandez, L., Aparicio, J., and Muhammed, M. The role of feed metal concentration in the coupled transport of zinc through a bis(2-ethylhexyl) phosphoric acid solid supported liquid membrane from aqueous perchlorate media. *Sep. Sci. Technol.*, **22** (6), pp. 1577-1595, 1987.
65. Huang, T.C. and Juang, R.S. Rate and mechanism of divalent metal transport through supported liquid membrane containing di(2-ethylhexyl) phosphoric acid as a mobile carrier. *J. Chem. Tech. Biotechnol.*, **42**, pp. 3-17, 1988.
66. Partridge, J.A. and Jensen, R.C. Purification of di(2-ethylhexyl) phosphoric acid by precipitation of copper(II) di(2-ethylhexyl) phosphate. *J. Inorg. Nucl. Chem.*, **31**, pp. 2587-2589, 1969.
67. Rossotti, F.J.C. and Rossotti, H. Potentiometric titrations using Gran plots. *J. Chem. Ed.*, **42** (7), pp. 375-378, 1965.

---

## APPENDIX A - Optical Tachometer

---

An optical tachometer was used to continuously measure the rotational speed of the RDC. A diagram of the physical setup is shown in Figure A.1. A circle with six alternating black and white sections was glued onto the top of the filter mount (Figure A.2). An infra-red photodiode-phototransistor pair was used to sense the black (light absorbing) to white (light reflecting) transitions, producing a signal output consisting of a series of pulses.

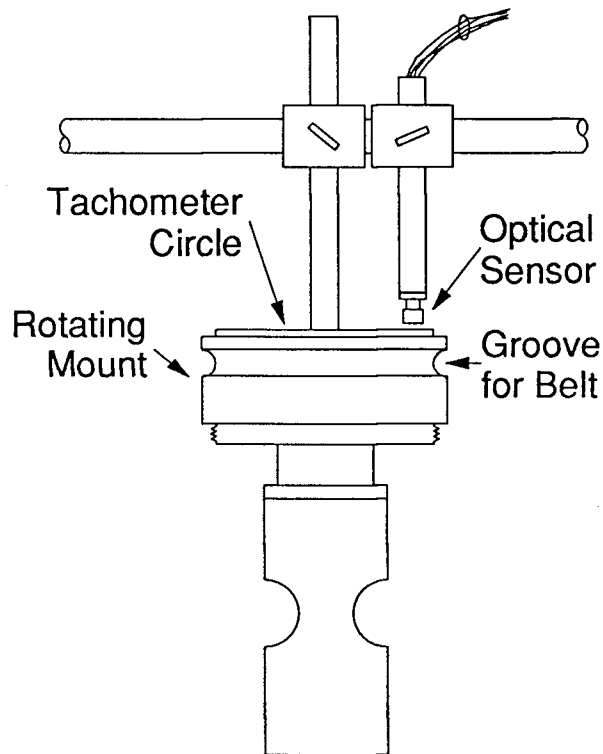


**Figure A.1** - The RDC and the Optical RPM Sensor

---

A frequency counter (Advance Instruments TC9A Timer/Counter) with adjustable sensitivity input (10mV, 100mV, or 1V - the 1V range was used) was used to process the signal. The advantage of this particular counter lay in its ability to acquire a signal for a fixed period (in this particular case, 10 seconds). By acquiring the signal for ten seconds, a reading for RPM could be directly determined according to the following equation:

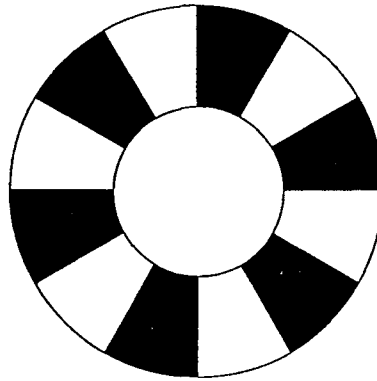


Figure A.2 - The Tachometer Circle

---

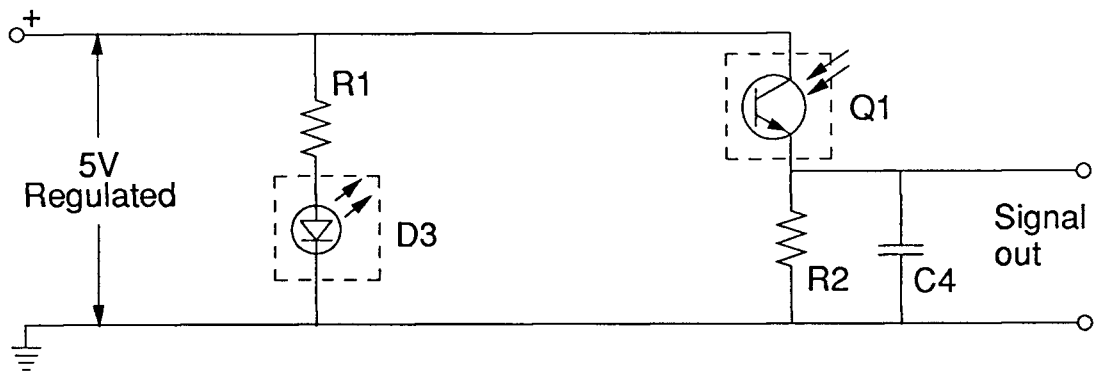
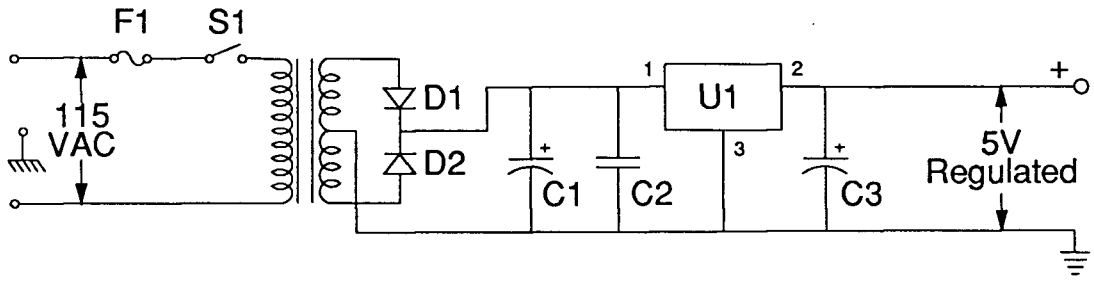
$$\begin{aligned} & \frac{6 \text{ counts}}{\text{revolution}} \times 10 \text{ second sampling time} \times \frac{1 \text{ minute}}{60 \text{ seconds}} \\ & = 1 \text{ count/revolution per minute} \\ & = 1 \text{ count/rpm} \end{aligned}$$

i.e. the observed count reading on the counter display was equal to the rotational speed of the RDC in RPM.

The photodiode/phototransistor pair was connected to the counter by a simple signal conditioner. The schematic diagram for the signal conditioner and its power supply is shown in Figure A.3. As can be seen in this figure, the entire signal conditioner (lower half of the schematic) consists of exactly four components: D3/Q1, R1, R2, and C4.

The power supply design shown in the upper half of Figure A.3 is a conventional design using a three-terminal voltage regulator (U1), and will not be discussed further. Photodiode D3 is connected to the 5 volt supply via resistor R1, which limits the current flow. Phototransistor Q1 conducts when it is exposed to infra-red light (reflected by the white portions of the tachometer circle) and makes the signal output positive. When Q1 is not conducting (i.e. a black portion of the tachometer circle), resistor R2 pulls the output signal to ground. Capacitor C4 is a noise filter.

The signal conditioner was modified from an existing unit which had previously been built for another experiment. The modification, which was necessary to reduce noise, involved placing capacitor C4 across the signal output terminals. No other changes were made to the existing unit.



- F1 - 1/2 Amp fuse
- D1, D2 - 1N4005 diodes
- C1 - 470 $\mu$ f, 40V electrolytic capacitor
- C2 - 0.333 $\mu$ f, 100V capacitor
- C3 - 10 $\mu$ f, 63V electrolytic capacitor
- C4 - 0.1 $\mu$ f ceramic disc capacitor
- R1 - 15 $\Omega$ , 1/2W resistor
- R2 - 2.8K, 1/2W resistor
- U1 - LM7805 5 volt voltage regulator
- D3/Q1 - infra-red photodiode/phototransistor - F104 607

Figure A.3 - Schematic Diagram of Optical Counter Signal Conditioner

---

## APPENDIX B - Data Acquisition Hardware and Software

---

This appendix will describe the hardware and software used for acquiring the NaOH volume/time profiles from the autoburette in each RDC run. The chart recorder feed output from the Radiometer ABU80 autoburette was connected to a Data Translation DT2805 data acquisition board via a DT707-T screw terminal panel. The board was configured with differential inputs, bipolar operation, and a range of +10/-10V; analog channel 1 was used for input.

Due to the unusual nature of the chart recorder feed output which was used for tracking the volume dispensed from the autotitrator, a custom computer program was written in Pascal to record the data. The chart recorder feed output was well suited for this application, because for every 1/4000th of total burette volume (10ml for the current study) one half of a +5V/GND square wave is output. Thus, by counting the number of positive/ground and ground/positive transitions, the total volume dispensed may be determined.

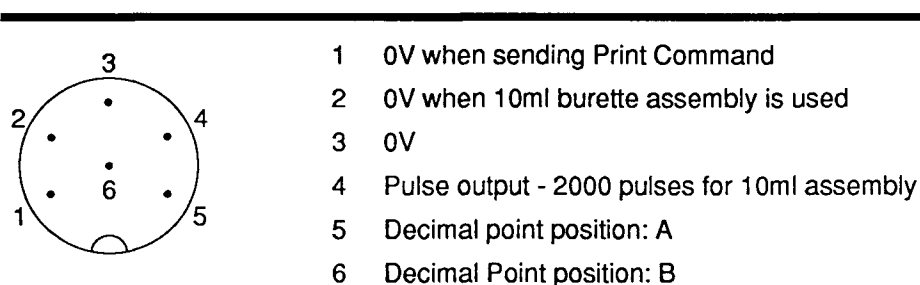


**Figure B.1** Chart Feed pin-out specifications

---

Data acquisition software was evaluated and found unsuitable. Most software records the input signal at discrete time intervals, a method which is clumsy for this particular application since the values of interest was not the value of the input signal at any particular time, but rather the time of each voltage transition, and the total number of voltage transitions. A program was therefore written which checked the chart recorder feed voltage, and incremented a counter if it changed. Once every second, if the number of counts had changed, the elapsed time, number of counts, and total number of counts were written to a file.

A flowsheet of the data acquisition program is shown in Figure B.2, and the Pascal program listing follows in Table B.1.

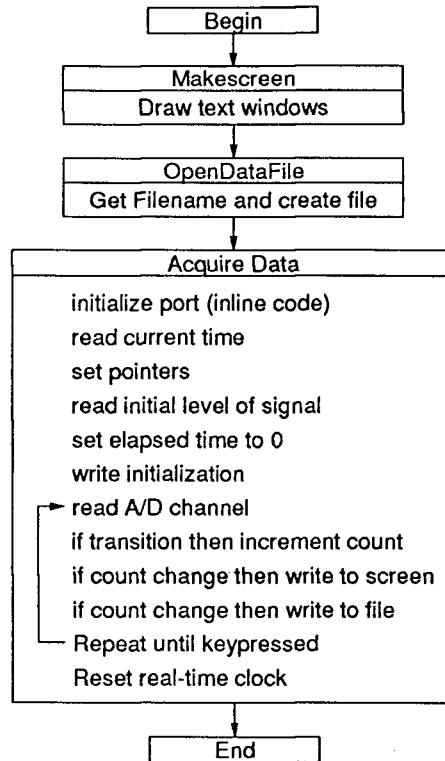


**Figure B.2** Major elements of the data acquisition program

**Table B.1:** Pascal Listing of Data Acquisition Computer Program

**Program AD\_Data\_Acquisition;**

```

const
  CountMAX = 12001; { Max. number of array elements - limit is imposed by memory restrictions }

type
  timestring = string[8];
  Filestring = string[14];
  timearray = array[0..countmax] of byte;
  countarray = array[0..countmax] of integer;
  Maxstring = string[255];
  Regpack = record
    AX,BX,CX,DX,BP,SI,DI,DS,ES,Flags: integer;
  end;

var i : integer;           { miscellaneous counter index }
    n : integer;          { index for arrays A, B, C, and tcount }
    A, B, C : timearray;  { arrays for hour, minute, and second values }
    tcount : countarray;  { array for count values }
    Datafile : text;      { Output text file }
    dummy : char;
    Base_Address, Data_Register : Integer;
  
```

**Function KeyboardInput : char;**

```

{ Waits until a key is pressed, and then reports the value of the key. }

var Key : char;

begin { KeyboardInput }
  Repeat Delay(50) until KeyPressed;
  
```

```

Read(Kbd,Key);
KeyboardInput := Key;
end; { KeyboardInput }

```

### Function Question (prompt:MaxString) : boolean;

```

{ Asks the Yes or No question contained in the string prompt and then waits until a Y or N }
{ answer has been received. The value of the answer is then reported by the value of this }
{ boolean function - True ≡ Yes and False ≡ No. }

var query : char;

begin { Question }
  Repeat
    Write( prompt + ' <Y/N> ' + chr(8) );
    query := KeyboardInput;
    writeln(query);
  Until (query in ['Y','y','N','n']);          { Keep asking until a Y or N answer is received }

  If (query in ['Y','y']) then Question := true else Question := false;

end; { Question }

```

### Procedure Beep;

```

{ Beeps the speaker - used when user has made a data entry error }
{ or to alert the user to a possible problem. }

begin { Beep }
  sound(880); { Beep at 880 Hz }
  Delay(125); { for 125 milliseconds. }
  Nosound; { Turn off sound. }
end; { Beep }

```

### Procedure MakeScreen;

```

{ This procedure draws the text screen which contains a status window, a window for }
{ user input, and a window for displaying acquired data. The windows are drawn using }
{ IBM extended graphics characters. }

var i : Integer;          { loop variable }

begin { MakeScreen }

  ClrScr;
  GotoXY(1, 1);          { upper left-hand corner }
  Write(chr(201));      { draw upper left corner character }
  for i := 2 to 78 do Write(chr(205)); { draw line }
  Write(chr(187));      { draw upper right corner character }

  GotoXY(1, 2); Write(chr(186)); { left margin, row 2 }
  GotoXY(79, 2); Write(chr(186)); { right margin, row 2 }

  GotoXY(1, 3);          { row 3 }
  Write(chr(204));      { left side line join character }
  for i := 2 to 78 do Write(chr(205)); { draw line }
  Write(chr(185));      { right side line join character }

  for i := 4 to 10 do   { rows 4 through 10 }
  begin
    GotoXY(1, i); Write(chr(186)); { draw left margin border }
    GotoXY(79, i); Write(chr(186)); { draw right margin border }
  end;

  GotoXY(1, 11);        { row 11 }
  Write(chr(204));      { left side line join character }
  for i := 2 to 78 do Write(chr(205)); { draw line }
  Write(chr(185));      { right side line join character }

  for i := 12 to 24 do  { rows 12 through 24 }
  begin
    GotoXY(1, i); Write(chr(186)); { draw left margin border }
    GotoXY(79, i); Write(chr(186)); { draw right margin border }
  end;

```

```

GotoXY(1, 25);                               { bottom line }
Write(chr(200));                             { draw bottom left corner character }
for i := 2 to 78 do Write(chr(205));         { draw bottom line }
Write(chr(188));                             { draw bottom right corner character }

LowVideo;                                    { select low intensity video }

end; {MakeScreen}

```

### Procedure ResetWindow;

```

{ Resets the text screen by setting the window back to full screen. }
{ Also moves the cursor to the bottom left-hand corner of the screen. }

begin { ResetWindow }
  Window(1,1,80,25);
  GotoXY(1,24);
end; { ResetWindow }

```

### Procedure Time(var hour,min,sec,frac:byte; var time : timestring);

```

{ Reads the real-time clock and sets the values hour, min, sec, frac (hundredths of seconds) }
{ using DOS Interrupt 21h. The variable string time is also set equal to the time, expressed }
{ in the form HH:MM:SS. }

var
  Regs    : Regpack;                          { register variable passed to interrupt handler }
  AH, AL  : byte;                             { 8 bit registers }
  temp1, temp2, temp3 : string[2];           { temporary variables used for holding time digits }

begin { Time }
  AL := $00;                                  { not required, just be neat }
  AH := $2C;                                  { select "get system time" function }
  Regs.AX := AH shl 8 + AL;                   { convert AH and AL to 16 bit AX value }

  Intr($21,Regs);                             { call interrupt 21 hexadecimal }
  hour := Regs.CX shr 8;                       { get value for hour }
  min  := Regs.CX mod 256;                     { get value for min }
  sec  := Regs.DX shr 8;                       { get value for sec }
  frac := Regs.DX mod 256;                     { get value for frac }

  str(hour,temp1);                             { convert numeric hour value into string }
  str(min, temp2);                             { convert numeric min value into string }
  str(sec, temp3);                             { convert numeric sec value into string }
  if hour < 10 then temp1 := '0' + temp1;      { add a leading zero if hour < 10 }
  if min < 10 then temp2 := '0' + temp2;      { add a leading zero if min < 10 }
  if sec < 10 then temp3 := '0' + temp3;      { add a leading zero if sec < 10 }
  time := temp1 + ':' + temp2 + ':' + temp3;   { create time string in the form HH:MM:SS }

end; { Time }

```

### Procedure SetTime(hour,min,sec:byte);

```

{ Sets the time to the values specified by the arguments hour, min, sec using DOS Interrupt }
{ 21h. This particular routine is not particularly efficient, but it is not in a time-critical }
{ section, and is much clearer the way it is structured here. }

var
  Regs    : Regpack;                          { register variable passed to interrupt handler }
  AH, AL, CH, CL, DH, DL : byte;             { 8 bit registers }

begin { SetTime }

  AL := $00;                                  { not required, just be neat }
  AH := $2D;                                  { select "set system time" function }
  CH := hour;                                 { set hour }
  CL := min;                                  { set minutes }
  DH := sec;                                  { set seconds }
  DL := 0;                                    { set hundredths of seconds equal to zero }

```

```

Regs.AX := AH shl 8 + AL;           { convert AH and AL to 16 bit AX value }
Regs.CX := CH shl 8 + CL;           { convert CH and CL to 16 bit CX value }
Regs.DX := DH shl 8 + DL;           { convert DH and DL to 16 bit DX value }

Intr($21,Regs);                     { call interrupt 21 hexadecimal }

end; { SetTime }

```

### Procedure Error;

```

{ Catastrophic error handler. This procedure is invoked if the A/D converter reports }
{ an error, something which should not happen under normal circumstances. When run, it }
{ resets the text window and immediately halts program execution. }

```

```

begin { Error }
  Writeln;
  Writeln('A/D CONVERSION ERROR');
  Writeln;
  ResetWindow;
  Halt;
end; { Error }

```

### Procedure ResetTime (oldhour, oldmin, oldsec, A, B, C:byte);

```

{ This procedure resets the real-time clock at the end of the acquisition run. The time }
{ at the start of acquisition was stored in oldhour, oldmin, & oldsec, and A, B, & C hold }
{ the elapsed time of the run (hours, minutes, and seconds, respectively. The clock time }
{ is obtained by summing the initial time and the elapsed time, with carry. }

```

```

var hour, min, sec : real;

begin { ResetTime }
  sec := oldsec + C;
  min := oldmin + B;
  hour := oldhour + A;

  if (sec >= 60) then
    begin
      sec := sec - 60;
      min := min + 1;
    end;
  if (min >= 60) then
    begin
      min := min - 60;
      hour := hour + 1;
    end;
  if (hour >= 24) then hour := hour - 24;
  SetTime(hour,min,sec);
end; { ResetTime }

```

### Procedure AcquireData (Data Register:integer; var A,B,C:timearray; var tcount : countarray; var n : integer; var Datafile : text);

```

{ AcquireData is the master data acquisition routine. It is divided into two sections:
initialization and acquisition. Two sections are written in IBM assembler (via inline
statements) - one section halts any acquisition activity and prepares the board for command
input, and the second section (duplicated twice in this procedure) acquires the A/D reading from
channel 1. }

```

```

{ The program constantly checks for a voltage transition in the chart feed output (read into the
A/D converter through analog channel #1. If a transition is detected, then countinc is
incremented and countflag is set. The detection loop then continues until (after reading the
clock) the new hundredths second value is less than the old hundredths second value (i.e. a new
second). At this point the array tcount[n] is set equal to tcount[n-1] plus the number of
transitions (countinc) detected in the previous second. The arrays A[n], B[n], & C[n] are set
equal to the elapsed time (hours, minutes, and seconds). The time and the count values are
output to the screen so that program operation may be verified; the values of n, A[n], B[n],
C[n], and tcount are also outputted to the file. Thus, at the end of acquisition, the arrays A,
B, C, and tcount contain the count/time profile, with a new array element whenever at least one
voltage transition occurred in a one second interval. }

```

```

var Aflag,Bflag : boolean;      { a pair of flags which indicate when a transition occurs }
High, Low : byte;              { High and Low bytes of A/D converted value }
countflag : boolean;           { indicates if a transition has occurred }
countinc : integer;            { number of transitions in the current second }

timex : timestring;           { string indicating the current time in HH:MM:SS format }
D : byte;                      { hundredths of a second digit from real-time clock }
oldhour,oldmin,oldsec : byte;  { Old time read from clock prior to acquisition }
Dold : byte;                   { old hundredths of a second value - for second detection }

dummy : char;                  { dummy character for keypressed function }
keyflag : boolean;             { flag which indicates when a key has been pressed }

volume : real;                 { total volume which has been dispensed }

begin { AcquireData }

{ Inline machine code which initializes the A/D converter. }

inline ($BA/$ED/$02/$B0/$0F/$EE/ { Port[Command_Register] := Command_Stop }
$BA/$EC/$02/$EC/ { TEMP := Port[Data_Register] }
$BA/$ED/$02/$EC/ { Repeat }
$24/$02/$75/$FB/ { until ((Port[Status_Register] and $02) = 0) }
$EC/$24/$04/ { Repeat }
$3C/$04/$75/$F9/ { until ((Port[Status_Register] and $04) = $4) }
$B0/$00/$EE/ { Port[Command_Register] := Command_Reset }
$EC/$24/$01/ { Repeat }
$3C/$01/$75/$F9/ { until ((Port[Status_Register] and $1) = $1) }
$BA/$EC/$02/$EC/ { TEMP := Port[Data_Register] }
$BA/$ED/$02/$EC/ { Repeat }
$24/$02/$75/$FB/ { until ((Port[Status_Register] and $02) = 0) }
$EC/$24/$04/ { Repeat }
$3C/$04/$75/$F9); { until ((Port[Status_Register] and $04) = $4) }

Time(oldhour,oldmin,oldsec,D,timex); { get time from clock prior to start of acquisition }

n := 0; { set the count index = 0 }
countinc := 0; { set the current count increment = 0 }
keyflag := false; { no key has been pressed to terminate execution }

{ Read A/D channel to get initial state of the chart feed }
{ LOW contains the low byte, and HIGH contains the high byte }

inline ($BA/$ED/$02/$B0/$0C/$EE/ { Port[Command_Register] := Command_ADIN }
$EC/ { Repeat }
$24/$02/$75/$FB/ { until ((Port[Status_Register] and $02) = 0) }
$BA/$EC/$02/$B0/$00/$EE/ { Port[Data_Register] := ADgain }
$BA/$ED/$02/$EC/ { Repeat }
$24/$02/$75/$FB/ { until ((Port[Status_Register] and $02) = 0) }
$BA/$EC/$02/$B0/$01/$EE/ { Port[Data_Register] := ADchannel }
$BA/$ED/$02/$EC/$24/$01/ { Repeat }
$3C/$01/$75/$F9); { until ((Port[Status_Register] and $01) = $1) }
LOW := Port[Data_Register];
inline ($BA/$ED/$02/$EC/$24/$01/ { Repeat }
$3C/$01/$75/$F9); { until ((Port[Status_Register] and $01) = $1) }
HIGH := Port[Data_Register];
inline ($BA/$ED/$02/$EC/ { Repeat }
$24/$02/$75/$FB/ { until ((Port[Status_Register] and $02) = 0) }
$EC/$24/$04/ { Repeat }
$3C/$04/$75/$F9); { until ((Port[Status_Register] and $04) = $4) }
IF ((Port[Data_Register] AND $80) = $80) then Error;

SetTime(0,0,0); { Set clock to 0,0,0 - zero elapsed time }
Time(A[0],B[0],C[0],D,timex); { Read back the time from the clock }
tcount[0] := 0; { Total counts at time zero = 0 }

countflag := false; { No transitions have occurred }
Aflag := (HIGH > 9); { Set Aflag if threshold output is exceeded ("HIGH") }
Bflag := Aflag; { Set Bflag so it is the same as Aflag }

Window(5,2,75,3); { Select status window }
GotoXY(1,1);
Write('Initialization : ',timex); { Display "Initialization" and time to show activation }
Window( 5,4,75,10); { Select data output window }
Clrscr;

Volume := tcount[0]/400; { Compute the dispensed volume }

{ Write the initialization information to the file }
Writeln(Datafile,A[0]:2,' ',B[0]:2,' ',C[0]:2,' ',tcount[0]:5,' ',Volume:7:4);

n := n + 1; { Increment the array index }

```

```

{ Master acquisition repeat loop. This loop repeats until an overflow occurs }
{ in the number of counts or a key is pressed to end acquisition. }
Repeat

  if Keypressed then Keyflag := true;

  { Read A/D channel to get state of the chart feed. }

  inline ($BA/$ED/$02/$B0/$0C/$EE/ { Port[Command_Register] := Command_ADIN }
    $EC/ { Repeat }
    $24/$02/$75/$FB/ { until ((Port[Status_Register] and $02) = 0) }
    $BA/$EC/$02/$B0/$00/$EE/ { Port[Data_Register] := ADgain }
    $BA/$ED/$02/$EC/ { Repeat }
    $24/$02/$75/$FB/ { until ((Port[Status_Register] and $02) = 0) }
    $BA/$EC/$02/$B0/$01/$EE/ { Port[Data_Register] := ADchannel }
    $BA/$ED/$02/$EC/$24/$01/ { Repeat }
    $3C/$01/$75/$F9); { until ((Port[Status_Register] and $01) = $1) }

  LOW := Port[Data_Register];
  inline ($BA/$ED/$02/$EC/$24/$01/ { Repeat }
    $3C/$01/$75/$F9); { until ((Port[Status_Register] and $01) = $1) }

  HIGH := Port[Data_Register];
  inline ($BA/$ED/$02/$EC/ { Repeat }
    $24/$02/$75/$FB/ { until ((Port[Status_Register] and $02) = 0) }
    $EC/$24/$04/ { Repeat }
    $3C/$04/$75/$F9); { until ((Port[Status_Register] and $04) = $4) }

  IF ((Port[Data_Register] AND $80) = $80) then Error;

  Dold := d; { Keep the old hundredths second value for comparison }
  Time(A[n],B[n],C[n],D,timex); { Read the elapsed time }

  { if a count has been measured and there is a new second then compute }
  { the total number of counts, clear countflag, write the data to the }
  { screen and to the file, increment n, and reset countinc. }
  if countflag and (D < Dold) then
  begin
    tcount[n] := tcount[n-1] + countinc;
    countflag := false;
    writeln(timex,' ',countinc:5,' counts; ',tcount[n]:5,' total counts');
    Volume := tcount[n]/400;
    writeln(Datafile,A[n]:2,' ',B[n]:2,' ',C[n]:2,' ',tcount[n]:5,' ',Volume:7:4);
    n := n + 1;
    countinc := 0;
  end;

  Aflag := (HIGH > 9); { if HIGH is greataer than voltage threshold, set Aflag }

  { if Aflag is not equal to Bflag, then a voltage transition has occurred. }
  { Increment countinc, set countflag, and reset Bflag so it is equal to Aflag. }
  If not (Aflag = Bflag) then
  begin
    countinc := countinc + 1;
    countflag := true;
    bflag := aflag;
  end;

  { If array space limit is hit or a key has been pressed then terminate acquisition }
  until ((n = CountMAX) OR Keyflag);

  while keypressed read(kbd,dummy); { clear keyboard buffer }
  Time(A[n],B[n],C[n],D,timex); { read the time }
  Writeln;
  Window(5, 14, 75, 24); { Select the output window }
  Clrscr;
  Writeln('Execution terminated: ',timex); { Display status, termination time (elapsed) }
  ResetTime(oldhour,oldmin,oldsec,A[n],B[n],C[n]); { Reset the real-time clock }

  writeln;
  writeln('Total volume dispensed: ',volume:7:4,' ml');

end; { AcquireData }

```

**Procedure OpenDataFile**(var Datafile : text);

```

{ This procedure prompts the user for the desired datafile filename, fills in the }
{ extension "dat" if it is not specified, and then checks to see if this name is }
{ already present on the disk. If it is, the user is given the choice of overwriting }
{ it. If the user declines, then they are prompted to enter the filename again. }
{ The file variable Datafile, is used in other routines for accessing the file. }

```

```

var  Filename : Filestring; { name of data file }
     Exist    : boolean;    { true if specified filename already exists on disk }
     OKflag   : boolean;    { flag indicates when filename has been successfully selected }

begin { OpenDataFile }

  Window(5,12,75,24);      { Set and select the user input window }
  OKflag := false;        { filename has not been successfully selected yet }

  repeat                   { repeat until OKFlag }
    Clrscr;                { clear the screen inside the window }

    repeat                 { Read filenames until at least one character is entered }
      Write('Save filename: ');
      Readln(Filename);
    until (length(filename) > 0);

    { if the filename is longer than 4 characters, check to see if the extension }
    { is ".dat". If so, strip it off }.
    if (length(filename) > 4) then
      if (copy(filename,length(filename)-3,length(filename))='.dat')
        then filename := copy(filename,1,length(filename)-4);

    { if the filename is longer than 8 characters, filename is equal to first 8 characters }
    if (length(filename) > 8) then filename := copy(filename,1,8);

    Filename := Filename + '.dat';          { Add the extension ".dat" }

    Assign(Datafile,Filename);             { Define the file variable }

    { Turn off error checking, Reset datafile, and then re-enable error checking. If }
    { Datafile exists, then IOresult will be equal to 0. }
    {$I-} Reset(Datafile) {$I+};
    Exist := (IOresult = 0);               { If the file already exists on the disk, Exist = true }
    OKflag := not Exist;                   { The filename is OK to use if it doesn't Exist }

    { If the filename exists, then warn the user and ask whether or not to overwrite }
    if Exist
      then
        begin
          Beep;
          Beep;
          Writeln;
          Writeln('WARNING: File "',Filename,'" already exists!');

          { If they answer yes to the question, then the filename is OK, so set }
          { OKflag=true. Close the Datafile and Erase it to start with a clean slate. }
          If question('Do you want to erase it?')
            then
              begin
                OKflag := true;
                Close(Datafile);
                Erase(Datafile);
              end;
        end

    until OKflag;                    { Repeat asking for filenames until one is OK }

    Clrscr;                            { Clear the window }

    writeln;
    writeln('Output datafile : ',Filename); { Identify the output filename selected }

end; { OpenDataFile }

{ Main - Main program code }
Begin { Main }

  Base_Address := $2EC;                { Memory Address of the Data Acquisition board }
  Data_Register := Base_Address;        { Data Register Address is the same as the Base Address }

  Makescreen;                        { Draw the text windows }

  OpenDataFile(Datafile);               { Get the file Filename and prepare for file write }
  Rewrite(Datafile);                    { Open and empty the file - set pointer to the beginning }

  AcquireData(Data_Register,A,B,C,tcount,n,DataFile); { Master Acquisition Routine }

  Close(Datafile);                      { Close the file }

```

```
for i := 1 to 20000 do;           { do-nothing wait loop to pause program - it is helpful to }
                                { see final count values before terminating program.      }

Writeln;
Write('Press any key to continue...');
dummy := KeyboardInput;         { Wait for a keypress before terminating execution }
ResetWindow;                    { Reset text screen }
Clrscr;
end. { Main }                    { that's all folks }
```

## APPENDIX C - Raw Experimental Data

NOTE: An asterisk (\*) signifies that the marked parameter is being varied from the baseline.

	[Zn] ( M )	[D2EHPA] ( F )	pH	Temp. ( °C )	Intercept ( $\times 10^7$ )	Slope ( $\times 10^7$ )	J(100rpm) kmol/m <sup>2</sup> /s	J(300rpm) kmol/m <sup>2</sup> /s
STUDYA01	0.05	0.05	5.50*	25	1.20225	0.48573	6.34E-08	7.04E-08
STUDYA02	0.05	0.05	4.50	25	1.27801	0.64266	5.63E-08	6.39E-08
STUDYA03	0.05	0.05	4.50	25	1.60495	0.52152	4.98E-08	5.44E-08
STUDYA04	0.05	0.05	4.50	25	1.44678	0.53018	5.38E-08	5.94E-08
STUDYA05	0.001*	0.05	4.50	25	0.46758	5.80803	2.01E-08	3.26E-08
STUDYA06	0.03*	0.05	4.50	25	1.56962	0.58608	4.94E-08	5.46E-08
STUDYA07	0.01*	0.05	4.50	25	1.62316	0.81708	4.43E-08	5.03E-08
STUDYA08	0.005*	0.05	4.50	25	1.87731	1.31886	3.45E-08	4.05E-08
STUDYA09	0.003*	0.05	4.50	25	1.44404	1.59222	3.74E-08	4.64E-08
STUDYA10	0.10*	0.05	4.50	25	1.56957	0.51383	5.08E-08	5.56E-08
STUDYA11	0.05	0.10*	4.50	25	0.87816	0.33828	8.77E-08	9.71E-08
STUDYA12	0.05	0.025*	4.50	25	2.78002	1.22596	2.68E-08	3.00E-08
STUDYA13	0.05	0.010*	4.50	25	5.63237	1.98924	1.39E-08	1.53E-08
STUDYA14	0.05	0.005*	4.50	25	0.93892	5.15378	2.03E-08	3.08E-08
STUDYA15	0.05	0.0025*	4.50	25	14.39475	11.31931	4.32E-09	5.14E-09
STUDYA16	0.05	0.005*	4.50	25	12.06940	4.45671	6.44E-09	7.11E-09
STUDYA17	0.05	0.05	5.00*	25	1.38820	0.58543	5.43E-08	6.06E-08
STUDYA18	0.05	0.05	3.25*	25	1.88770	0.12249	5.04E-08	5.15E-08
STUDYA19	0.05	0.05	4.00*	25	1.56045	0.53104	5.07E-08	5.56E-08
STUDYA20	0.05	0.05	3.75*	25	1.33529	0.68410	5.36E-08	6.09E-08
STUDYA21	0.05	0.05	3.50*	25	1.41360	0.77253	4.97E-08	5.68E-08
STUDYA22	0.05	0.05	5.50*	25	1.40901	0.63507	5.26E-08	5.91E-08
STUDYA25	0.05	0.05	4.50	30*	1.15114	0.49328	6.52E-08	7.29E-08
STUDYA26	0.05	0.05	4.50	15*	1.62001	0.63318	4.74E-08	5.25E-08
STUDYA27	0.05	0.05	4.50	20*	1.63941	0.28731	5.37E-08	5.66E-08
STUDYA28	0.05	0.05	4.50	35*	1.07196	0.44648	7.05E-08	7.86E-08
STUDYA30	0.005*	0.05	4.50	25	1.27783	1.03012	4.82E-08	5.75E-08
STUDYA31	0.10*	0.05	4.50	25	1.25067	0.56321	5.93E-08	6.66E-08
STUDYA32	0.005*	0.05	4.50	25	1.31220	1.09904	4.62E-08	5.54E-08
STUDYA33	0.05	0.05	4.50	25	1.21560	0.59272	5.97E-08	6.75E-08
STUDYA34	0.05	0.05	4.50	25	1.44421	0.57371	5.29E-08	5.88E-08
STUDYA35	0.05	0.05	4.50	25	1.35095	0.61098	5.48E-08	6.16E-08
STUDYA36	0.005*	0.05	4.50	25	1.30828	1.12605	4.59E-08	5.52E-08
STUDYA37	0.10*	0.05	4.50	25	1.01799	0.84444	5.98E-08	7.17E-08
STUDYA38	0.20*	0.05	4.50	25	1.23857	0.49103	6.18E-08	6.86E-08
STUDYA39	0.20*	0.05	4.50	25	1.33987	0.43416	5.97E-08	6.52E-08
STUDYA40	0.02*	0.05	4.50	25	1.34332	0.64144	5.43E-08	6.13E-08
STUDYA41	0.04*	0.05	4.50	25	1.40675	0.54474	5.47E-08	6.06E-08
STUDYA42	0.05	0.10*	4.50	25	0.71916	0.30998	1.04E-07	1.17E-07
STUDYA43	0.05	0.075*	4.50	25	0.92083	0.36531	8.31E-08	9.22E-08
STUDYA44	0.05	0.035*	4.50	25	1.87262	0.68720	4.16E-08	4.59E-08
STUDYA45	0.05	0.05	4.50	35*	1.09105	0.41156	7.09E-08	7.84E-08
STUDYA48	0.05	0.05	4.50	50*	0.92457	0.47012	7.76E-08	8.81E-08
STUDYA50	0.05	0.05	4.50	50*	0.88095	0.43449	8.21E-08	9.30E-08
STUDYA51	0.05	0.05	4.50	40*	1.03295	0.38181	7.53E-08	8.31E-08
STUDYA52	0.05	0.05	4.50	45*	0.95741	0.39778	7.90E-08	8.81E-08

	[Zn] ( M )	[D2EHPA] ( F )	% Loading	Intercept ( $\times 10^7$ )	Slope ( $\times 10^7$ )	J(100rpm) kmol/m <sup>2</sup> /s	J(300rpm) kmol/m <sup>2</sup> /s
STUDYB01	0.05	0.05	8.2	1.44008	0.62974	5.19E-08	5.81E-08
STUDYB02	0.05	0.05	24.3	1.87071	0.75522	4.07E-08	4.53E-08
STUDYB03	0.05	0.05	0	1.29804	0.58299	5.72E-08	6.42E-08
STUDYB04	0.05	0.05	18.7	1.77354	0.87059	4.09E-08	4.62E-08
STUDYB05	0.05	0.05	40.0	2.45371	1.32527	2.87E-08	3.28E-08
STUDYB06	0.05	0.05	49.2	3.29994	1.49803	2.24E-08	2.52E-08
STUDYB07	0.05	0.05	28.5	2.02465	0.95048	3.62E-08	4.08E-08
STUDYB08	0.05	0.05	57.7	4.03017	2.09985	1.77E-08	2.01E-08
STUDYB09	0.05	0.05	82.2	12.01515	3.40072	6.83E-09	7.39E-09
STUDYB10	0.05	0.05	67.6	6.45097	2.35808	1.21E-08	1.33E-08
STUDYB11	0.05	0.05	88.1	28.52638	14.30439	2.52E-09	2.86E-09

	[Zn] ( M )	[D2EHPA] ( F )	filter	Intercept ( $\times 10^7$ )	Slope ( $\times 10^7$ )	J(100rpm) kmol/m <sup>2</sup> /s	J(300rpm) kmol/m <sup>2</sup> /s
STUDYD01	0.05	0.05	0.22 $\mu$ m	1.34584	0.61641	5.48E-08	6.17E-08
STUDYD02	0.05	0.05	0.80 $\mu$ m	1.27965	0.47415	6.07E-08	6.70E-08
STUDYD03	0.05	0.05	0.05 $\mu$ m	2.86257	0.56463	3.03E-08	3.21E-08
STUDYD04	0.05	0.05	0.80 $\mu$ m	1.25882	0.54710	5.94E-08	6.65E-08
STUDYD05	0.05	0.05	0.22 $\mu$ m	1.27255	0.54201	5.91E-08	6.60E-08
STUDYD06	0.05	0.05	0.05 $\mu$ m	2.87390	0.50528	3.06E-08	3.23E-08
STUDYD07	0.05	0.05	0.22 $\mu$ m	1.38042	0.54523	5.55E-08	6.16E-08

---

## APPENDIX D - Basic Mathematical Model

---

The mathematical derivation and program flowchart for the basic mathematical model have been given in Section 4.2, and will not be reproduced here. The program employs an incremental search / bisection routine to determine the steady-state flux under different bulk conditions. The source code for the program follows as Table D.1.

**Table D.1:** Pascal Listing of Basic Mathematical Model

### Program Model;

```
{ guide to variable notation: Zn ≡ Zn2+(aq),
                             Hp ≡ H+(aq),
                             HL ≡ HL(org),
                             HL2 ≡ (HL)2(org),
                             ZnL2HL1 ≡ ZnL2·HL(org),
                             and ZnL2HL2 ≡ ZnL2·(HL)2(org) }
{ a suffix of b indicates a bulk species, and i indicates an interfacial species }

const beta13_over_beta14 = 1e-3;      { ratio of ZnL2·HL and ZnL2·(HL)2 formation constants,
                                       = 10-3 }
Kd = 5.012e4;                         { Dimerization constant for D2EHPA, = 104.7 }
K_ex = 3.236e-2;                       { Equilibrium constant extraction reaction }
c_ZL_bulk = 0;                         { Total organic bulk zinc concentration = 0 }
w = 100;                                { RDC rotational speed, in rpm }

type Filestring = string[14];
    MaxString = string[255];
    Extension = string[4];

var k_aq_Zn, k_aq_Hp, k_or_HL2, k_or_ZL1, k_or_ZL2,      { mass transfer coefficients }
    c_HL_eff_bulk, c_Zn_bulk, pH, c_Hp_bulk,           { species bulk concentrations }
    c_Zn_i, c_HL2tot_i, c_Hp_i, c_ZLtot_i,            { species interfacial concentrations }
    c_HL_i, c_HL2_i, c_ZnL2HL1_i, c_ZnL2HL2_i,       { species interfacial concentrations }
    JZn,                                                { zinc flux in kmol/m2/sec }
    n,                                                  { association factor }
    Vary_i, Vary_f, Vary_inc, Vary_value : real;       { initial, final, increment, and
                                                         current parameter values }
```

### Procedure Beep;

```
{ Beeps the speaker - used when user has made a data entry error }
{ or to alert the user to a possible problem. }

begin { Beep }
    sound(880); { Beep at 880 Hz }
    Delay(125); { for 125 milliseconds. }
    Nosound; { Turn off sound. }
end; { Beep }
```

### Function KeyboardInput : char;

```
{ Waits until a key is pressed, and then reports the value of the key. }

var Key : char;

begin { KeyboardInput }
    Repeat Delay(50) until KeyPressed;
    Read(Kbd,Key);
    KeyboardInput := Key;
end; { KeyboardInput }
```

```

Function Question (prompt:MaxString) : boolean;
{ Asks the Yes or No question contained in the string prompt and then waits until a Y or N }
{ answer has been received. The value of the answer is then reported by the value of this }
{ boolean function - True ≡ Yes and False ≡ No. }

var query : char;

begin { Question }
  Repeat
    Write( prompt + ' <Y/N> ' + chr(8) );
    query := KeyboardInput;
    writeln(query);
  Until (query in ['Y','y','N','n']);           { Keep asking until a Y or N answer is received }

  If (query in ['Y','y']) then Question := true else Question := false;
end; { Question }

```

```

Procedure OpenDataFile(var Datafile : text; filename_extension : extension);
{ This procedure prompts the user for the desired datafile filename, adds the extension }
{ specified, and then checks to see if this name is already present on the disk. If it }
{ is, the user is given the choice of overwriting it. If the user declines, then they }
{ are prompted to enter the filename again. The file variable Datafile, is used in }
{ other routines for accessing the file.}

var  Filename : Filestring; { name of data file }
     Exist : boolean;       { true if specified filename already exists on disk }
     OKflag : boolean;      { flag indicates when filename has been successfully selected }

begin { OpenDataFile }

  OKflag := false;          { filename has not been successfully selected yet }

  repeat                    { repeat until OKFlag }
    repeat                  { Read filenames until at least one character is entered }
      Write('Save filename: ');
      Readln(Filename);
    until (length(filename) > 0);

    { if the filename is longer than 4 characters, check to see if the extension }
    { matches filename_extension. If so, strip it off. }
    if (length(filename) > 4) then
      if (copy(filename,length(filename)-3,length(filename))=filename_extension)
        then filename := copy(filename,1,length(filename)-4);

    { if the filename is longer than 8 characters, filename is equal to first 8 characters }
    If (length(filename) > 8) then filename := copy(filename,1,8);

  Filename := Filename + filename_extension;           { Add the extension }

  Assign(Datafile,Filename);                          { Define the file variable }

  { Turn off error checking, Reset datafile, and then re-enable error checking. If }
  { Datafile exists, then IOResult will be equal to 0. }
  {$I-} Reset(Datafile) {$I+};
  Exist := (IOResult = 0 );                            { If the file already exists on the disk, Exist = true }
  OKflag := not Exist;                                { The filename is OK to use if it doesn't Exist }

  { If the filename exists, then warn the user and ask whether or not to overwrite }
  if Exist
  then
    begin
      Beep;
      Beep;
      Writeln;
      Writeln('WARNING: File "',Filename,'" already exists!');

      { If they answer yes to the question, then the filename is OK, so set }
      { OKflag=true. Close the Datafile and Erase it to start with a clean slate. }
      If Question('Do you want to erase it?')
      then
        begin
          OKflag := true;
          Close(Datafile);
          Erase(Datafile);
        end
    end
  end;

```

```

                end;
    end
until OKflag;                { Repeat asking for filenames until one is OK }

Writeln('Output datafile : ',Filename);        { Identify the output filename selected }
Writeln;

Rewrite(Datafile);          { Open and empty the file - set pointer to the beginning }

{ Write file header }
Writeln(Datafile,'w = ',w:4);
Write (Datafile,'[Zn]bulk [HL]eff,b [ZnL]b    pH,b JZn      n      [Zn]i      [HL]i      ');
Writeln(Datafile,'[(HL)2]i [HL2]ieff [ZnL1]i  [ZnL2]i  [ZnL]i,t [H+]i');

end; { OpenDataFile }

```

**Function Power(x, n : real):real;**

{ Computes the value of  $x^n$  and returns the value as Power. }

```

begin { Power }
    power := exp(n*ln(x));
end; { Power }

```

**Procedure Quadratic(a,b,c : real; var root1, root2 : real);**

{ Solves the quadratic equation and returns the two roots as root1 and root2. }

```

begin { Quadratic }
    root1 := (-b + sqrt(b*b-4*a*c))/(2*a);
    root2 := (-b - sqrt(b*b-4*a*c))/(2*a);
end; { Quadratic }

```

**Procedure Calculate\_Constants;**

{ Computes the mass transfer coefficients for each species. The Levich }  
 { equivalent boundary layer thickness is first calculated, and then the }  
 { mass transfer coefficient is computed using the appropriate formula. }

```

const  D_HL2      = 1.003e-9;
       D_ZnL2HL1 = 0.781e-9;
       D_ZnL2HL2 = 0.659e-9;
       D_HClO4   = 2.854e-9;
       D_Zn      = 1.038e-9;
       nu_H2O    = 8.93e-7;
       nu_heptane = 5.64e-7;
       L_over_alpha = 1.90e-4;

```

```

var    zD_aq_Zn, zD_aq_Hp, zD_or_HL2, zD_or_ZL1, zD_or_ZL2 : real;

```

```

begin { Calculate_Constants }

```

```

    zD_aq_Zn := 0.643/sqrt(w/60)*Power(nu_H2O,(1/6)) * Power(D_Zn,(1/3));
    zD_aq_Hp := 0.643/sqrt(w/60)*Power(nu_H2O,(1/6)) * Power(D_HClO4,(1/3));
    zD_or_HL2 := 0.643/sqrt(w/60)*Power(nu_heptane,(1/6)) * Power(D_HL2,(1/3));
    zD_or_ZL1 := 0.643/sqrt(w/60)*Power(nu_heptane,(1/6)) * Power(D_ZnL2HL1,(1/3));
    zD_or_ZL2 := 0.643/sqrt(w/60)*Power(nu_heptane,(1/6)) * Power(D_ZnL2HL2,(1/3));

```

```

    k_aq_Zn := D_Zn / zD_aq_Zn;
    k_aq_Hp := D_HClO4 / zD_aq_Hp;
    k_or_HL2 := D_HL2 / (zD_or_HL2 + L_over_alpha);
    k_or_ZL1 := D_ZnL2HL1 / (zD_or_ZL1 + L_over_alpha);
    k_or_ZL2 := D_ZnL2HL2 / (zD_or_ZL2 + L_over_alpha);

```

```

end; { Calculate_Constants }

```

**Procedure Vary\_Setup;**

{ This procedure just gets the initial, final, and increment value when }  
 { a range of concentrations is examined. }

```

begin { Vary_Setup }
  Write ('      Initial Value: ');
  Readln (Vary_i);
  Write ('      Final   Value: ');
  Readln (Vary_f);
  Write ('      Increment   : ');
  Readln (Vary_inc);
  if Vary_i > Vary_f          { recurse to get correct values if initial is > than final }
  then
    Vary_Setup
  else
    if Vary_inc <= 0          { recurse to get correct values if increment is < 0 }
    then Vary_Setup;
end; { Vary_Setup }

```

```

Procedure Input_Parameters(var c_Zn_bulk, c_HL_eff_bulk, pH : real;
                             var code : integer);

```

```

{ This procedure prompts the user for values for the bulk zinc concentration, bulk D2EHPA }
{ concentration (expressed as dimer), and bulk pH. The user can examine a range of values }
{ by entering a value of -1. In this case, the subroutine Vary_Setup is called which }
{ prompts the user for the initial, final, and incremental values. code tells the program }
{ whether a range has been selected or not; a value of zero indicates no range, while 1, }
{ 2, and 3 indicate zinc, HL, and H+, respectively. }

```

```

var   input : real;          { temporary storage variable }

begin { Input_Parameters }
  code := 0;                 { no range yet }
  Writeln;
  Writeln('Enter model parameters:      (to vary, enter -1 at the prompt)');
  Write ('      [Zn]bulk = ');
  Readln (Input);
  if (Input = -1)           { select a range of values }
  then
    begin
      code := 1;            { range is for Zn }
      Vary_setup;          { get the range }
    end
  else
    c_Zn_bulk := input;

  Write ('      [HL]bulk = ');
  Readln (Input);
  if (Input = -1)           { select a range of values }
  then
    begin
      code := 2;            { range is for HL }
      Vary_setup;          { get the range }
    end
  else
    c_HL_eff_bulk := input;

  Write ('      pH = ');
  Readln (Input);
  if (Input = -1)           { select a range of values }
  then
    begin
      code := 3;            { range is for H+ }
      Vary_setup;          { get the range }
    end
  else
    pH := input;
end; { Input_Parameters }

```

```

Procedure Compute_Interface_Concentrations(JZn:Real);

```

```

{ This procedure computes the interfacial concentrations from Fick's first law for the specified }
{ flux JZn. The existence of both ZnL,HL and ZnL,(HL), complicates the procedure somewhat, so that }

```

an iterative approach is needed to find the correct value for  $n$ , the association factor. The iteration is carried out until the fractional difference between the  $n_{new}$  and  $n_{old}$  is less than the error criteria  $eps$ . }

```

const   eps = 1e-4;

var JHL2eff, JHp, JZL : Real;
    a, b, c, root1, root2 : real;
    n_old, n_new : real;

begin { Compute_Interface_Concentrations }

    c_Zn_i := - JZn / k_aq_Zn + c_Zn_bulk;      { Compute the interfacial [Zn2+] }
    if c_Zn_i < 0 then c_Zn_i := 1e-10;        { if it's negative, make it very small }

    JHp := -2 * JZn;                          { from the mass balance }
    c_Hp_i := - JHp / k_aq_Hp + c_Hp_bulk;     { Compute the interfacial [H+] }
    if c_hp_i < 0 then c_hp_i := 1e-10;       { if it's negative, make it very small }

    n_new := n;                                { set up initial value }

    repeat                                     { iterate n's until within error eps }
        n_old := n;
        n := n_new;

        JHL2eff := JZn * n;                   { from the mass balance }
        c_HL2tot_i := - JHL2eff / k_or_HL2 + 0.5 * c_HL_eff_bulk;
        if c_HL2tot_i < 0 then c_HL2tot_i := 1e-10; { if it's negative, make it very small }

        { solve for partition between HL and (HL)2 using the quadratic equation }
        a := Kd;
        b := 1/2;
        c := -c_HL2tot_i;
        Quadratic(a,b,c,root1,root2);

        c_HL_i := root1;                      { interfacial HL is equal to the first root }
        c_HL2_i := c_HL2tot_i - 1/2 * c_HL_i; { compute interfacial (HL)2 from mass balance }

        JZL := JZn;                          { from the mass balance }
        { compute the interfacial concentrations of ZnL2HL and ZnL2(HL)2 }
        c_ZnL2HL1_i := (JZL) / (k_or_ZL1 + k_or_ZL2 * c_HL_i / beta13 over_beta14);
        c_ZnL2HL2_i := (JZL) / (k_or_ZL1 * beta13 over_beta14 / c_HL_i + k_or_ZL2);
        c_ZLtot_i := c_ZnL2HL1_i + c_ZnL2HL2_i;

        n_new := (1.5 * c_ZnL2HL1_i + 2 * c_ZnL2HL2_i) / c_ZLtot_i;

    Until ( (abs(n_new-n_old)/n_new) < eps );

    n := n_new;

end; { Compute_Interface_Concentrations }

```

**Function F(x:real) : real;**

{ The interfacial concentrations are computed for the given flux  $X$  by the function Compute\_Interface\_Concentrations. The equilibrium constant for the given interfacial concentrations is then computed and compared with the actual equilibrium constant. Note that interfacial concentrations are used in the  $K_{ex}$  expression rather than activities, i.e. all activity coefficients are assumed to be equal to 1. }

```

begin { F }

    Compute_Interface_Concentrations(X);

    F := c_ZnL2HL1_i * Power(c_Hp_i,2) / c_Zn_i / Power(c_HL2_i,1.5) - K_ex;

end { F };

```

**Procedure Solve( Xinitial,Xfinal,dX,eps : real; var X3 : real);**

{ this procedure uses an incremental search followed by a bisection routine to find the root of the function  $F(X)$ .  $F(X)$  is defined as the difference between the equilibrium constant computed

from the interfacial concentrations and the actual value of the equilibrium constant. In the function, the interfacial concentrations are first computed for a zinc flux  $X$ , and then the difference between the two equilibrium constants is computed. }

```

var X1, Y1, X2, Y2, X3OLD, Y3 : REAL;

LABEL LOOP;

begin { Solve }

  X1 := Xinitial;
  Y1 := F(X1);
  IF (Y1 = 0) then
    begin
      X3 := X1;
      Exit;
    end;

  repeat
    X2 := X1 + dX;
    if (X2 > Xfinal) then
      begin
        Writeln('Solution not found on search interval');
        Exit;
      end;
    Y2 := F(X2);

    if (Y1*Y2) > 0
    then
      begin
        X1 := X2;
        Y1 := Y2;
      end
    else
      if (Y1*Y2) = 0
      then
        begin
          X3 := X2;
          Exit;
        end;
      until (Y1*Y2) < 0;

    { Start Bisection until accuracy in X falls within error eps }

  LOOP:
    X3 := (X1 + X2) / 2;
    if (abs((X3 - X1) / X1) < eps) then Exit;
    Y3 := F(X3);
    if (Y1 * Y3) = 0 then Exit;
    if (Y1 * Y3) < 0
    then
      begin { y1*y3 < 0 }
        X2 := X3;
        Y2 := Y3;
      end
    else
      begin { y1*y3 > 0 }
        X1 := X3;
        Y1 := Y3;
      end;
    Goto LOOP;

end; { Solve }

```

### Procedure Write\_Console\_Data;

{ This procedure writes the zinc flux, the association factor, the bulk concentrations, }  
 { and the computed interfacial concentrations to the screen. }

```

begin { Write Console Data }
  Writeln('Flux = ', Jzn:8, ' kmol/m^2/sec      n = ', n:6:4);
  Write (' [Zn], b = ', c_Zn_bulk:6:4, ' ');
  Write (' [HL]eff, b = ', c_HL_eff_bulk:6:4, ' ');
  Writeln(' [ZnL2], b = ', c_ZL_bulk:6, ' pH = ', pH:4:2);
  Writeln(' [Zn], i = ', c_Zn_i:8:6);
  Write (' [HL]2eff, i = ', c_HL2tot_i:8:6);
  Writeln(' [HL], i = ', c_HL_i:8:6, ' [HL]2, i = ', c_HL2_i:8:6);
  Write (' [ZnL]tot, i = ', c_ZLtot_i:8:6);
  Writeln(' [ZnL2HL], i = ', c_ZnL2HL1_i:8:6, ' [ZnL2HL2], i = ', c_ZnL2HL2_i:8:6);
  Writeln;
end; { Write_Console_Data }

```

```
Procedure Write_File_Data( var Datafile : text );
```

```
{ This procedure writes the values for the bulk concentrations, the zinc flux, the }
{ association factor, and interfacial concentrations to the Datafile. }
```

```
begin { Write File Data }
```

```
  Write (Datafile,c_Zn_bulk:9,' ',c_HL_eff_bulk:9,' ',c_ZL_bulk:9,' ');
  Write (Datafile,pH:4:2,' ',JZn:9,' ',n:6:4,' ',c_Zn_i:9,' ',c_HL_i:9,' ');
  Write (Datafile,c_HL2_i:9,' ',c_HL2tot_i:9,' ',c_ZnL2HL1_i:9,' ');
  Writeln(Datafile,c_ZnL2HL2_i:9,' ',c_ZLtot_i:9,' ',c_Hp_i:9);
```

```
end; { Write_File_Data }
```

```
{ Main - Main program code }
```

```
{ This is the main program. Procedures are called which calculate the mass transfer }
{ coefficients, obtain a datafile filename and set up the file for writing, and obtain the bulk }
{ concentrations ( or concentration ranges). A loop is then executed which finds the zinc flux }
{ for the conditions specified, and writes values to the screen and the datafile. This loop }
{ continues until the flux for all concentration values specified has been computed. The datafile }
{ is then closed and execution is terminated. }
```

```
{ The variable vary in its various permutations is used to accomodate the circumstance where the }
{ zinc flux is computed for a range of values. In this case, code is set to some value other than }
{ zero, its particular value specifying the parameter to be altered. Vary_i, vary_f, vary_inc, and }
{ vary_value are then used to cycle the parameter through the range. }
```

```
const Xi = 1e-9;      { Initial flux value for iterative search routine }
      Xf = 5e-7;      { Final flux value for iterative search routine }
      dX = 5e-9;      { Incremental flux value for iterative search routine }
      eps = 1e-4;     { Error criteria for iterative search routine }
```

```
var Datafile : text; { Output Datafile }
    code : integer;  { Parameter code }
```

```
begin { Main }
```

```
  Clrscr;
  Calculate_Constants;          { Compute mass transfer coefficients }
  OpenDataFile(Datafile,'.out'); { Get the file Filename and prepare for file write }
```

```
{ Execute I/O routine to get values for the aqueous zinc concentration, D2EHPA concentration }
{ (expressed as monomer), and aqueous pH. The routine returns these values, as well as a }
{ code which indicates if a parameter has been selected to be varied over a range. }
Input_Parameters(c_Zn_bulk, c_HL_eff_bulk, pH, code);
```

```
Vary_value := Vary_i;          { set the range variable equal to the range initial value }
```

```
{ if code is nonzero, set the appropriate parameter equal to the range variable }
```

```
if code = 1 then c_Zn_bulk := Vary_value;
if code = 2 then c_HL_eff_bulk := Vary_value;
if code = 3 then pH := Vary_value;
```

```
Repeat                          { Loop once, or until range maximum is exceeded }
```

```
  n := 1.5;                      { An initial value for n }
  c_Hp_bulk := exp(-pH * 2.303);  { convert pH into H+ concentration }
```

```
  Solve(Xi,Xf,dX,eps,JZn);       { Conduct an iterative search for JZn over the }
                                { range Xi - Xf, interval dX, and error criteria eps. }
```

```
  Write_Console_Data;           { Display the solution on the screen }
  Write_File_Data(Datafile);    { Output values to specified Datafile }
```

```
{ If code is not equal to zero, i.e. run for a range of values, increment the range }
{ variable and then set the appropriate parameter equal to the new range value. }
```

```
if not (code = 0) then
  begin
    Vary_value := Vary_value + Vary_inc;
    if code = 1 then c_Zn_bulk := Vary_value;
    if code = 2 then c_HL_eff_bulk := Vary_value;
    if code = 3 then pH := Vary_value;
  end;
```

```
until ((code = 0) or (Vary_value > Vary_f));
```

```
Close(Datafile);                { Close the file }
```

```
end. { Main }
```

# APPENDIX E - Extended Mathematical Model

The mathematical derivation and program flowchart for the extended mathematical model have been given in Section 4.4, and will not be reproduced here. The source code for the program follows as Table E.1.

**Table E.1:** Pascal Listing of Extended Mathematical Model

**Program Preload;**

```
{ guide to variable notation: Zn ≡ Zn2+(aq),
                             Hp ≡ H+(aq),
                             HL ≡ HL(org),
                             HL2 ≡ (HL)2 (org),
                             ZL ≡ total organic zinc,
                             ZnL2HLO ≡ ZnL2 (org),
                             ZnL2HL1 ≡ ZnL2HL(org),
                             and ZnL2HL2 ≡ ZnL2(HL)2 (org) }
{ a suffix of b indicates a bulk species, and i indicates an interfacial species }

const  b12_over_b13 = 6e-5;           { ratio of ZnL2 and ZnL2HL2 formation constants }
       b13_over_b14 = 1e-3;         { ratio of ZnL2HL and ZnL2(HL)2 formation constants,
                                     = 10-3 }
       Kd = 5.012e4;                { Dimerization constant for D2EHPA, = 104.7 }
       K_ex = 3.236e-2;             { Equilibrium constant extraction reaction }
       c_Zn_bulk = 0.05;            { Aqueous zinc concentration }
       pH = 4.5;                    { Bulk pH }
       c_HL_total_bulk = 0.05;     { Total D2EHPA (as monomer) in organic bulk }
       w = 100;                     { RDC rotational speed, in rpm }

type
  Filestring = string[14];
  MaxString  = string[255];
  Extension  = string[4];

var   k_aq_Zn, k_aq_Hp, k_or_HL, k_or_HL2,
       k_or_ZL0, k_or_ZL1, k_or_ZL2,
       c_Hp_bulk, loading,
       c_HL_eff_bulk, c_HL_bulk, c_HL2_bulk,
       c_ZL_bulk, c_ZnL2HLO_b, c_ZnL2HL1_b, c_ZnL2HL2_b,
       c_Zn_i, c_Hp_i, c_HL2tot_i, c_HL_i, c_HL2_i,
       c_ZLtot_i, c_ZnL2HLO_i, c_ZnL2HL1_i, c_ZnL2HL2_i,
       JZn, JZL,
       n,
       KCZnbulk, KCbulk,
       Vary_i, Vary_f, Vary_inc, Vary_value : real;
      { mass transfer coefficients }
      { mass transfer coefficients }
      { species bulk concentrations }
      { species bulk concentrations }
      { species bulk concentrations }
      { species interfacial concentrations }
      { species interfacial concentrations }
      { zinc flux in kmol/m2/sec }
      { association factor }
      { intermediate mass transfer values }
      { initial, final, increment, and
        current parameter values }

Procedure Beep;

{ Beeps the speaker - used when user has made a data entry error }
{ or to alert the user to a possible problem. }

begin { Beep }
  sound(880); { Beep at 880 Hz }
  Delay(125); { for 125 milliseconds. }
  Nosound;   { Turn off sound. }
end; { Beep }
```

```
Function KeyboardInput : char;
```

```
{ Waits until a key is pressed, and then reports the value of the key. }
```

```
var Key : char;
```

```
begin { KeyboardInput }  
  Repeat Delay(50) until KeyPressed;  
  Read(Kbd,Key);  
  KeyboardInput := Key;  
end; { KeyboardInput }
```

```
Function Question (prompt:MaxString) : boolean;
```

```
{ Asks the Yes or No question contained in the string prompt and then waits until a Y or N }  
{ answer has been received. The value of the answer is then reported by the value of this }  
{ boolean function - True ≡ Yes and False ≡ No. }
```

```
var query : char;
```

```
begin { Question }  
  Repeat  
    Write( prompt + ' <Y/N> ' + chr(8) );  
    query := KeyboardInput;  
    writeln(query);  
  Until (query in ['Y','y','N','n']);           { Keep asking until a Y or N answer is received }  
  
  If (query in ['Y','y']) then Question := true else Question := false;  
end; { Question }
```

```
Procedure OpenDataFile(var Datafile : text; filename_extension : extension);
```

```
{ This procedure prompts the user for the desired datafile filename, adds the extension }  
{ specified, and then checks to see if this name is already present on the disk. If it }  
{ is, the user is given the choice of overwriting it. If the user declines, then they }  
{ are prompted to enter the filename again. The file variable Datafile, is used in }  
{ other routines for accessing the file.}
```

```
var  Filename : Filestring; { name of data file }  
     Exist : boolean;      { true if specified filename already exists on disk }  
     OKflag : boolean;     { flag indicates when filename has been successfully selected }
```

```
begin { OpenDataFile }  
  
  OKflag := false;           { filename has not been successfully selected yet }  
  
  repeat                     { repeat until OKFlag }  
    repeat                   { Read filenames until at least one character is entered }  
      Write('Save filename: ');  
      Readln(Filename);  
    until (length(filename) > 0);  
  
    { if the filename is longer than 4 characters, check to see if the extension }  
    { matches filename_extension. If so, strip it off. }  
    if (length(filename) > 4) then  
      if (copy(filename,length(filename)-3,length(filename))=filename_extension)  
        then filename := copy(filename,1,length(filename)-4);  
  
    { if the filename is longer than 8 characters, filename is equal to first 8 characters }  
    If (length(filename) > 8) then filename := copy(filename,1,8);  
  
    Filename := Filename + filename_extension;           { Add the extension }  
  
    Assign(Datafile,Filename);                           { Define the file variable }  
  
    { Turn off error checking, Reset datafile, and then re-enable error checking. If }  
    { Datafile exists, then IOresult will be equal to 0. }  
    {$I-} Reset(Datafile) {$I+};  
    Exist := (IOresult = 0);                             { If the file already exists on the disk, Exist = true }  
    OKflag := not Exist;                                 { The filename is OK to use if it doesn't Exist }
```

```

{ If the filename exists, then warn the user and ask whether or not to overwrite }
if Exist
  then
    begin
      Beep;
      Beep;
      Writeln;
      Writeln('WARNING: File "',Filename,'" already exists!');

      { If they answer yes to the question, then the filename is OK, so set      }
      { OKflag=true. Close the Datafile and Erase it to start with a clean slate. }
      If Question('Do you want to erase it?')
        then
          begin
            OKflag := true;
            Close(Datafile);
            Erase(Datafile);
          end;
    end
  until OKflag;          { Repeat asking for filenames until one is OK }

  Writeln('Output datafile : ',Filename);          { Identify the output filename selected }
  Writeln;

  Rewrite(Datafile);          { Open and empty the file - set pointer to the beginning }

  { Write file header }
  Writeln(Datafile,'w = ',w:4);
  Write (Datafile,'loading  [Zn]bulk  [HL]eff,b [ZnL]b ');
  Write (Datafile,'[HL]bulk  [HL2]bulk [ZnL0]b  [ZnL1]b  [ZnL2]b');
  Write (Datafile,' pH,b JZn      n');
  Write (Datafile,'          [Zn]i      [HL]i      [(HL)2]i  [HL2]ieff');
  Writeln(Datafile,' [ZnL0]i  [ZnL1]i  [ZnL2]i  [ZnL]i,t  {H+}i');

end; { OpenDataFile }

```

**Function Power(x, n : real):real;**

```

{ Computes the value of  $x^n$  and returns the value as Power. }

begin { Power }
  power := exp(n*ln(x));
end; { Power }

```

**Procedure Quadratic(a,b,c : real; var root1, root2 : real);**

```

{ Solves the quadratic equation and returns the two roots as root1 and root2. }

begin { Quadratic }
  root1 := (-b + sqrt(b*b-4*a*c))/(2*a);
  root2 := (-b - sqrt(b*b-4*a*c))/(2*a);
end; { Quadratic }

```

**Procedure Calculate\_Constants;**

```

{ Computes the mass transfer coefficients for each species. The Levich }
{ equivalent boundary layer thickness is first calculated, and then the }
{ mass transfer coefficient is computed using the appropriate formula. }

```

```

const  D_HL      = 1.520e-9;
       D_HL2     = 1.003e-9;
       D_ZnL2HL0 = 0.993e-9;
       D_ZnL2HL1 = 0.781e-9;
       D_ZnL2HL2 = 0.659e-9;
       D_HClO4   = 2.854e-9;
       D_Zn      = 1.038e-9;
       nu_H2O    = 8.93e-7;
       nu_heptane = 5.64e-7;
       L_over_alpha = 1.90e-4;

var    zD_aq_Zn, zD_aq_Hp, zD_or_HL, zD_or_HL2, zD_or_ZL0, zD_or_ZL1, zD_or_ZL2 : real;

begin { Calculate_Constants }

  zD_aq_Zn := 0.643/sqrt(w/60)*Power(nu_H2O,(1/6)) * Power(D_Zn,(1/3));

```

```

zD_aq_Hp := 0.643/sqrt(w/60)*Power(nu_H2O, (1/6)) * Power(D_HClO4, (1/3));
zD_or_HL := 0.643/sqrt(w/60)*Power(nu_heptane, (1/6)) * Power(D_HL, (1/3));
zD_or_HL2 := 0.643/sqrt(w/60)*Power(nu_heptane, (1/6)) * Power(D_HL2, (1/3));
zD_or_ZL0 := 0.643/sqrt(w/60)*Power(nu_heptane, (1/6)) * Power(D_ZnL2HL0, (1/3));
zD_or_ZL1 := 0.643/sqrt(w/60)*Power(nu_heptane, (1/6)) * Power(D_ZnL2HL1, (1/3));
zD_or_ZL2 := 0.643/sqrt(w/60)*Power(nu_heptane, (1/6)) * Power(D_ZnL2HL2, (1/3));

```

```

k_aq_Zn := D_Zn / zD_aq_Zn;
k_aq_Hp := D_HClO4 / zD_aq_Hp;
k_or_HL := D_HL / (zD_or_HL + L_over_alpha);
k_or_HL2 := D_HL2 / (zD_or_HL2 + L_over_alpha);
k_or_ZL0 := D_ZnL2HL0 / (zD_or_ZL0 + L_over_alpha);
k_or_ZL1 := D_ZnL2HL1 / (zD_or_ZL1 + L_over_alpha);
k_or_ZL2 := D_ZnL2HL2 / (zD_or_ZL2 + L_over_alpha);

```

```
end; { Calculate_Constants }
```

### Procedure Vary\_Setup;

```
{ This procedure just gets the initial, final, and increment value when }
{ a range of concentrations is examined. }
```

```

begin { Vary_Setup }
  Write ('          Initial Value: ');
  Readln (Vary_i);
  Write ('          Final Value: ');
  Readln (Vary_f);
  Write ('          Increment : ');
  Readln (Vary_inc);
  if Vary_i > Vary_f
  then
    Vary_Setup
  else
    if Vary_inc <= 0
    then Vary_Setup;
end; { Vary_Setup }

```

### Procedure Input\_Parameters(var loading : real; var varycode : integer);

```
{ This procedure prompts the user for a value for the percentage zinc loading in the organic }
{ phase. The user can examine a range of values by entering a value of -1. In this case, }
{ the subroutine Vary_Setup is called which prompts the user for the initial, final, and }
{ incremental values. varycode tells the program whether a range has been selected or not; }
{ a value of zero indicates no range, while 1 indicates a loading range. }
```

```

var input : real; { temporary storage variable }

begin { Input_Parameters }
  varycode := 0;
  Writeln;
  Writeln(' Enter model parameters: (to vary, enter -1 at the prompt)');
  Write (' loading = ');
  Readln (input);
  if (input = -1)
  then
    { select a range of values }
    begin
      varycode := 1;
      Vary_setup; { get the range }
    end
  else
    loading := input;
end; { Input_Parameters }

```

### Procedure Solve( Xinitial, Xfinal, dX, eps : real; var X3 : real; functioncode : integer); forward;

```
{ Master root finding routine. Since Solve references Solvefunction, which references }
{ Compute_Interface_Concentrations, which references Solve, a forward declaration is }
{ required. functioncode indicates which function is to be solved for; it also }
{ selects the increment method; if functioncode is equal to 1 then dX is added to the }
{ current value of X for each interval, but if functioncode is not equal to 1, then X }
{ is multiplied by dX for each interval. }
```

### Procedure Compute\_Bulk\_Concentrations;

```
{ This procedure computes the concentration of HL, (HL)2, ZnL2, ZnL2HL, and ZnL2(HL)2 }
{ based on the conditions in the bulk (total D2EHPA concentration and loading). }

const Xi= 1e-10;
      dX = 2;
      eps = 1e-4;

var Xf, temp : real;

begin { Compute_Bulk_Concentrations }

  c_Hp_bulk := exp(-pH * 2.303);           { compute [H+] from pH }
  c_ZL_bulk := c_HL_total_bulk / 2 * loading; { compute zinc concentration from loading }

  { if the bulk zinc concentration is equal to zero, then there is no speciation of }
  { organic zinc in the bulk. Therefore, the effective concentration of HL is equal }
  { to the total concentration of HL in the bulk. The partition between HL and }
  { (HL)2 can therefore be calculated. }
  if (c_ZL_bulk = 0)
  then
    begin
      c_HL_eff_bulk := c_HL_total_bulk;
      Quadratic(Kd,0.5,-c_HL_eff_bulk/2,c_HL_bulk,temp);
      c_HL2_bulk := (c_HL_eff_bulk-c_HL_bulk)/2;

      c_ZnL2HL0_b := 0;
      c_ZnL2HL1_b := 0;
      c_ZnL2HL2_b := 0;
    end
  else
    begin
      Xf := 2 * c_HL_total_bulk;
      Solve(Xi,Xf,dX,eps,c_HL_bulk,3);      { Solve over the interval, SOLVEFUNCTION #3 }

      c_HL2_bulk := Kd * c_HL_bulk * c_HL_bulk;
      c_HL_eff_bulk := c_HL_bulk + 2 * c_HL2_bulk;
      c_ZnL2HL1_b := c_ZL_bulk / (b12 over b13 / c_HL_bulk + 1 + c_HL_bulk / b13 over b14);
      c_ZnL2HL0_b := c_ZnL2HL1_b * b12 over b13 / c_HL_bulk;
      c_ZnL2HL2_b := c_ZnL2HL1_b * c_HL_bulk / b13 over b14;
    end;
  end;

end; { Compute_Bulk_Concentrations }
```

### Procedure Compute\_Interface\_Concentrations( x : real );

{ This procedure computes the interfacial concentrations for the specified flux *JZn*. The interfacial concentrations for zinc and the hydrogen ion can be calculated directly from Fick's first law, but an iterative approach must be used to compute the interfacial concentrations of the five organic species. The procedure Solve is used to compute the concentration of HL at the interface. The upper limit for the search interval, *Yf*, is set at 1.5 times the total HL concentration in the bulk; a multiplier of 1.5 is used since *dY* is multiplicative and also equal to 1.5. Thus, complete coverage of the entire interval is ensured. The interfacial dimer concentration is then calculated, and the effective total dimer concentration at the interface is found by adding the dimer and monomer contributions. Finally, the concentrations of the organic zinc species may be computed. }

```
const Yi = 1e-10;
      dY = 1.5;
      eps = 1e-4;

var JHL2eff, JHp, JZn : real;
    Yf : real;
begin { Compute_Interface_Concentrations }

  JZn := x;
  c_Zn_i := - Jzn / k_aq_Zn + c_Zn_bulk;
  if c_zn_i < 0 then c_zn_i := 1e-10;

  JHp := -2 * Jzn;
  c_Hp_i := - JHp / k_aq_Hp + c_Hp_bulk;
  if c_hp_i < 0 then c_hp_i := 1e-10;

  JZL := JZn;

  Yf := c_HL_eff_bulk * 1.5;
  Solve(Yi,Yf,dY,eps,c_HL_i,2);          { Solve over the interval, SOLVEFUNCTION #2 }

  c_HL2_i := Kd * c_HL_i * c_HL_i;
```

```

c_HL2tot_i := c_HL_i / 2 + c_HL2_i;

c_ZnL2HL1_i := (JZL + KCZnbulk) / (k_or_ZL0 * b12_over_b13 / c_HL_i + k_or_ZL1
+ k_or_ZL2 * c_HL_i / b13_over_b14);
c_ZnL2HL0_i := c_ZnL2HL1_i * b12_over_b13 / c_HL_i;
c_ZnL2HL2_i := c_ZnL2HL1_i * c_HL_i / b13_over_b14;
c_ZLtot_i := c_ZnL2HL0_i + c_ZnL2HL1_i + c_ZnL2HL2_i;

{ compute the association factor at the interface }
n := (c_ZnL2HL0_i + 1.5 * c_ZnL2HL1_i + 2 * c_ZnL2HL2_i) / c_ZLtot_i;

end; { Compute_Interface_Concentrations }

```

**Function SolveFunction**( x : real; FunctionCode : integer ):real;

{ This function is a generalized function which is called by the root-finding procedure SOLVE. SOLVE is used to find the roots of three different functions; the particular function is selected by the value of *Functioncode*. If *Functioncode* is equal to 1, then SOLVE has been called from Main, where it is used to find the Zinc flux, *JZn*. This particular function calls the procedure Compute\_Interface\_Concentrations, which finds the interfacial concentration of HL via an iterative approach. It therefore calls SOLVE again, this time with a *Functioncode* equal to 2. Finally, SOLVE is used by the procedure Compute\_Bulk\_Concentrations to find the bulk concentration of HL, and Solvefunction is called with *Functioncode* equal to 3. }

```

var CZNL1_i, temp1, temp2 : real;
begin
  if (FunctionCode = 1)
  then
    begin
      Compute_Interface_Concentrations(X);
      SolveFunction := c_ZnL2HL1_i * Power(c_Hp_i,2) / c_Zn_i / Power(c_HL2_i,1.5) - K_ex;
    end;

  if (FunctionCode = 2)
  then
    begin
      CZNL1_i := (JZL+KCZnbulk) / (k_or_ZL0*b12_over_b13/x + k_or_ZL1
+ k_or_ZL2*x/b13_over_b14);
      SolveFunction := k_or_HL*x + 2*k_or_HL2*Kd*x*x + 2*k_or_ZL0*CZNL1_i*b12_over_b13/x
+ 3*k_or_ZL1*CZNL1_i + 4*k_or_ZL2*CZNL1_i*x/b13_over_b14 - KCbulk;
    end;

  if (FunctionCode = 3) then
    SolveFunction := c_HL_total_bulk - x - 2 * Kd * x*x - ( 2*b12_over_b13/x + 3
+ 4*x/b13_over_b14 ) * c_ZL_bulk / (b12_over_b13/x + 1 + x/b13_over_b14);

end;

```

**Procedure Solve**{( Xinitial,Xfinal,dX,eps : real; var X3 : real; functioncode : integer)};

{ Master root finding routine. This procedure uses an incremental search followed by a bisection method to find the root of the function SOLVEFUNCTION(x,functioncode). *functioncode* indicates which function is to be solved for; it also selects the increment method; if *functioncode* is equal to 1 then *dX* is added to the current value of *X* for each interval, but if *functioncode* is not equal to 1, then *X* is multiplied by *dX* for each interval. For function #1, the value of the function changes very rapidly, and therefore small steps were required. Conversely, for functions #2 and 3, the equilibrium changes slowly with *x* and a large interval must be searched, and therefore instead of adding *dX* to *X*, a multiplicative approach is used. }

```

var X1, Y1, X2, Y2, X3OLD, Y3 : REAL;

LABEL LOOP;

begin { Solve }

  X1 := Xinitial;
  Y1 := SolveFunction(X1,FunctionCode);
  IF (Y1 = 0) then
    begin
      X3 := X1;
      Exit;
    end;

```

```

Repeat
  if (FunctionCode = 1) then X2 := X1 + dx
                                else X2 := X1 * dx;
                                { select iteration method }
  if (X2 > Xfinal) then
  begin
    Writeln('Solution not found on search interval');
    Exit;
  end;
  Y2 := SolveFunction(X2,FunctionCode);

  if (Y1*Y2) > 0
  then
  begin
    X1 := X2;
    Y1 := Y2;
  end
  else
  IF (Y1*Y2) = 0
  then
  begin
    X3 := X2;
    Exit;
  end;
until (Y1*Y2) < 0;

{ Start Bisection until accuracy in X falls within error eps }

LOOP:
  X3 := (X1 + X2) / 2;
  if (abs((X3 - X1) / X1) < eps) then Exit;
  Y3 := SolveFunction(X3,FunctionCode);
  IF (Y1 * Y3) = 0 then Exit;
  IF (Y1 * Y3) < 0
  then
  begin { y1*y3 < 0 }
    X2 := X3;
    Y2 := Y3;
  end
  else
  begin { y1*y3 > 0 }
    X1 := X3;
    Y1 := Y3;
  end;
GOTO LOOP;

end; { Solve }

```

### Procedure Write\_Console\_Data;

```

{ This procedure writes the zinc flux, the association factor, and the }
{ computed bulk and interfacial concentrations to the screen. }

begin { Write Console Data }
  Writeln('Flux = ',JZn:8,' kmol/m^2/sec          n = ',n:6:4);
  Write  ('[Zn],b = ',c_Zn_bulk:6:4,' ');
  Writeln('[ZnL2],b = ',c_ZL_bulk:6:4,'      pH = ',pH:4:2);
  Writeln('[Zn],i = ',c_Zn_i:8:6);
  Write  ('[HL]eff,b = ',c_HL_eff_bulk:6:4,' ');
  Writeln('      [HL],b = ',c_HL_bulk:8:6,'      [HL]2,b = ',c_HL2_bulk:8:6);
  Write  ('[HL]2eff,i = ',c_HL2tot_i:8:6);
  Writeln('      [HL],i = ',c_HL_i:8:6,'      [HL]2,i = ',c_HL2_i:8:6);
  Writeln('[ZnL]tot,i = ',c_ZLtot_i:8:6);
  Writeln('      [ZnL2],i = ',c_ZnL2HL0_i:8:6,'      [ZnL2HL],i = ',c_ZnL2HL1_i:8:6,'      [ZnL2HL2],i = ',c_ZnL2HL2_i:8:6);
  Writeln;
end; { Write_Console_Data }

```

### Procedure Write\_File\_Data( var Datafile : text );

```

{ This procedure writes the values for the bulk concentrations, the zinc flux, the }
{ association factor, and interfacial concentrations to the Datafile. }

```

```

begin { Write_File_Data }
  Write (Datafile,loading:6:4,' ',c_Zn_bulk:9,' ',c_HL_eff_bulk:9,' ',c_ZL_bulk:9,' ');
  Write (Datafile,c_HL_bulk:9,' ',c_HL2_bulk:9,' ');
  Write (Datafile,c_ZnL2HL0_b:9,' ',c_ZnL2HL1_b:9,' ',c_ZnL2HL2_b:9,' ');
  Write (Datafile,pH:4:2,' ',JZn:9,' ',n:6:4,' ',c_Zn_i:9,' ',c_HL_i:9,' ');
  Write (Datafile,c_HL2_i:9,' ',c_HL2tot_i:9,' ',c_ZnL2HL0_i:9,' ',c_ZnL2HL1_i:9,' ');
  Writeln(Datafile,c_ZnL2HL2_i:9,' ',c_ZLtot_i:9,' ',c_Hp_i:9);
end; { Write_File_Data }

{ Main - Main program code }

{ This is the main program. Procedures are called which calculate the mass transfer
coefficients, obtain a datafile filename and set up the file for writing, and obtain the loading
value (or range). A loop is executed which then computes the bulk species concentrations, finds
the zinc flux for the conditions specified, and writes values to the screen and the datafile.
This loop continues until the zinc flux for all loading values specified has been computed. The
datafile is then closed and execution is terminated. }

{ The variable vary in its various permutations is used to accomodate the circumstance where the
zinc flux is computed for a range of loading values. varycode equal to 1 indicates that the flux
search routine is to be executed for loadings in the interval Vary_i - vary_f, with step size
vary_inc. }

const Xi = 1e-11; { Initial flux value for iterative search routine }
      Xf = 5e-7; { Final flux value for iterative search routine }
      dX = 5e-9; { Incremental flux value for iterative search routine }
      eps = 1e-4; { Error criteria for iterative search routine }

var Datafile : text; { Output Datafile }
    varycode : integer; { Parameter code }

begin { Main }

  Clrscr;
  Calculate_Constants; { Compute mass transfer coefficients }
  OpenDataFile(Datafile,'.out'); { Get the file Filename and prepare for file write }

  { Execute I/O routine to get a value for the loading. The routine returns the loading, as }
  { well as varycode which indicates if the user wishes to vary the parameter over a range. }
  Input_Parameters(loading, varycode);

  if varycode = 1 { If a range is selected, initialize vary_value }
  then { and loading }
  begin
    Vary_value := Vary_i;
    loading := Vary_value;
  end;

  Repeat { Loop once, or until range maximum is exceeded }

    Compute_Bulk_Concentrations;

    { Compute constants which are used by Compute_Interface_Concentrations and Solvefunction }
    KCZnbulk := k_or_ZL0*c_ZnL2HL0_b + k_or_ZL1*c_ZnL2HL1_b + k_or_ZL2*c_ZnL2HL2_b;
    KCbulk := k_or_HL*c_HL_bulk + 2*k_or_HL2*c_HL2_bulk + 2*k_or_ZL0*c_ZnL2HL0_b
              + 3*k_or_ZL1*c_ZnL2HL1_b + 4*k_or_ZL2*c_ZnL2HL2_b;

    Solve(Xi,Xf,dX,eps,JZn,1); { Conduct an iterative search for JZn over the
                                range Xi - Xf, interval dX, and error criteria eps. }

    Write_Console_Data; { Display the solution on the screen }
    Write_File_Data(Datafile); { Output values to specified Datafile }

    { If varycode is equal to one, increment the range variable and then set }
    { loading equal to the new range value. }
    if varycode = 1
    then
    begin
      Vary_value := Vary_value + vary_inc;
      loading := Vary_value;
    end;

  until ((varycode = 0) or (Vary_value > Vary_f));

  Close(Datafile); { Close the file }

end. { Main }

```